AD-A144 196 ATMOSPHERE TEMPERATURE PROFILE RECOVERY USING PARTIAL INTERFEROMETRY.. (U) UTAH STATE UNIV BEDFORD MA STEWART RADIANCE LAB M H BRUCE ET AL. 30 SEP 83 SDL-SRL-83-2 1/1

UNCLASSIFIED AFGL-TR-83-0317 F19628-83-C-0056 F/G 4/1 NL

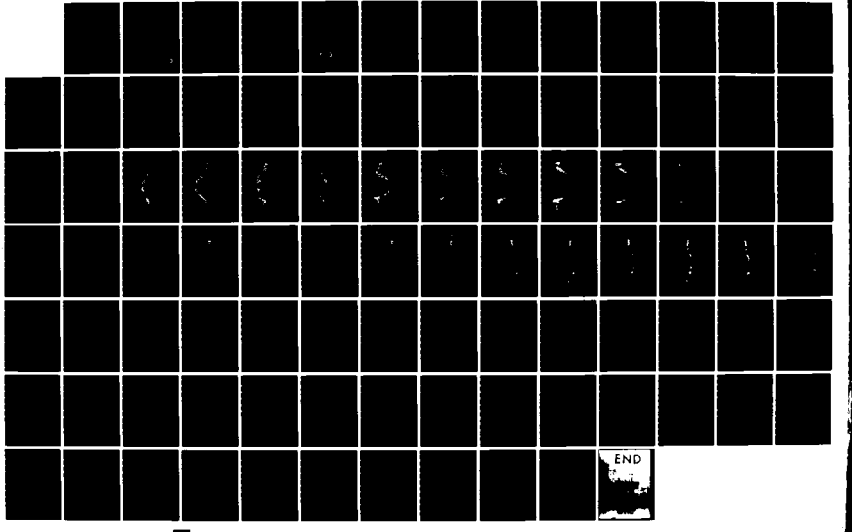

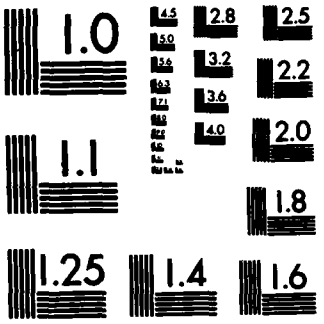

MICROCOPY RESOLUTION TEST CHART
NATIONAL BUREAU OF STANDARDS-1963-A

(12)

AFGL-TR-83-0317

ATMOSPHERE TEMPERATURE PROFILE RECOVERY USING PARTIAL INTERFEROMETRY

Marshall H. Bruce
Charles W. Eastman

STEWART RADIANCE LABORATORY
UTAH STATE UNIVERSITY
139 The Great Road
Bedford, MA. 01730

SCIENTIFIC REPORT NO. 1

30 September 1983

AIR FORCE GEOPHYSICS LABORATORY
AIR FORCE SYSTEMS COMMAND
UNITED STATES AIR FORCE
HANSCOM AFB, MA. 01731

This technical report has been reviewed and is approved for publication

(Signature)
FRANCIS X. ROBERT
Contract Manager
Atmospheric Backgrounds Branch
Infrared Technology Division

(Signature)
RANDALL E. MURPHY, Chief
Atmospheric Backgrounds Branch
Infrared Technology Division

FOR THE COMMANDER

(Signature)
RANDALL E. MURPHY
Acting Director
Infrared Technology Division

Qualified requestors may obtain additional copies from the Defense Technical Information Center.

If you address has changed, or if you wish to be removed from the mailing list, or if the addressee is no longer employed by your organization, please notify AFGL/DAA, Hanscom AFB, MA 01731. This will assist us in maintaining a current mailing list.

Do not return copies of this report unless contractual obligations or notices on a specific document requires that it be returned.

UNCLASSIFIED

SECURITY CLASSIFICATION OF THIS PAGE *(When Data Entered)*

REPORT DOCUMENTATION PAGE		READ INSTRUCTIONS BEFORE COMPLETING FORM
1. REPORT NUMBER AFGL-TR-83-0317	2. GOVT ACCESSION NO. AD-A134196	3. RECIPIENT'S CATALOG NUMBER
4. TITLE *(and Subtitle)* ATMOSPHERE TEMPERATURE PROFILE RECOVERY USING PARTIAL INTERFEROMETRY		5. TYPE OF REPORT & PERIOD COVERED Scientific Report No. 1 6. PERFORMING ORG. REPORT NUMBER SDL-SRL-83-2
7. AUTHOR(s) Marshall H. Bruce Charles W. Eastman		8. CONTRACT OR GRANT NUMBER(s) F19628-83-C-0056
9. PERFORMING ORGANIZATION NAME AND ADDRESS Stewart Radiance Laboratory Utah State University 139 The Great Road, Bedford, MA. 01730		10. PROGRAM ELEMENT, PROJECT, TASK AREA & WORK UNIT NUMBERS 62101F 767010AK
11. CONTROLLING OFFICE NAME AND ADDRESS Air Force Geophysics Laboratory Hanscom AFB, MA., 01731 Monitor: Francis X. Robert/LSP		12. REPORT DATE 30 September 1983 13. NUMBER OF PAGES 91
14. MONITORING AGENCY NAME & ADDRESS *(if different from Controlling Office)*		15. SECURITY CLASS. *(of this report)* UNCLASSIFIED 15a. DECLASSIFICATION/DOWNGRADING SCHEDULE

16. DISTRIBUTION STATEMENT *(of this Report)*

Approved for public release; distribution unlimited.

17. DISTRIBUTION STATEMENT *(of the abstract entered in Block 20, if different from Report)*

18. SUPPLEMENTARY NOTES

19. KEY WORDS *(Continue on reverse side if necessary and identify by block number)*

Remote sensing, atmospheric temperature, carbon dioxide radiation transfer, interferometers, partial scan.

20. ABSTRACT *(Continue on reverse side if necessary and identify by block number)*

A model for the radiative transfer of CO_2 at 15μm through representative earth atmospheres is constructed in order to investigate the efficiency of temperature profile recovery using selected partial interferograms. The recovered profiles and their root mean square errors are then compared in order to evaluate the apparent advantage in using partial interferometry.

DD FORM 1 JAN 73 1473

UNCLASSIFIED

SECURITY CLASSIFICATION OF THIS PAGE *(When Data Entered)*

TABLE OF CONTENTS

LIST OF FIGURES

LIST OF TABLES

INTRODUCTION

The recovery of temperature profiles of the earth's atmosphere by a top-side sounder in the 15 μm region has been investigated. A modeled radiative transfer of CO_2 through a structured atmosphere is created and analyzed by a least squares method in the presence of varying amounts of random noise. This is done both in the spectral domain using either a 135 cm^{-1} window centered at 15 μm or by using 10 selected spectral channels 0.5 cm^{-1} wide or in the interferogram domain using either the entire continuous region from zero path to an optical path difference corresponding to the spectral domain resolution, or by using selected portions (partial interferograms) to recover temperature profiles. The recovered profiles and their root mean square errors are then compared both in the spectral and interferogram domains in order to evaluate the apparent advantage in using partial interferograms as first proposed by Kyle (1977) and investigated by Smith et al., (1979) and at Santa Barbara Research Center (1981) and Perkin-Elmer (1982).

First a computation of synthetic line spectra for the nine strongest bands of CO_2 at 15 μm was done. These are general spectra parameterized by temperature, pressure, column density, and general line widths. The model then convolves a Lorentz, or a Lorentz-Gaussian (Voigt) profile with the line spectra and forms the transmission and absorption as a function of wavenumber.

The radiative transfer for multiple atmospheric layers (up to 14 distinct layers) was then computed and, for spectral domain studies, convolved with an instrument function, either triangular, sinc, or preferably $sinc^2$. Fourier transforms of the separate and composite atmospheric layer spectra were also done, since they are required for the interferometer

domain analysis. The final result is an artificial spectrum representative of that observed by a satellite or balloon-borne interferometer looking down through a radiating atmosphere to a hot earth surface. The possible gain advantages are then discussed and conclusions drawn.

Radiative Transfer in a Plane Parallel Atmosphere:

We assume a plane parallel atmosphere with no scattering, and in local thermodynamic equilibrium, so that a particular layer may be characterized by a pressure, temperature, and density, and a constant mixing ratio of CO_2. Under such a condition, the radiative transfer calculations are done using the expression for the intensity of radiation $I(\sigma)$ emerging from the top of the last layer (looking at nadir) as

$$I(\sigma) = \int_{\text{bottom}}^{\text{top}} B(\sigma,T)d\tau(\sigma) + B(\sigma,T_g)\tau_g(\sigma) \quad , \qquad (1)$$

where $\tau(\sigma)$ is the wavelength dependent transmission from a given layer at height z to the top layer, and $B(\sigma,\tau)$ is the black body function for a given layer (z dependent), and the subscript g is the ground contribution. Of course our integration is done with only a finite number of layers (up to 14 homogeneous layers of about 2 km thickness plus the ground contribution) so the expression becomes a summation, so that we have

$$I(\sigma) = \sum_{i=1}^{N} \omega_i B(\sigma,T_i)(\tau_{1,i} - \tau_{1,i+1}) + B(\sigma,T_g)\tau_{1,N} \quad , \qquad (2)$$

where ω_i are numerical weights for integration.

Because of the nature of the transmission function in the form of an exponential whose argument is proportional to the thickness and optical absorption coefficient for a particular layer, the total transmission from level 1 to level i is the product of the individual transmissions within each homogeneous layer, so we have, for example, $\tau_{13} = \tau_{12}\tau_{23}$, $\tau_{14} = \tau_{12}\tau_{23}\tau_{34} = \tau_{13}\tau_{34}$, etc. In this way we build up the total expression for $I(\sigma)$ for a given temperature profile. Such a calculation is illustrated from Figures 1-11 for ten atmospheric levels and a ground contribution, and represents the contribution of each layer to the radiance at height 30 km for a down-looking instrument. Figure 12 shows the total radiance.

Least Squares Procedure for Recovering Temperature Profiles. Spectral Space.

In order to derive a temperature profile from experimental measurements of intensity, the most direct method is to assume a reasonable "most probable" profile appropriate for the season and region and work with the difference spectra, with deviations indicating actual temperature variations from the assumed standard profile. For small changes in temperature a Taylor series expansion is sufficient, and we retain only the first differences. Thus an intensity profile giving a nadir intensity of $I(\sigma)$ may be represented as

$$I(\sigma) = I_0(\sigma) + \sum_{i=1}^{N} \left[\frac{\partial I(\sigma,T)}{\partial T}\right]_{T_i} \Delta T_i \quad , \qquad (3)$$

where

$$\left[\frac{\partial I(\sigma,T)}{\partial T}\right]_{\substack{\sigma=\sigma_j \\ T=T_i}} \equiv f(\sigma_j,T_i) \equiv f_{ji} \quad . \tag{4}$$

We minimize $\phi(\Delta T_i)$ in the least squares sense as (for a set of discrete wavenumbers, σ_j, $1 \leq j \leq M$)

$$\phi(\Delta T_i) = \sum_{j=1}^{M}\left[I(\sigma_j) - \left(I_0(\sigma_j) + \sum_{i=1}^{N} f(\sigma_j,T_i)\Delta T_i\right)\right]^2 \quad . \tag{5}$$

The set ΔT_i is chosen such that ϕ is a minimum, $d\phi=0$, or since the set ΔT_i is independent

$$\frac{\partial \phi}{\partial(\Delta T_k)} = 0 = (-2)\sum_{j=1}^{M}\left[\left(I(\sigma_j)-I_0(\sigma_j)\right) - \sum_{i=1}^{N} f(\sigma_j,T_i)\Delta T_i\right]\cdot f(\sigma_j,T_k) \quad . \tag{6}$$

Letting $\mathcal{I}(\sigma_j) \equiv I(\sigma_j) - I_0(\sigma_j)$, the difference between the observed

spectra and the spectra from the standard profile, we have

$$\sum_{j=1}^{M} \mathcal{J}(\sigma_j) f(\sigma_j, T_k) = \sum_{i=1}^{N} \left[\sum_{j=1}^{M} f(\sigma_j, T_i) f(\sigma_j, T_k) \right] \Delta T_i \quad . \qquad (7)$$

This set comprises N equations for the profile differences from a set of M points of spectra data.

We define the following matrices, first the MxN matrix of coefficients,

$$f \equiv \begin{bmatrix} f_{11} & f_{12} & \cdots & f_{1N} \\ f_{21} & f_{22} & \cdots & \\ \vdots & \vdots & & \\ \vdots & & & \vdots \\ f_{M1} & & \cdots & f_{MN} \end{bmatrix} \quad . \qquad (8)$$

Next the temperature difference column Nx1 matrix,

$$\Delta T \equiv \begin{bmatrix} \Delta T_1 \\ \Delta T_2 \\ \vdots \\ \Delta T_N \end{bmatrix}$$

and the intensity difference matrix,

$$\mathcal{J} \equiv \begin{bmatrix} \mathcal{J}(\sigma_1) \\ \mathcal{J}(\sigma_2) \\ \vdots \\ \mathcal{J}(\sigma_m) \end{bmatrix} . \qquad (9)$$

Then the expression for the temperature differences can be written in

matrix form as

$$f^T \mathcal{J} = f^T f \, \Delta T \quad , \tag{10}$$

where f^T is the transpose operation on f, and makes the product matrix $f^T f$ square, and possessing an inverse.

By including a "noise" term in the expression (3) we can determine the variance in the temperature. Thus, adding a noise term n, we have, in matrix notation

$$\mathcal{J} + n = f\Delta T \quad , \tag{11}$$

where n is an Mx1 column matrix. Then ϕ, the quandratic expression to be minimized, may be written as

$$\phi = \left[\mathcal{J} + n - f\Delta T\right]^T S \left[\mathcal{J} + n - f\Delta T\right] \quad , \tag{12}$$

where S is a symmetric weighting matrix to be determined.

Multiply (11) on the left by $f^T S$,

$$f^T S \mathcal{J} + f^T S n = f^T S f \, \Delta T \quad . \tag{13}$$

Now $f^T S f$ usually has an inverse, called the Moore-Penrose pseudo-inverse with weight S. Thus we may solve for ΔT as

$$\Delta T = (f^T S f)^{-1} f^T S \mathcal{J} + (f^T S f)^{-1} f^T S n \quad . \tag{14}$$

The "best estimate" $\tilde{\Delta T}$ of ΔT is the first term,

$$\widetilde{\Delta T} \equiv (f^T S f)^{-1} f^T S \mathcal{J} \quad , \tag{15}$$

and the "estimation of the error" is then

$$(\Delta T - \widetilde{\Delta T}) = (f^T S f)^{-1} f^T S n \quad . \tag{16}$$

Now the nature of n is stochastic, and the only meaningful measurements of our error are its expectation in the probability sense. So if we define a functional operation as the expectation of a function g, as E(g), and use a probability density function p, such that

$$\int_{-\infty}^{\infty} p(v)dv = 1 \quad , \tag{17}$$

and where

$$P(a,b) \equiv \int_a^b p(v)dv \quad , \tag{18}$$

is the probability of an event occurring between a and b, then

$$E(g) \equiv \int_{-\infty}^{\infty} g(v)p(v)dv \tag{19}$$

is the "expectation value of g". Then the variance of the estimation error may be expressed as

$$E(\Delta T - \widetilde{\Delta T})(\Delta T - \widetilde{\Delta T})^T$$

$$= E\left\{\left[(f^TSf)^{-1}f^TSn\right]\left[(f^TSf)^{-1}f^TSn\right]^T\right\}$$

$$= E\left\{(f^TSf)^{-1}f^TSn\ n^TSf(f^TSf)^{-1}\right\}$$

$$= (f^TSf)^{-1}f^TS\ E(nn^T)\ Sf(f^TSf)^{-1} \quad . \qquad (20)$$

Now $E(nn^T)$ is the variance of the matrix Q, the noise, and we may minimize ϕ and $E\left[(\Delta T - \widetilde{\Delta T})(\Delta T - \widetilde{\Delta T})^T\right]$ simultaneously by choosing our weighting matrix to be the inverse of the noise matrix, Q. Thus,

$$S \equiv Q^{-1} \quad . \qquad (21)$$

Then

$$E\left[(\Delta T - \widetilde{\Delta T})(\Delta T - \widetilde{\Delta T})^T\right] = (f^TQ^{-1}f)^{-1} \quad , \qquad (22)$$

and the "best estimate" of the temperature profile is

$$\Delta T = (f^TQ^{-1}f)^{-1}\ f^TQ^{-1}\mathcal{J} \quad . \qquad (23)$$

Now in general the noise matrix nn^T is

$$nn^T = \begin{pmatrix} n_1 \\ n_2 \\ n_3 \\ \cdot \\ \cdot \\ \cdot \\ n_u \end{pmatrix} \quad (n_1 n_2 n_3 \ldots n_u) \quad = \begin{bmatrix} n_1^2 & n_1n_2 & \ldots\ldots \\ n_1n_2 & n_2^2 & \ldots. \\ \cdot & & \\ \cdot & & \\ \cdot & & \\ \cdot & & \\ \cdot & & \end{bmatrix} \quad . \qquad (24)$$

For uncorrelated noise, the expectation value of nn^T leaves only the diagonal elements, as

$$Q \equiv E(n\, n^T) = \begin{bmatrix} E(n_1^2) & 0 & 0 & \cdots \\ 0 & E(n_2^2) & & \\ 0 & & \ddots & \\ \vdots & & & \ddots \\ \vdots & & & \end{bmatrix} \quad . \tag{25}$$

We may further reasonably assume the noise to be distributed uniformally, so the diagonal terms all have the same value, so Q becomes proportional to the unit matrix,

$$Q = \sigma_n^2 \begin{bmatrix} 1 & 0 & 0 \\ 0 & 1 & 0 \\ . & . & . \end{bmatrix} \quad , \tag{26}$$

where σ_n^2 is the variance of the noise. This being the case we can then write our expressions for the estimation of the temperature variance as

$$E\left[(\Delta T - \widetilde{\Delta T})(\Delta T - \widetilde{\Delta T})^T\right] = \sigma_n^2 (f^T f)^{-1} \quad , \tag{27}$$

and the best estimate of the profile difference as

$$\widetilde{\Delta T} = (f^T f)^{-1}\, f^T \not{g} \quad . \tag{28}$$

The Recovery of Temperature Profiles from Interferograms.

The interferogram E(x) is essentially the Fourier cosine integral transform of the spectrum, I(σ), as (Vanasse et al., 1971)

$$E(x) = 2\varepsilon \int_0^{\infty} I(\sigma)\cos 2\pi\sigma x \, d\sigma \quad , \tag{29}$$

where ε is the efficiency of the interferometer.

In practice the spectrum is computed at 2N discrete points, as shown

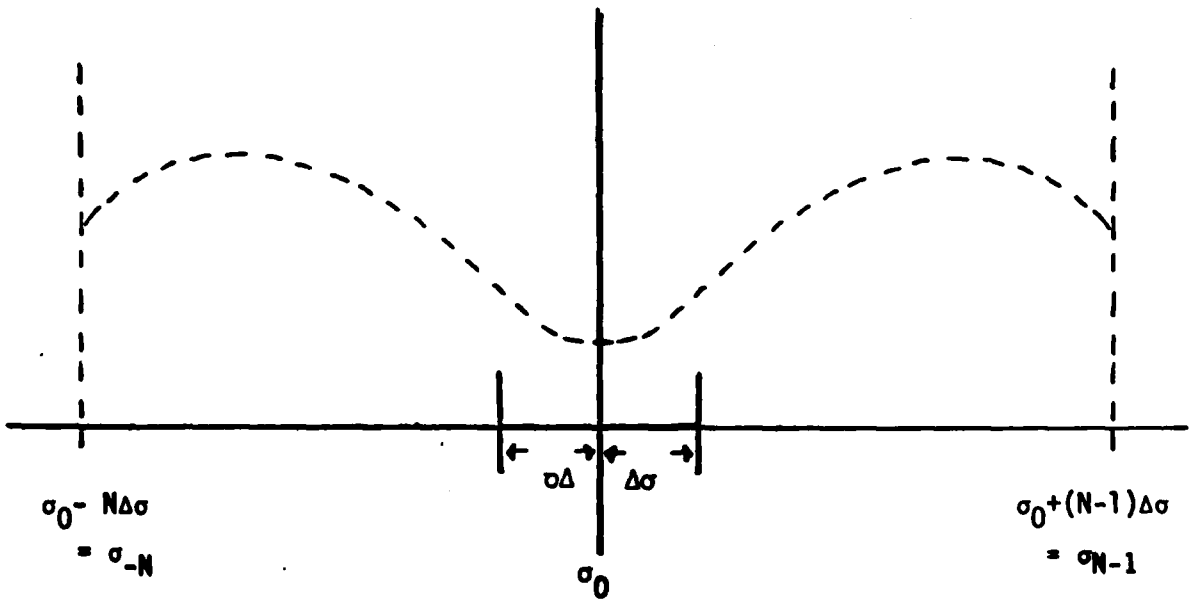

We assume that I(σ) is an even function around σ_0, $f(\sigma_0 + \sigma) = f(\sigma_0 - \sigma)$, and that it is periodic, $f(\sigma + N\Delta\sigma) = f(\sigma)$.

The integral is then related to the complex Fourier transform as, first

$$\int_{-\infty}^{\infty} I(\sigma) e^{-i2\pi\sigma x} d\sigma = 2 \int_{0}^{\infty} I(\sigma) \cos 2\pi\sigma x d\sigma \quad , \tag{30}$$

and then converted to a discrete sum by multiplying $I(\sigma)$ by the Dirac comb function and by band limiting by a rectangular function, as

$$\int_{-\infty}^{\infty} I(\sigma) \text{ comb} \left(\frac{\sigma - \sigma_0}{\Delta\sigma} \right) \text{Rect} \left[\frac{\sigma - (\sigma_0 - \frac{\Delta\sigma}{2})}{(2N-1)\Delta\sigma} \right] e^{-i2\pi\sigma x} \, d\sigma \quad , \tag{31}$$

where

$$\Delta\sigma = \frac{(\sigma_N - \sigma_0)}{N} \quad , \tag{32}$$

is the wave number sampling increment. Also note that the n^{th} sample point, σ_n, is expressed as

$$\sigma_n = \sigma_0 + n\Delta\sigma \quad , \tag{33}$$

and that the width of the rectangular function window is

$$2(\sigma_{N-1} - \sigma_{-N}) = (2N-1)\Delta\sigma \quad . \tag{34}$$

We may complete this as

$$E(x) = \Delta\sigma \int_{-\infty}^{+\infty} I(\sigma)\ \text{Rect}\left[\frac{\sigma - (\sigma_0 - \frac{\Delta\sigma}{2})}{(2N-1)\Delta\sigma}\right] \sum_{n=-\infty}^{+\infty} \delta(\sigma-\sigma_0-n\Delta\sigma)e^{-i2\pi\sigma x}\, d\sigma$$

$$= \Delta\sigma \sum_{n=-\infty}^{\infty} I(\sigma_0+n\Delta\sigma)\ \text{Rect}\left[\frac{n+\frac{1}{2}}{2N-1}\right]\ e^{-i2\pi x(\sigma_0+n\Delta\sigma)} \quad . \tag{35}$$

Since the definition for a rectangular function Rect x is

$$\text{Rect } x = \begin{cases} 1, & -\frac{1}{2} \leq x \leq \frac{1}{2} \quad , \\ 0, \text{ otherwise} & \quad , \end{cases} \tag{36}$$

then the sum is limited to $-N \leq n \leq N - 1$.

In addition the optical path difference, x, is also measured at discrete intervals, so $x_m \equiv m\Delta x$, m integer, so we may write

$$E(m\Delta x) = \Delta\sigma \sum_{-N}^{N-1} I(\sigma_0 + n\Delta\sigma)e^{-i2\pi m\Delta x(\sigma_0+n\Delta\sigma)}$$

$$= \Delta\sigma\ e^{-i2\pi\Delta x\sigma_0 m} \sum_{-N}^{N-1} I(\sigma_0 + n\Delta\sigma)e^{-i2\pi\Delta x\Delta\sigma mn} \quad . \tag{37}$$

For $I(\sigma_0 + n\Delta\sigma) = I(\sigma_0 - n\Delta\sigma)$, and $\Delta x\Delta\sigma = \frac{1}{2N}$ (making use of the sampling theorem $\Delta x = \frac{1}{2(\sigma_{N-1} - \sigma_0)}$) we have

$$E(m\Delta x) = \Delta\sigma e^{-i2\pi\Delta x\sigma_0 m}\left[\sum_{n=-N}^{-1} I(\sigma_0 + n\Delta\sigma)e^{-i2\pi\Delta x\Delta\sigma mn}\right.$$

$$\left. + I(\sigma_0) + \sum_{n=1}^{N-1} I(\sigma_0 + n\Delta\sigma)e^{-i2\pi\Delta x\Delta\sigma mn}\right]$$

$$= \Delta\sigma\, e^{-i2\pi\Delta x\sigma_0 m}\left[\sum_{n=1}^{N-1}\left(I(\sigma_0 - n\Delta\sigma)e^{+\frac{i\pi mn}{N}} + I(\sigma_0 + n\Delta\sigma)e^{-\frac{i\pi mn}{N}}\right)\right.$$

$$\left. + I(\sigma_0) + I(\sigma_0 + N\Delta\sigma)(-1)^m\right]$$

$$= \Delta\sigma\, e^{-i2\pi\Delta x\sigma_0 m}\left[I(\sigma_0) + I(\sigma_0 + N\Delta\sigma)(-1)^m + 2\sum_{n=1}^{N-1} I(\sigma_0 + n\Delta\sigma)\cos\frac{\pi mn}{N}\right]. \quad (38a)$$

In addition, by choosing $\Delta x\sigma_0 = h$, integer, $e^{-i2\pi\Delta x\sigma_0 m} = 1$, (which makes σ_0 an even multiple of the bandwidth $(\sigma_{N-1} - \sigma_0)$ or $\sigma_0 = 2h\,(\sigma_{N-1} - \sigma_0)$ and so we finally have for the discrete Fourier cosine transform

$$E(m\Delta x) \equiv \mathcal{F}_c\, I(\sigma) = \left[I(\sigma_0) + 2 \sum_{n}^{N-1} I(\sigma_0 + n\Delta\sigma) \cos \frac{\pi mn}{N} + I(\sigma_0 + N\Delta\sigma)\,(-1)^m \right] \Delta\sigma. \quad (38b)$$

Profile Recovery from Interferometer Data:

By applying the discrete Fourier cosine transform to the spectral space matrix equation (11), we have

$$\mathcal{F}_c \left[\mathcal{J}(\sigma) + n(\sigma) \right] = \mathcal{F}_c \left[f(\sigma) \right] \Delta T \quad . \quad (39)$$

We retain the linear nature of the analysis, since the two column matrices $\mathcal{J}(\sigma)$ and $n(\sigma)$ and the rectangular matrix $f(\sigma)$ transform directly, and gives

$$\mathcal{E}(x) + N(x) = F(x) \Delta T \quad . \quad (40)$$

Then by applying a similar analysis as before we have for the estimation of the temperature variance

$$E\left[(\Delta T - \Delta\tilde{T})(\Delta T - \Delta\tilde{T})^T \right] = \sigma_N^2 (F^T F)^{-1} \quad , \quad (41)$$

and the best estimate of the profile difference

$$\Delta\tilde{T} = (F^T F)^{-1} F^T \mathcal{E} \quad , \quad (42)$$

where σ_N^2 is the variance of the delay-space noise.

How Noise Transforms:

We use Parseval's theorem as

$$\int_0^\infty n^2(\sigma)d\sigma = \int_0^\infty N^2(x)dx \quad , \tag{43}$$

where N(x) is the Fourier cosine transform of n(σ). For the discrete, band limiting procedure previously applied to the Fourier cosine transform, we get

$$\frac{\Delta\sigma}{N}\left[n^2(\sigma_0) + 2\sum_{n=1}^{N-1} n^2(\sigma_0 + n\Delta\sigma) + n^2(\sigma_0+N\Delta\sigma)\right]$$

$$= \frac{\Delta x}{N}\left[N^2(0) + 2\sum_{n=1}^{N-1} N^2(n\Delta x) + (\sigma_0+N\Delta\sigma)\right] \tag{44}$$

These expressions are just the noise variances, and so we have

$$\Delta\sigma\ \sigma_n^2 = \Delta x\ \sigma_N^2 \quad . \tag{45}$$

This is used to compare the effect of equivalent noise in the two transform domains when we make our numerical analysis.

Some Numerical Relations and Parameters Used in Our analysis:

We present here some parameters used, along with pertinent algebraic relations. The number of points to model the spectral domain is $N = 4096$. The beginning wavenumber $\sigma_0 = 600\ cm^{-1}$ and the end wavenumber $\sigma_{N-1} = 750\ cm^{-1}$, giving a

$$\Delta\sigma = \frac{(\sigma_{N-1} - \sigma_0)}{N} = \frac{150}{4096} = .036621\ cm^{-1} \quad . \tag{46}$$

Since by the sampling theorem the maximum O.P.D. delay L is

$$\Delta\sigma = \frac{1}{2L}, \qquad \text{then} \qquad L = \frac{4096}{300} = 13.653\ cm \quad . \tag{47}$$

The delay space increment is

$$\Delta x = \frac{1}{2(\sigma_{N-1} - \sigma_0)} = .00333+\ cm \quad . \tag{48}$$

The relation between the noise variances may be written

$$\sigma_N^2 = \frac{2(\sigma_{N-1} - \sigma_0)^2}{N} \quad \sigma_n^2 \quad . \tag{49}$$

The computer program returns the Fourier cosine transform without the $\Delta\sigma$ term, thus we have

$$F(x) = \Delta\sigma\ F_{comp}(x) = \frac{(\sigma_{N-1} - \sigma_0)}{N} F_{comp}(x)$$

$$= .036621\ F_{comp}(x) \quad . \qquad (50)$$

Also, this is true for the noise variances, so

$$\sigma_N = \sqrt{\frac{2(\sigma_{N-1} - \sigma_0)^2}{N}} \qquad \sigma_n = 3.3146\ \sigma_n \quad . \qquad (51)$$

But

$$\sigma_{N_{comp}} = \sqrt{2N}\ \sigma_n = \sqrt{8192}\ \sigma_n$$

$$= 90.5097\ \sigma_n \quad . \qquad (52)$$

So, for example, r.m.s. noise of $\sigma_N = 10^{-8}$ watts/cm^2-sr is a spectral r.m.s. noise of $\frac{10^{-8}}{3.3146}\ \frac{\text{watts}}{\text{cm}^2\text{-sr-cm}^{-1}} = 3.0170 \times 10^{-9}$ watts/cm^2-sr-cm^{-1} and an r.m.s. noise returned by the computer of $(90.5097)(3.0170 \times 10^{-9}) = 2.7307 \times 10^{-7}$ watts/cm^2-sr.

Actual Profile Recovery for Simulated Spectral Models.

Table 3 shows the location for ten "optimal" filters suggested by Kaplan et al. (1977). These were applied to the spectral region, using each filter region as a sum over the window to give the equivalent response for ten separate radiometers, and then the spectral space covariance matrix $(f^T f)^{-1}$, Eq. (27) was found. The ten atmospheric layers captioned in Figures 1-10 were used for the spectral space filters. Table 15 shows the covariance error matrix, with the diagonal elements being the coefficients for the temperature variance to be multiplied by the variance of the noise present from detectors, etc. The r.m.s. noise temperature for the ten levels becomes

$$\widetilde{\Delta T} = (1.95 \times 10^{8})(3.017 \times 10^{-9}) = .587\ ^{o}K \qquad (53)$$

where we assume that $3.017 \times 10^{-9} \frac{\text{watts}}{cm^2\text{-}sr\text{-}cm^{-1}}$ r.m.s. noise is present.

A second analysis uses the full spectral information from 600-750 cm^{-1}, assuming fourteen atmospheric layers. The noise temperature error matrix $(f^T f)^{-1}$, is shown in Table 16 with an r.m.s. noise temperature of $.15^{o}K$, again assuming the same amount of noise as previously.

For the transform domain simulation, Fourier transforms of the separate and composite atmospheric layer spectra are performed and the error covariance matrix $(F^T F)^{-1}$ is constructed, using either the entire transform optical path difference interferogram (0-13.653 cm), or various partial interferograms, as displayed in Tables 4-14. Note that in comparing the two domains we use the equivalent amount of noise for each, and <u>are not</u> considering the obvious multiplex advantage in gain available from $\sqrt{\frac{\sigma_{max} - \sigma_{min}}{\Delta\sigma}}$, by observing all elements at the same time (as with an interferometer versus a grating

spectrometer). This is done to emphasize the information content of the two domains.

Gain

Figure 41 shows the r.m.s. noise temperature given by the matrix $(F^TF)^{-1}$ for various partial interferograms with 10^{-8} watts/cm^2-sr noise. The most promising region appears to be the continuous interferogram (0-2.167 cm), which has a r.m.s. value of .276 ^oK for 650 points of data. If we were to spend an equal amount of time measuring the partial interferograms from either (.500 - .833 cm) with an r.m.s. noise temperature of 1.011 ^oK for 100 points, or the region (1.167 - 1.500 cm) with an r.m.s. noise temperature of .969^oK for 100 points, we would expect the r.m.s. noise to decrease by the ratio $\sqrt{100/650}$ = 1/2.550 , and thus we could expect to determine the temperature for the (1.167 - 1.500 cm) region to within $\frac{.969}{2.550}$ = .380^oK, which is still not as good as the .276^oK r.m.s. for the 0-2.167 cm region. Figure 42 shows the comparison for the (0-2.167 cm) region with the (.500 - .833 cm) region using equal measuring times. Thus, under the limited cases studied and subject to the model accuracy we find no gain advantage for using partial interferograms in the 15 μm region.

REFERENCES

Abbas, M.M., Shapiro, G.L., and Alvarez, J.M. (1981) "Inversion Techniques for IR Heterodyne Sounding of Stratospheric Constituents from Space Platforms" Appl. Opt. Vol. 20, No. 21, 3755.

Kaplan, L.D., Chahine, M.T., Susskind, J., and Searl, J.E., (1977) "Spectral Bandpasses for a High Precision Satellite Sounder", Appl. Opt. Vol. 16, No. 2, 322.

Kyle, T.G., "Temperature Soundings with Partially Scanned Interferograms" (1977), Appl. Opt. Vol 16, Nov. 2, 326.

McClatchey, R.A., Benedict, W.S., Clough, S.A., Burch, D.E., Calfee, R.F., Fox, K., Rothman, L.S., and Garing, J.S., (1973) "AFCRL Atmospheric Absorption Line Parameters Compilation" Air Force Cambridge Research Laboratories, Environmental Research Papers, No. 434, AFCRL-TR-73-0096 AD762904.

Niple, E., (1980), "Nonlinear Least Squares Analysis of Atmospheric Absorption Spectra", Appl. Opt. Vol. 19, Nov. 20, 3481.

Perkin-Elmer report, (1982) "Feasibility of a Fourier Transform Spectrumeter for the Advanced Moisture and Temperature Sounder", Final Report, Perkin-Elmer Report No. 15407.

Rothman, L.S., and Young, L.D.G., (1981), "Infrared Energy Levels and Intensities of Carbon Dioxide-II", J. Quant. Spectrosc. Radiat. Transfer, Vol. 25, 505.

Santa Barbara Research Center Report (1981), "A Design Feasibility Study for the High-Resolution Interferometer Sounder (HIS).

Smith, W.L., Howell, H.B., and Woolf, H.M., "The Use of Interferometric Radiance Measurements for Sounding the Atmosphere", J. Atm. Sci., Vol. 36, 566 (1979).

Valley, S.L., Ed., "U.S. Standard Atmosphere Supplements, 1966" compiled in "Handbook of Geophysics and Space Environment", AFCRL, Bedford, Mass.

Vanasse, G.A., Stair, A.T., Jr. and Baker, D.J., editors, (1971), "Aspen International Conference on Fourier Spectroscopy, 1970", Air Force Cambridge Research Laboratories, Bedford, Mass., Special Report No. 114 AFCRL-71-0019, AD 724100.

Weinreb, M.P., and Crosby, D.S., (1972) "Optimization of Spectral Intervals for Remote Sensing of Atmospheric Temperature Profiles" Remote Sensing of Environment 2, 193-201.

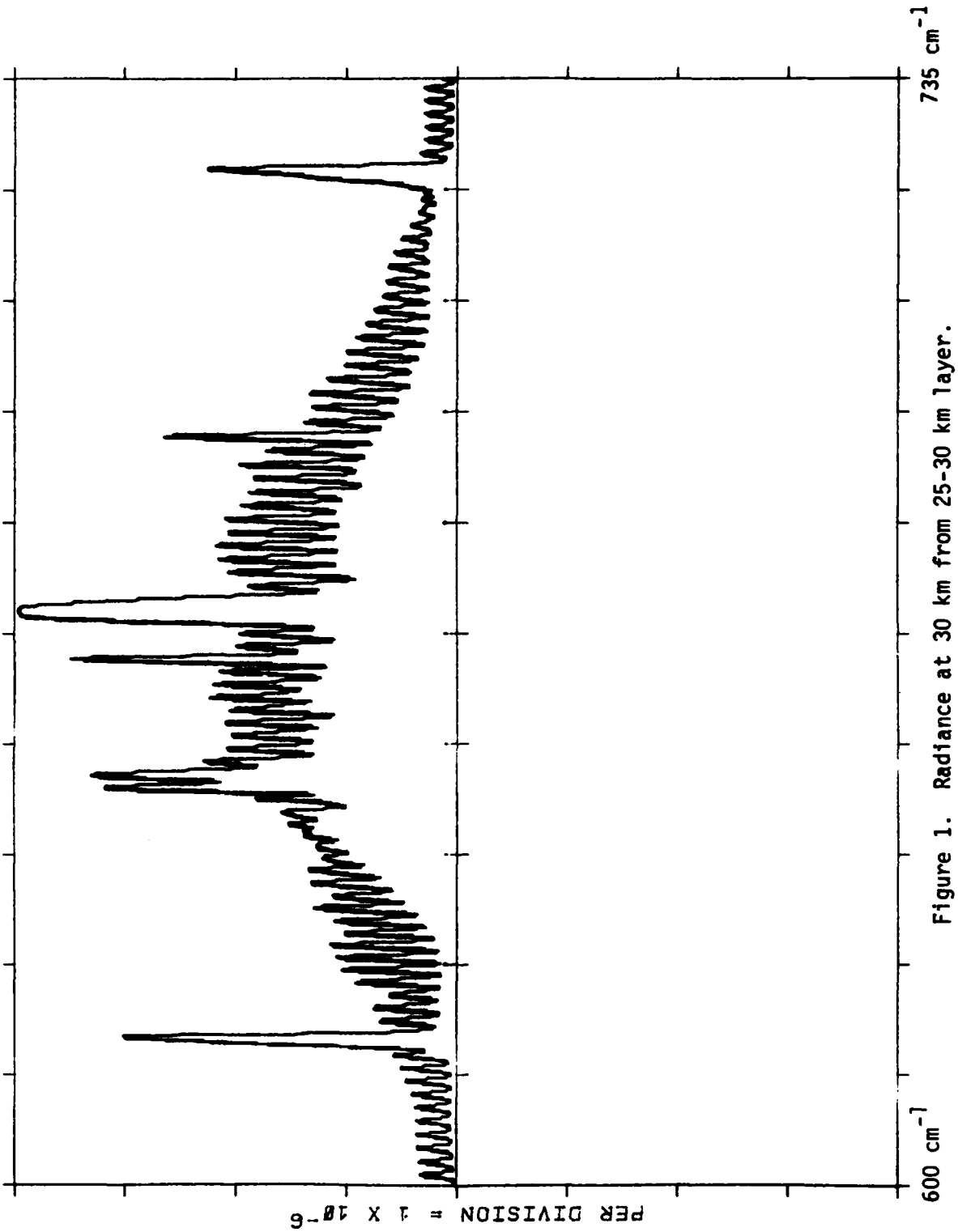

Figure 1. Radiance at 30 km from 25-30 km layer.

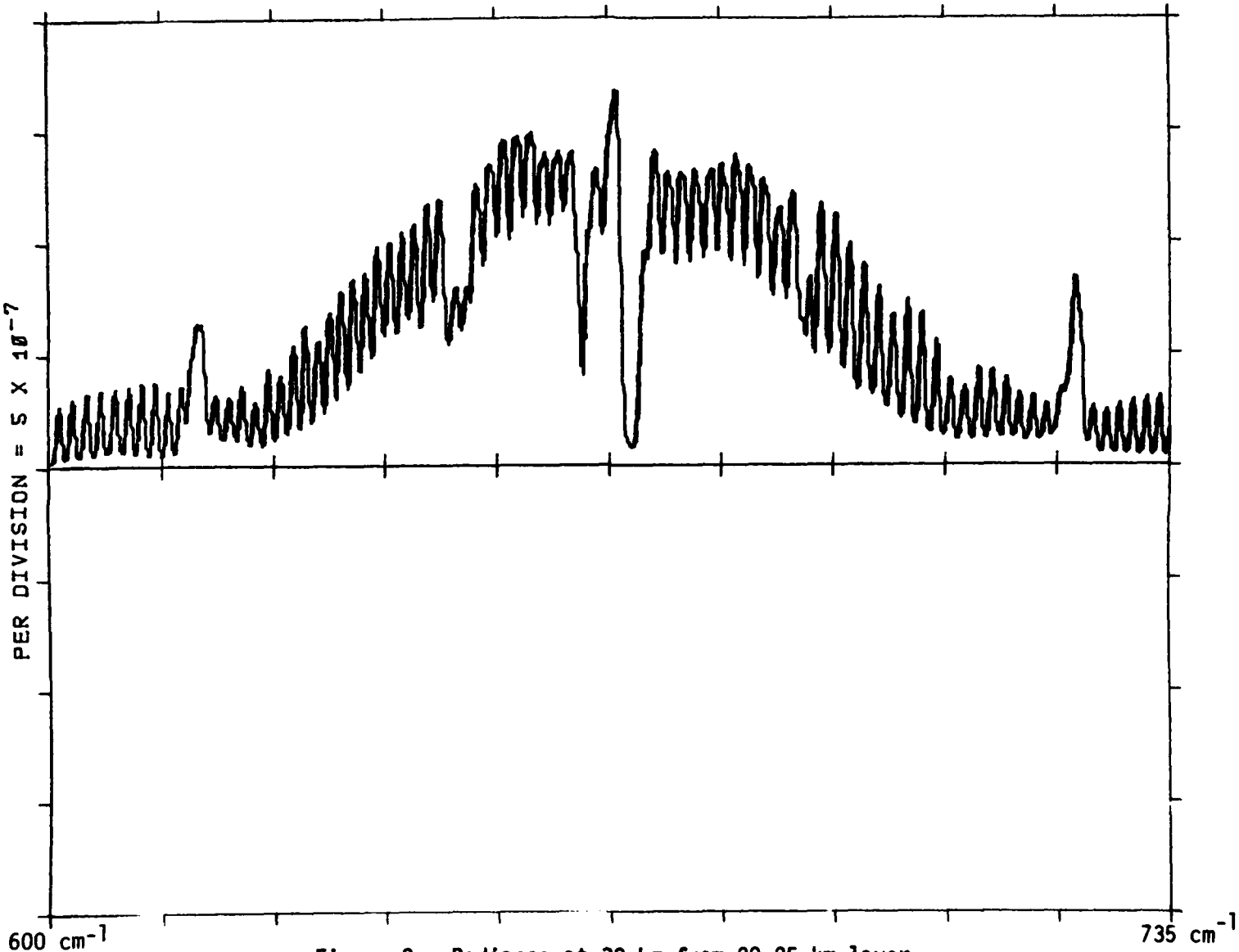

Figure 2. Radiance at 30 km from 20-25 km layer.

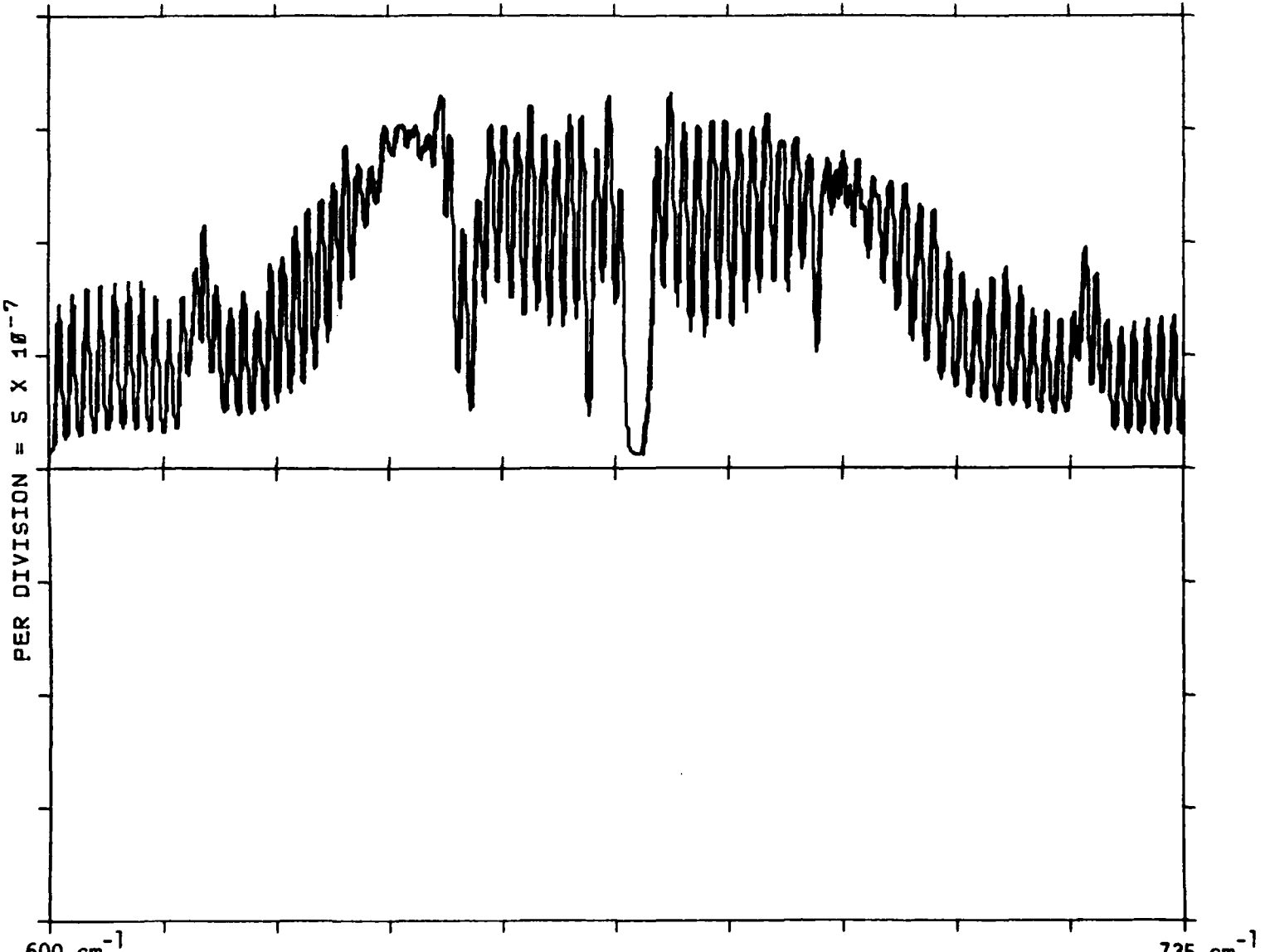

Figure 3. Radiance at 30 km from 15-20 km layer.

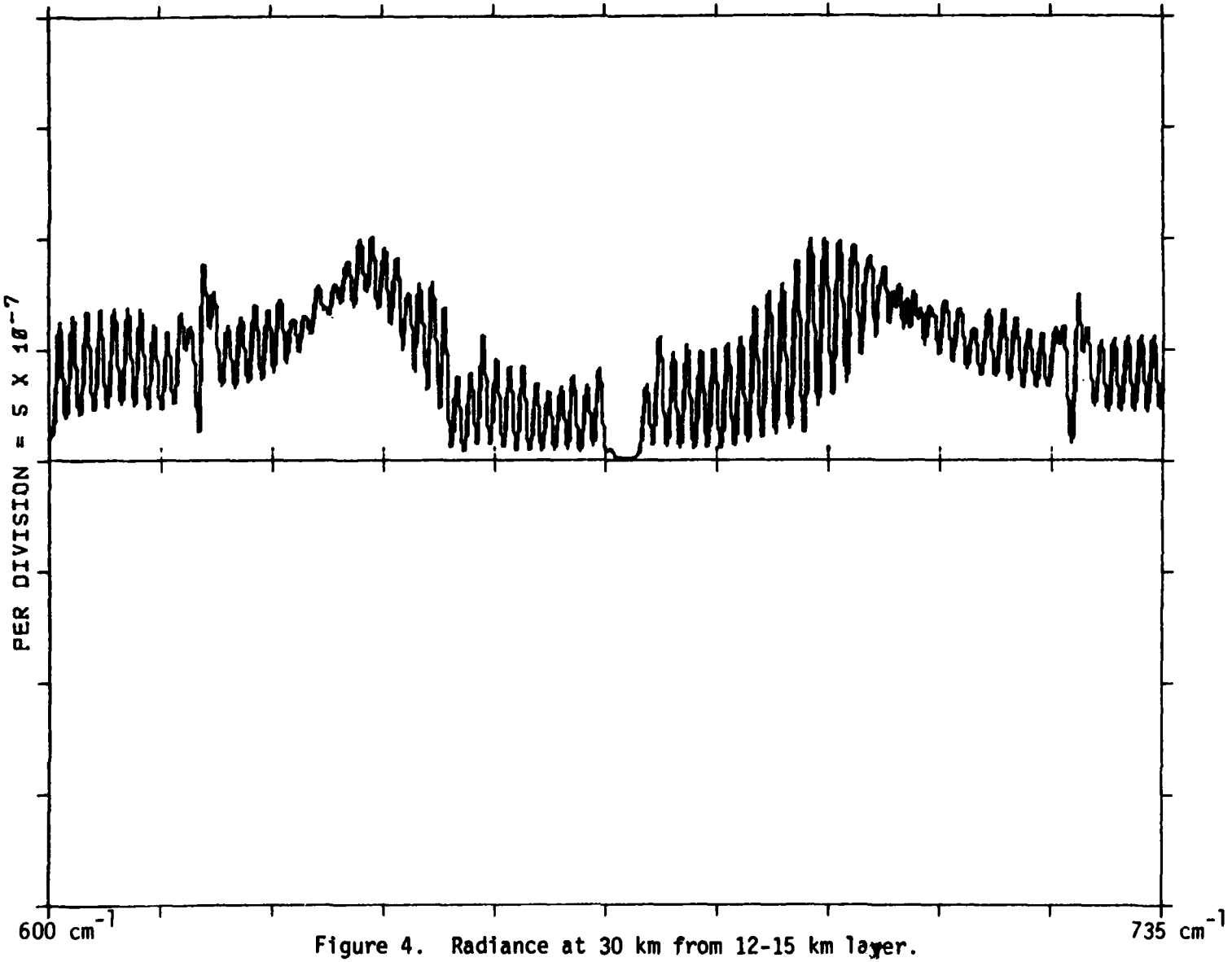

Figure 4. Radiance at 30 km from 12-15 km layer.

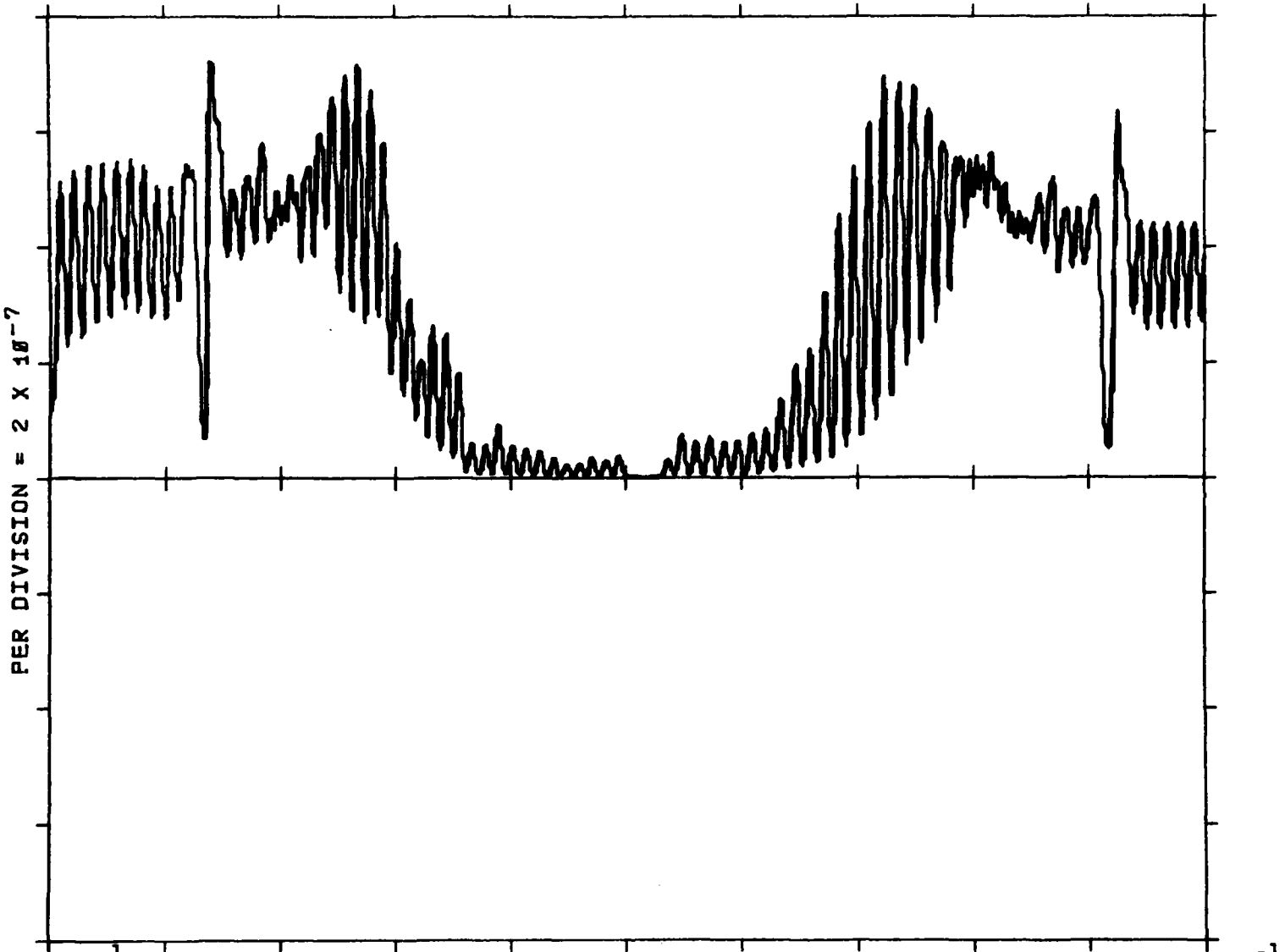

Figure 5. Radiance at 30 km from 10-12 km layer.

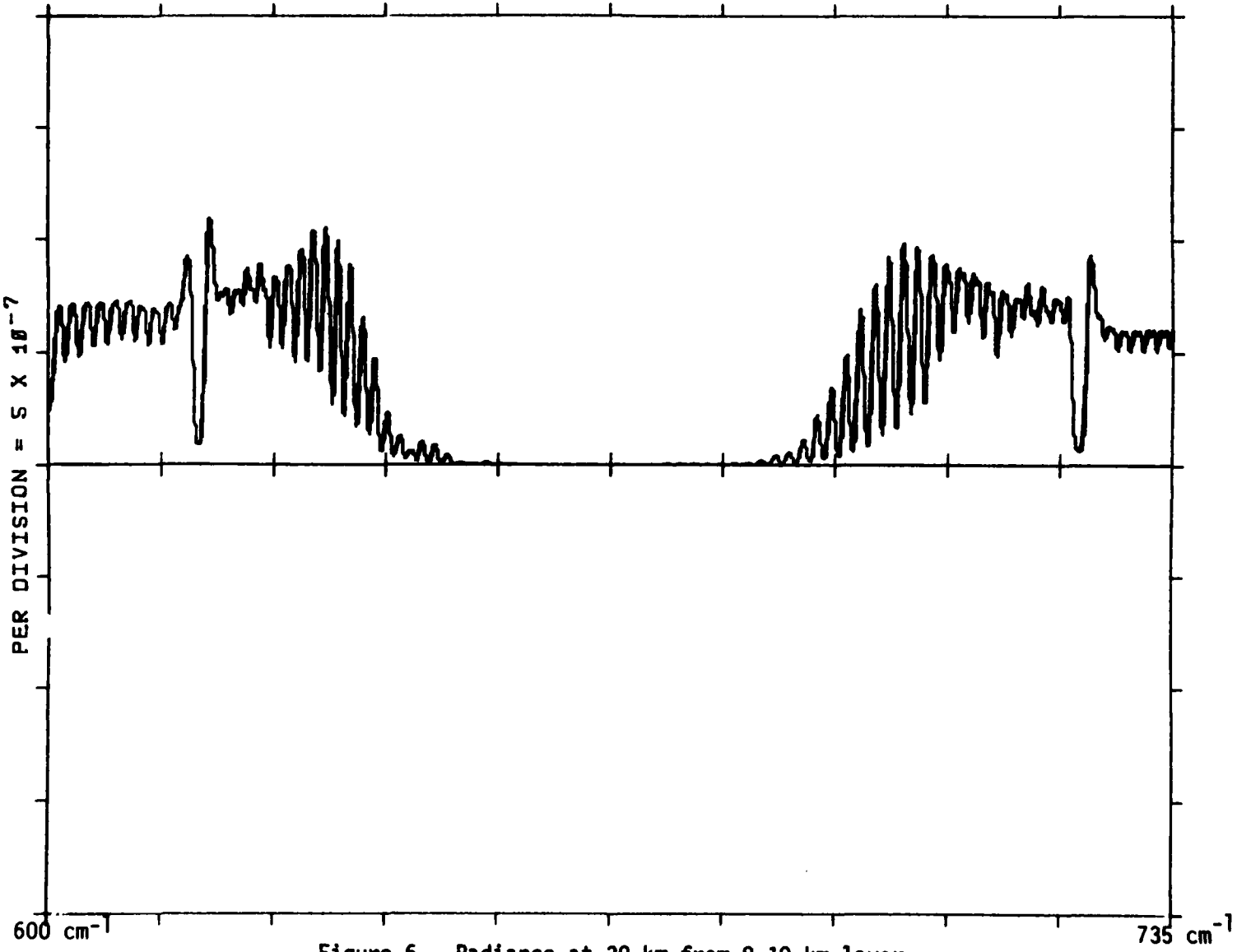

Figure 6. Radiance at 30 km from 8-10 km layer.

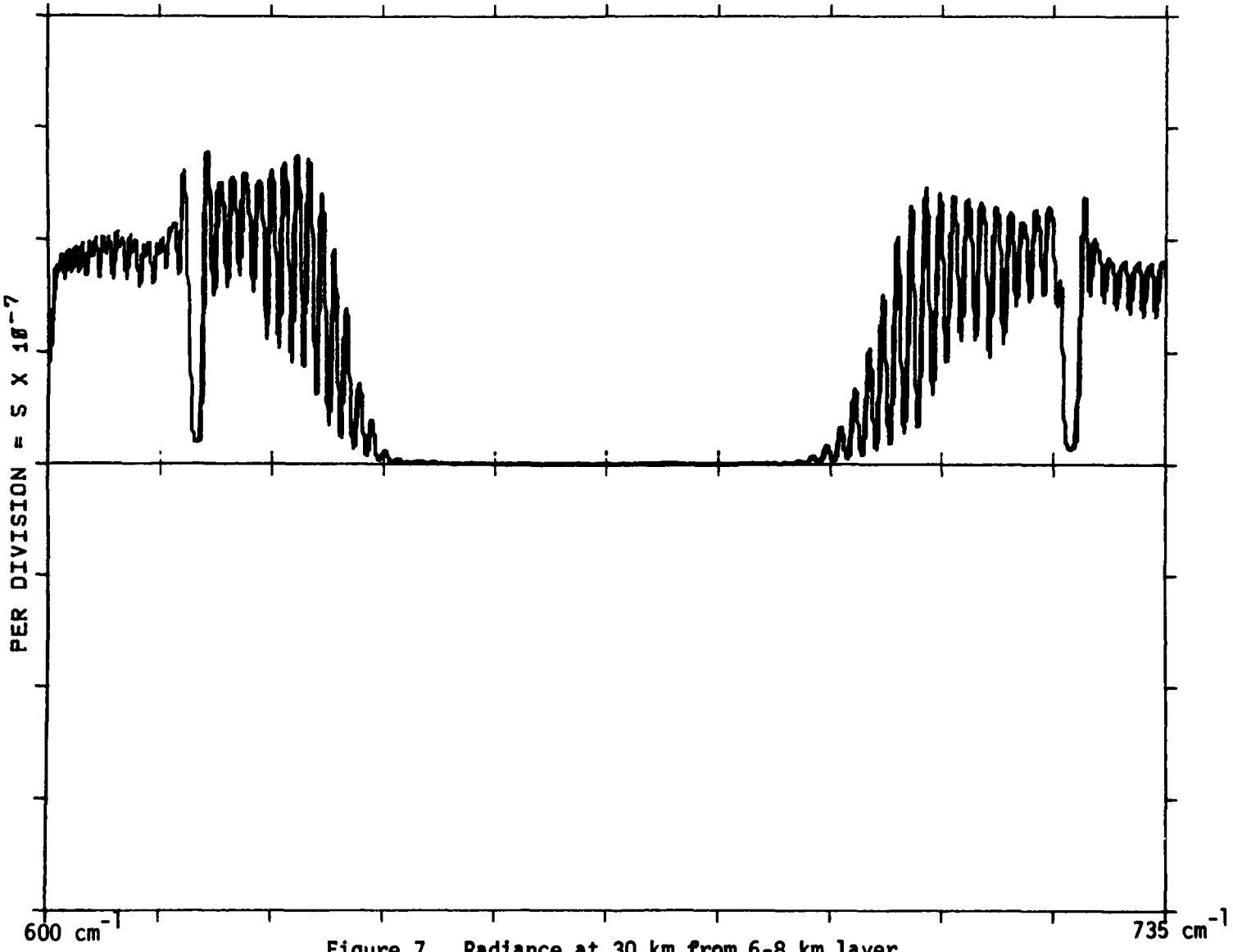

Figure 7. Radiance at 30 km from 6-8 km layer.

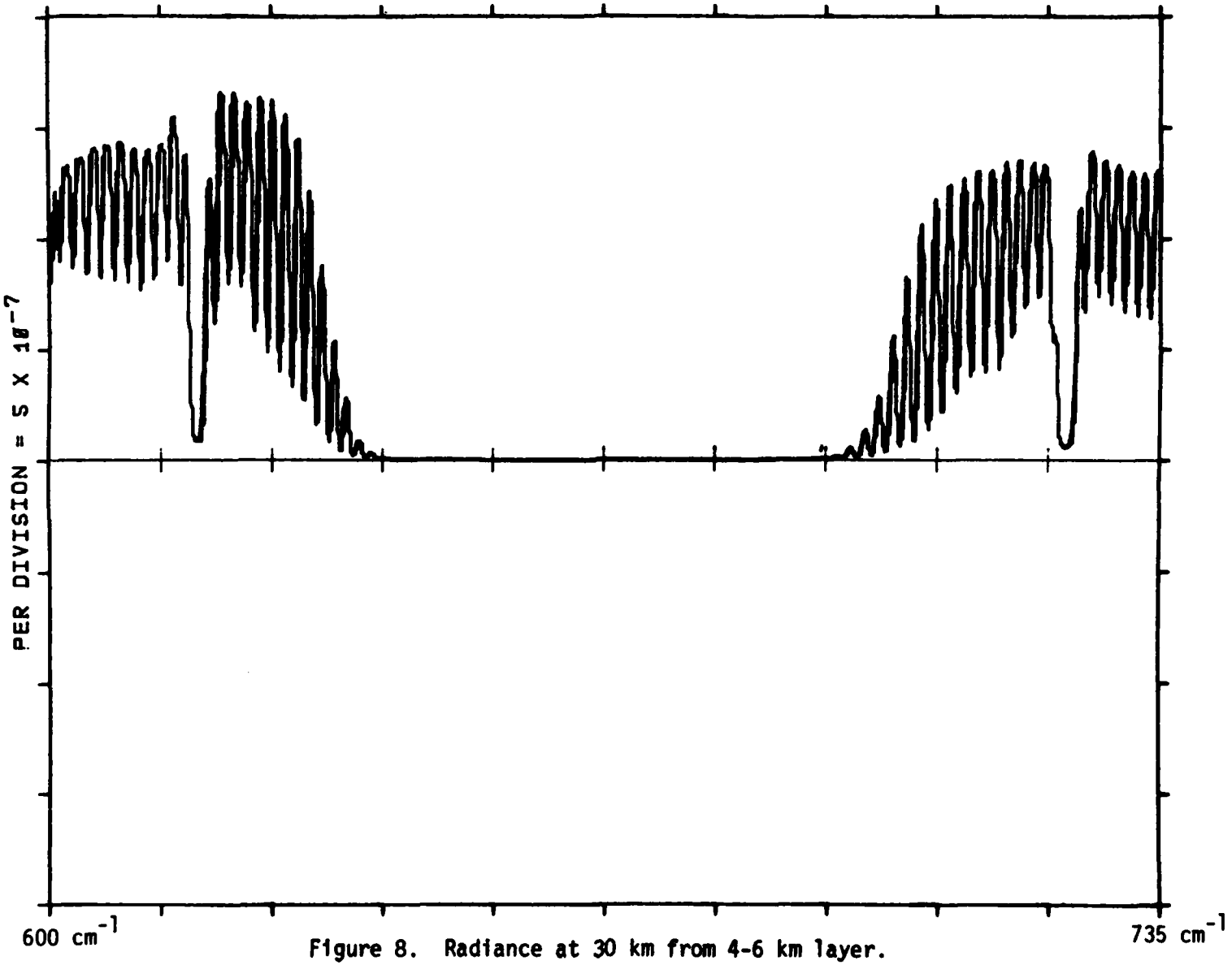

Figure 8. Radiance at 30 km from 4-6 km layer.

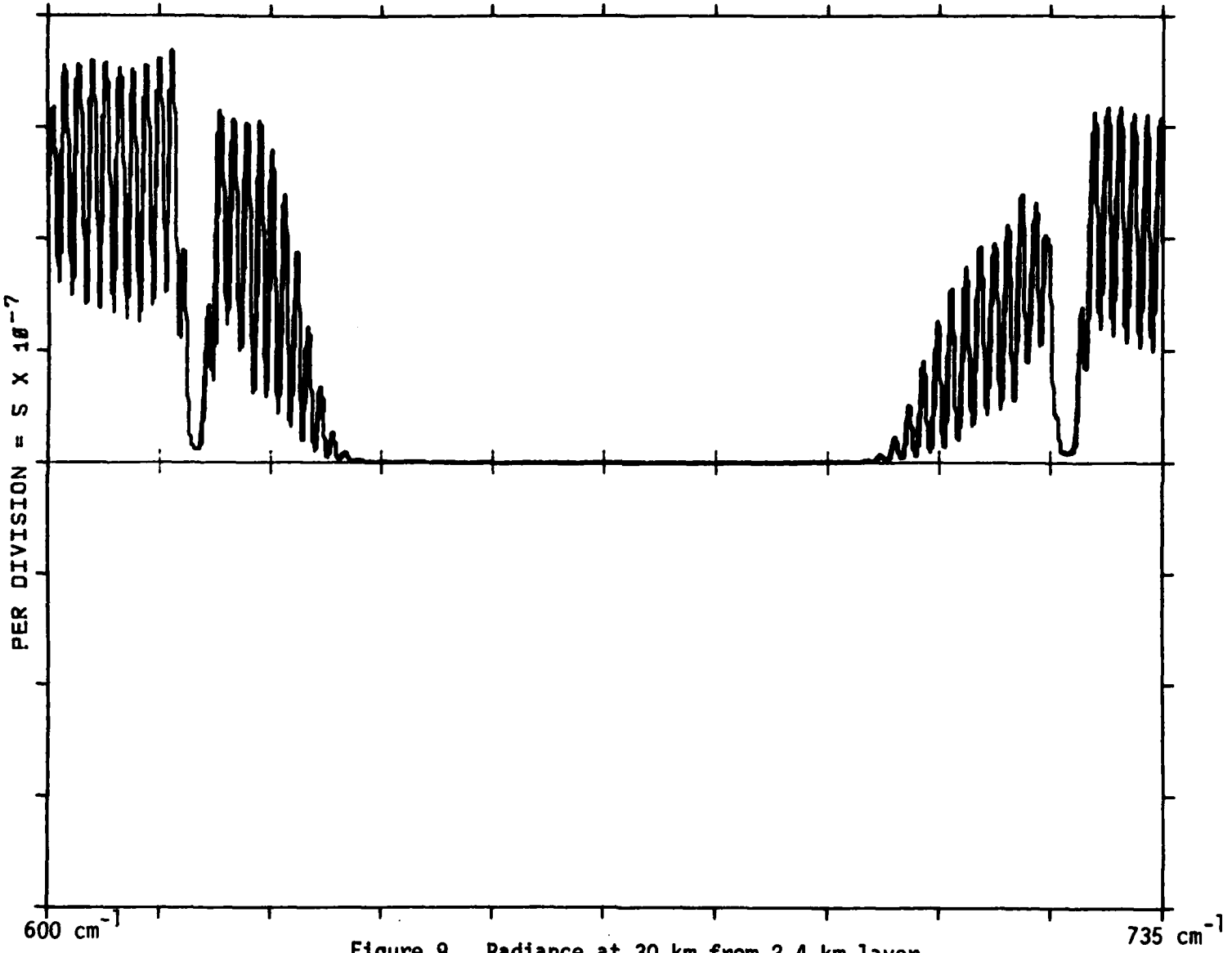

Figure 9. Radiance at 30 km from 2-4 km layer.

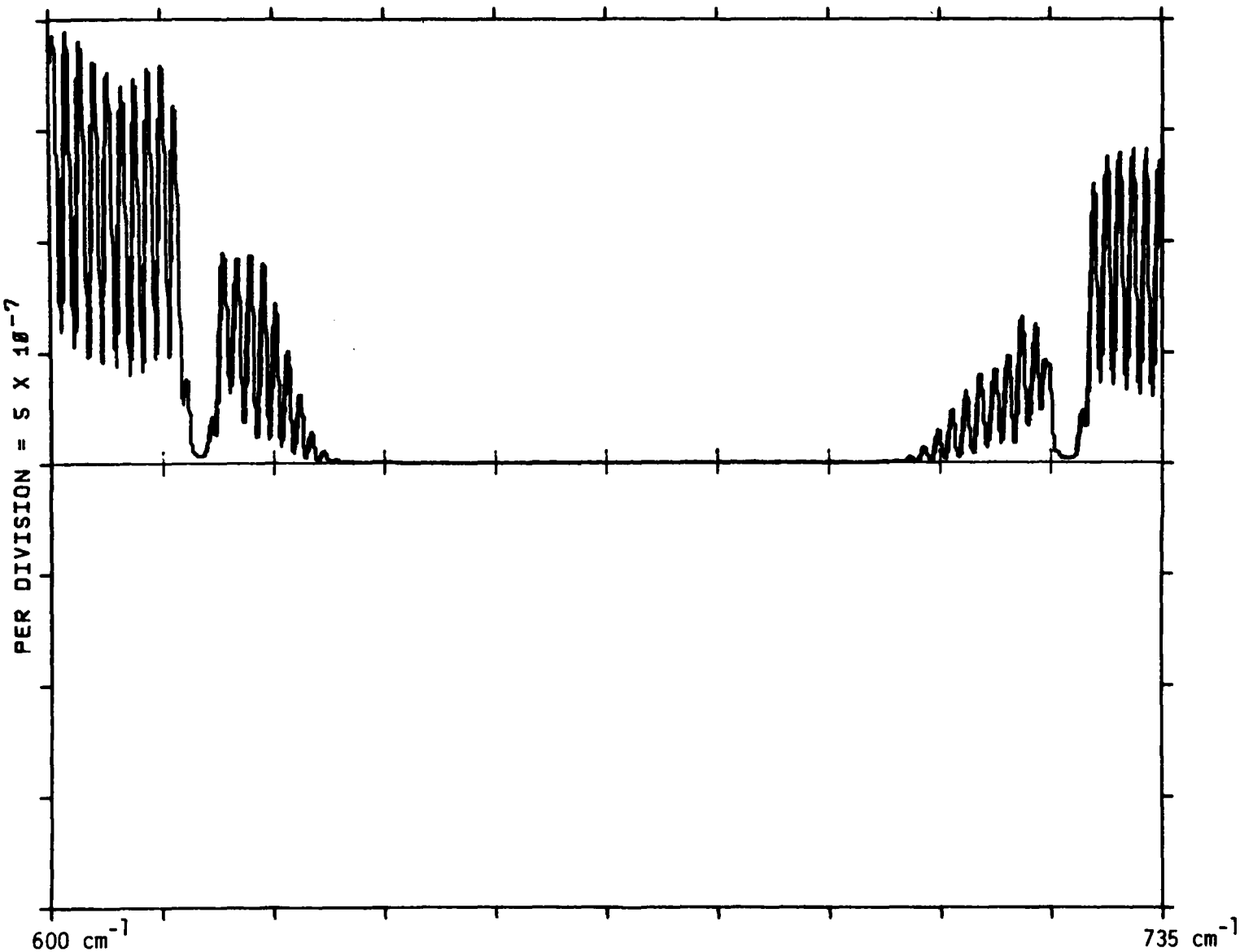

Figure 10. Radiance at 30 km from 0-2 km layer.

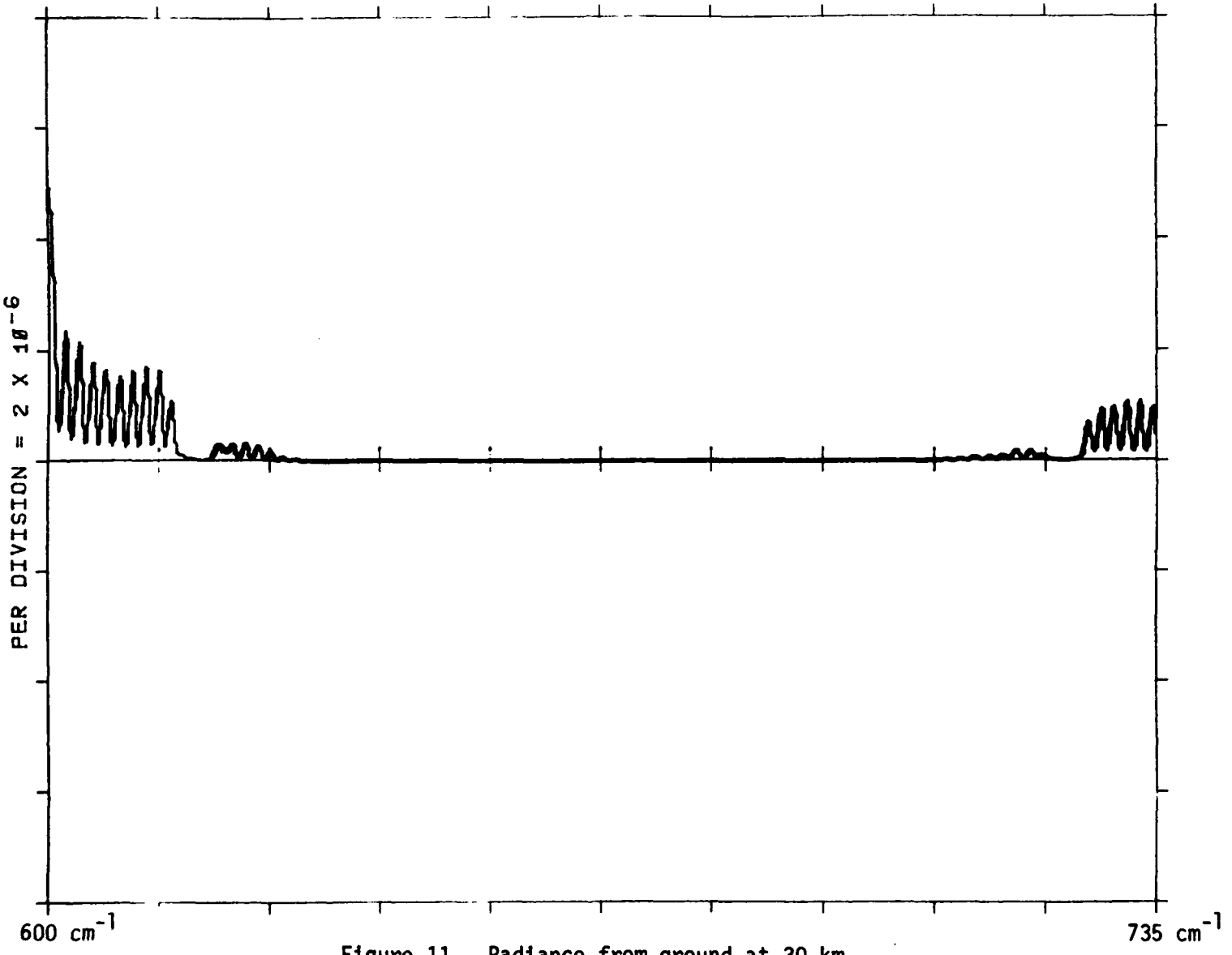

Figure 11. Radiance from ground at 30 km.

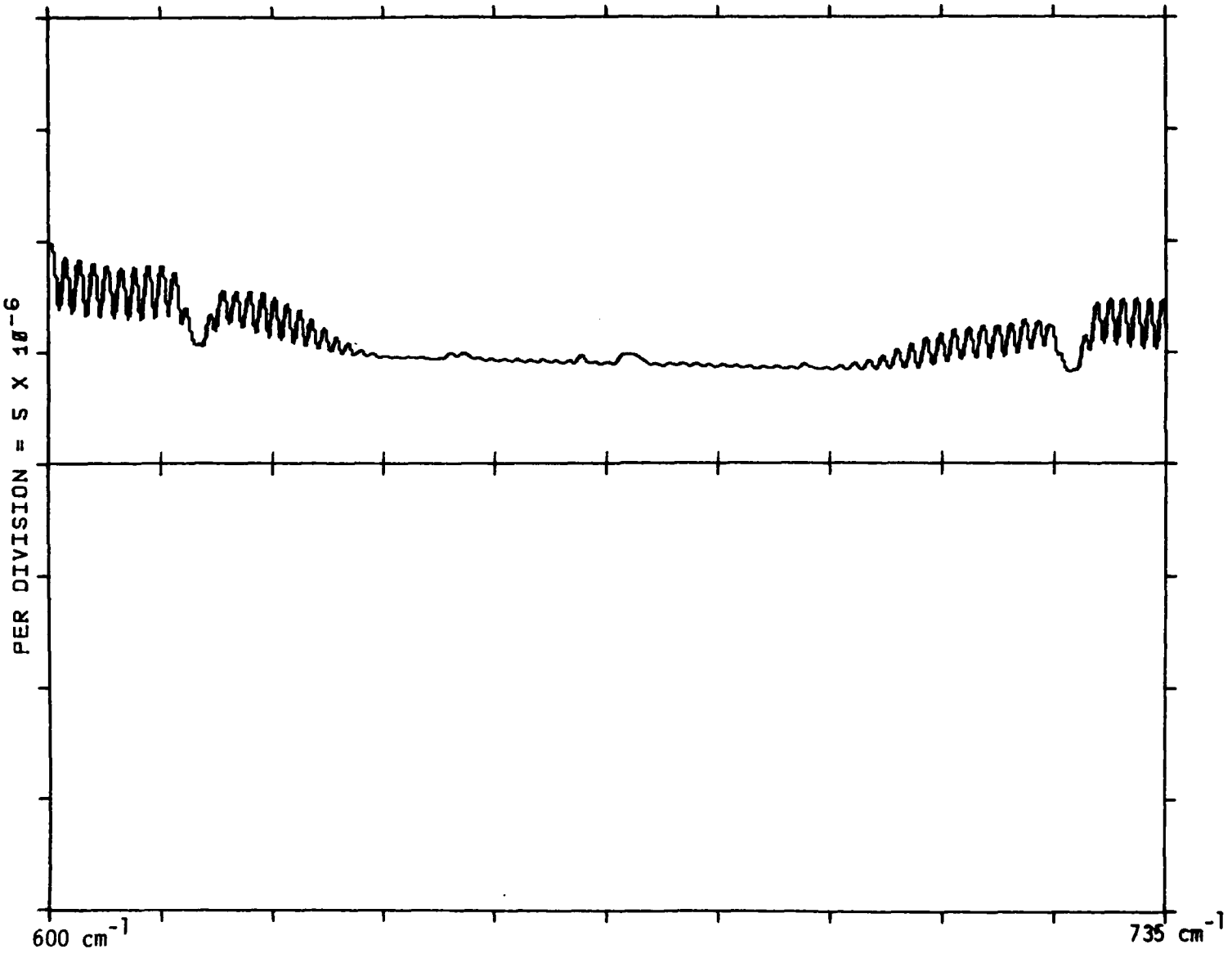

Figure 12. Total Radiance at 30 km (Down Looking)

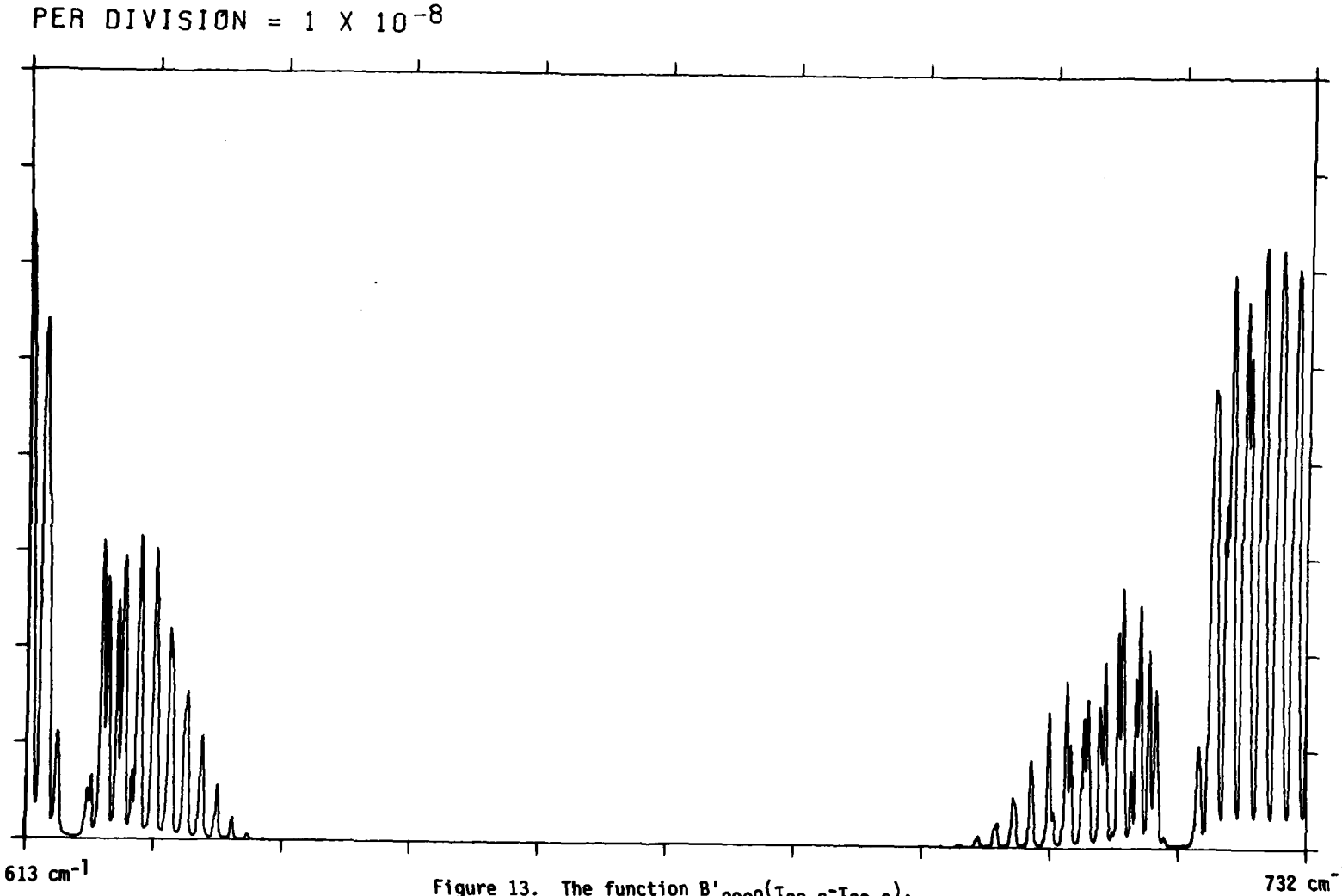

Figure 13. The function $B'_{290}(\tau_{30-2}-\tau_{30-0})$.

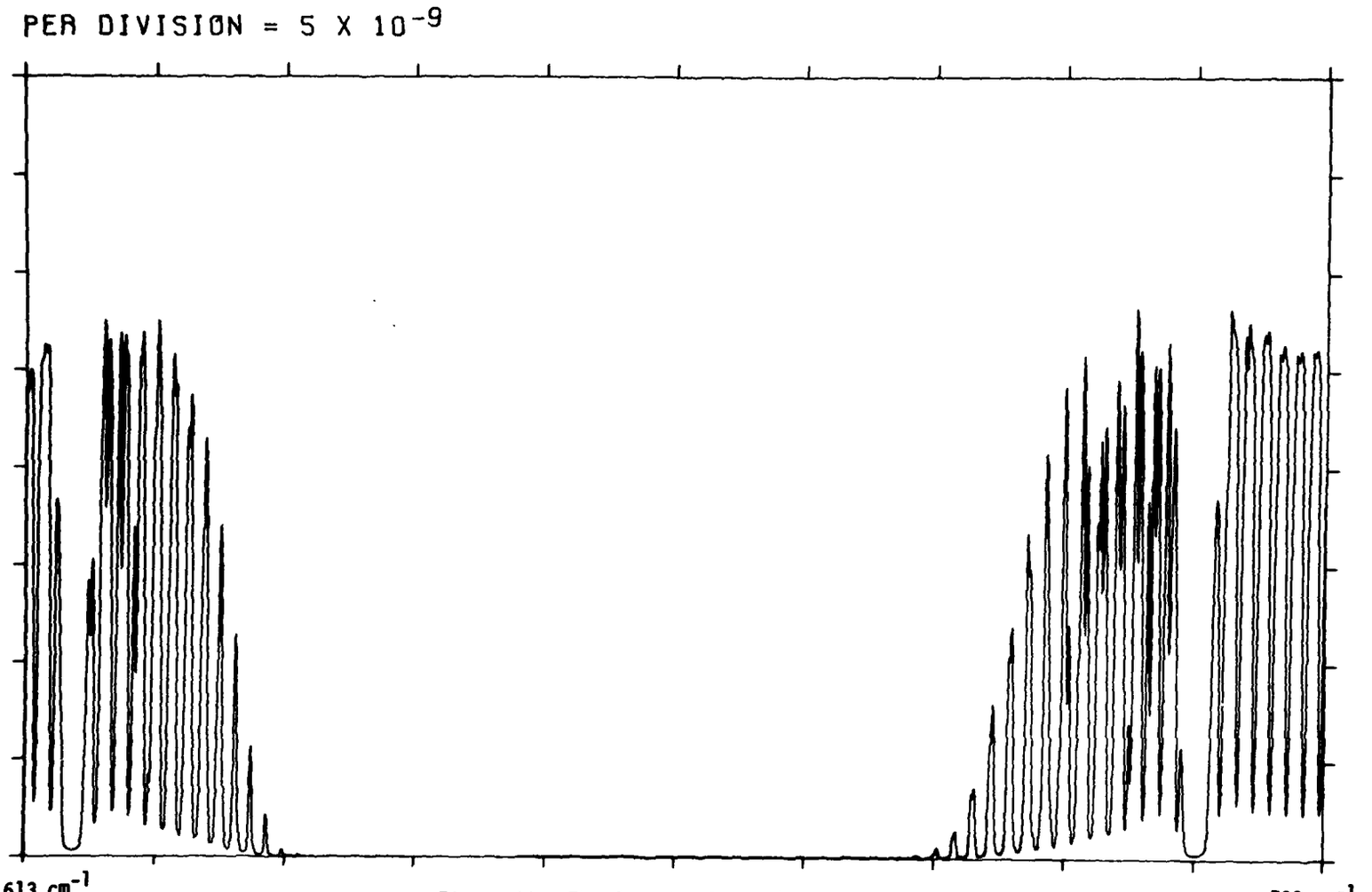

Figure 14. The function $B'_{279^0}(\tau_{30-4} - \tau_{30-2})$.

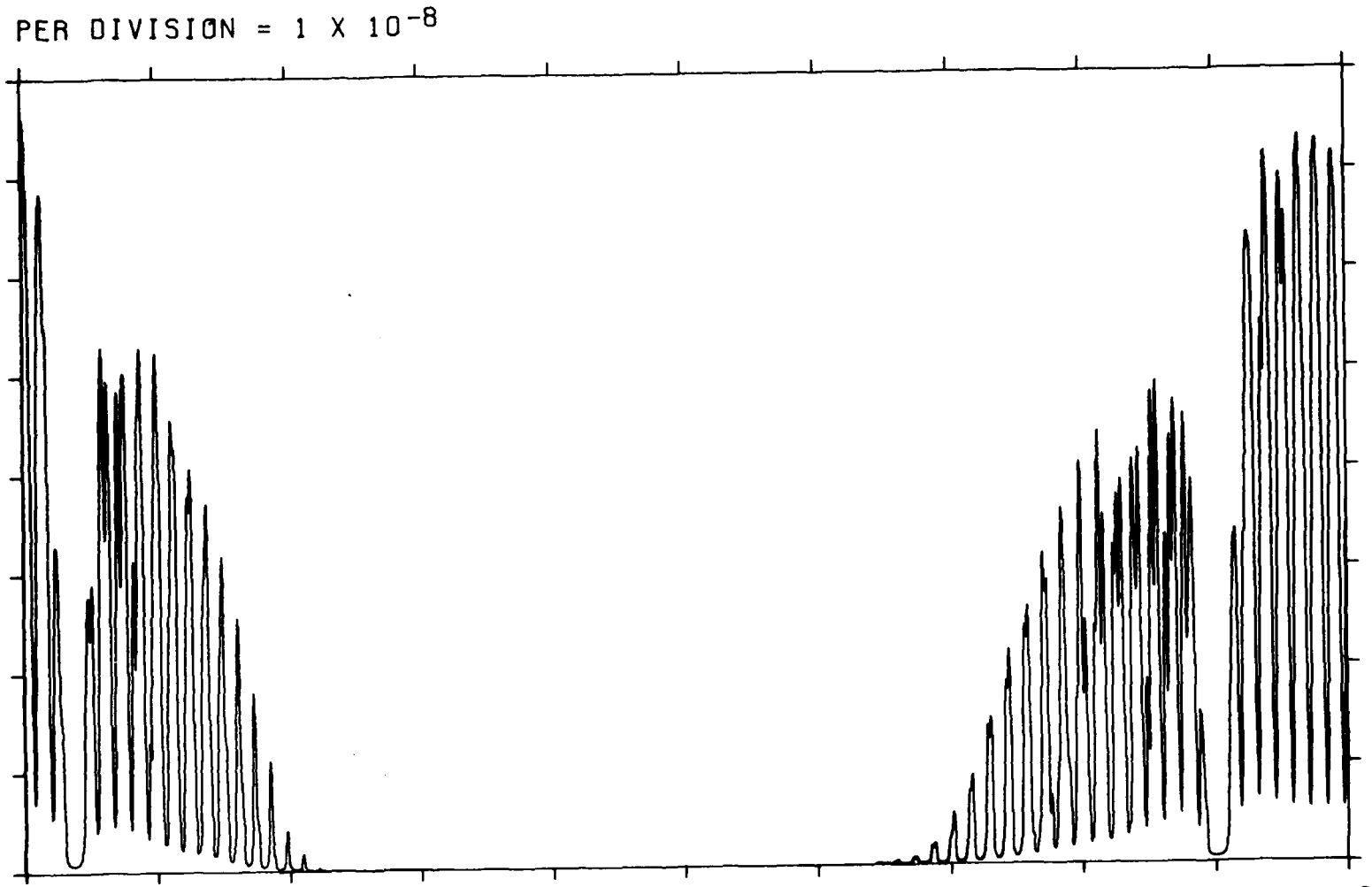

Figure 15. The function $B'_{267^0}(\tau_{30-6} - \tau_{30-4})$.

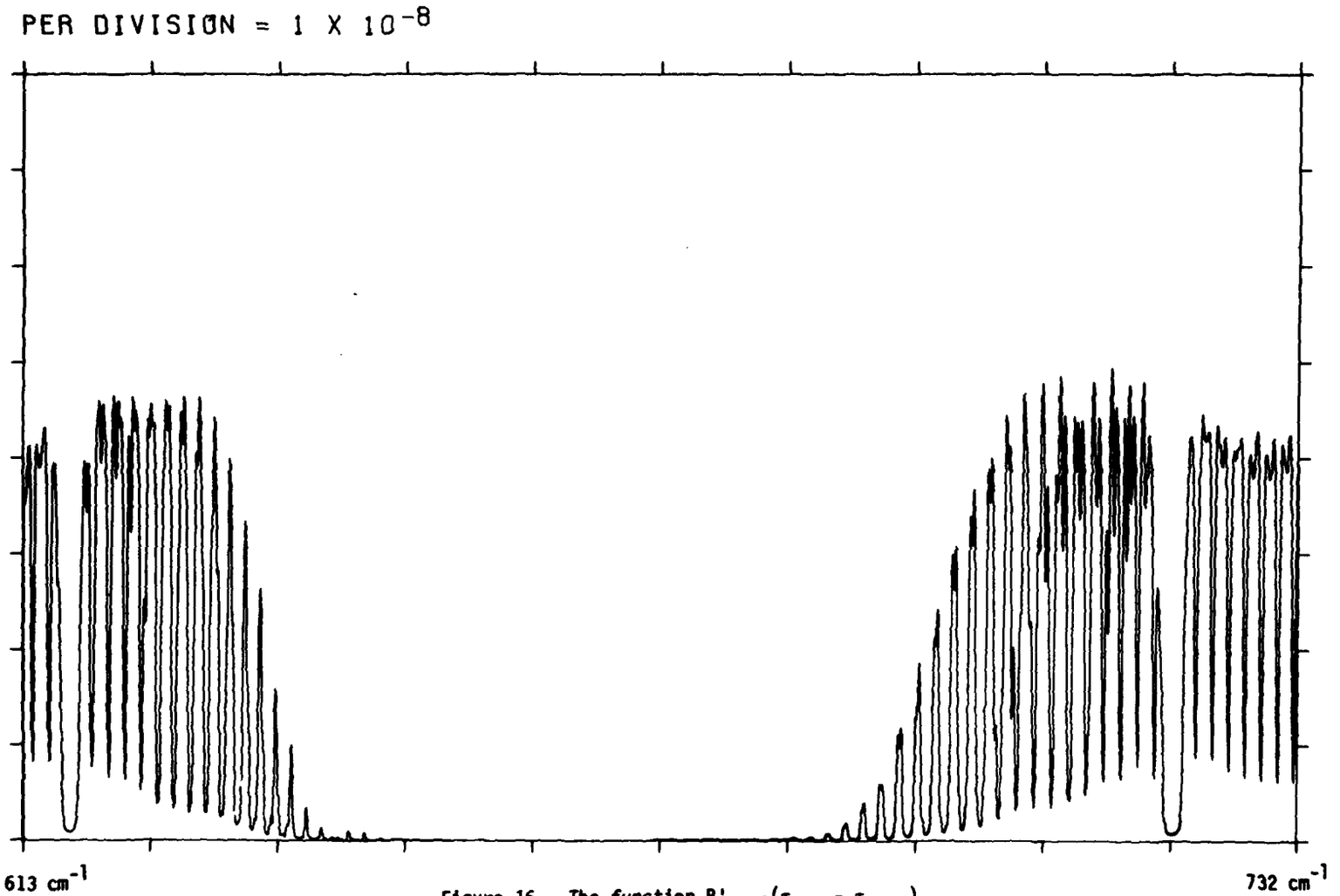

Figure 16. The function $B'_{265}o(\tau_{30-8} - \tau_{30-6})$.

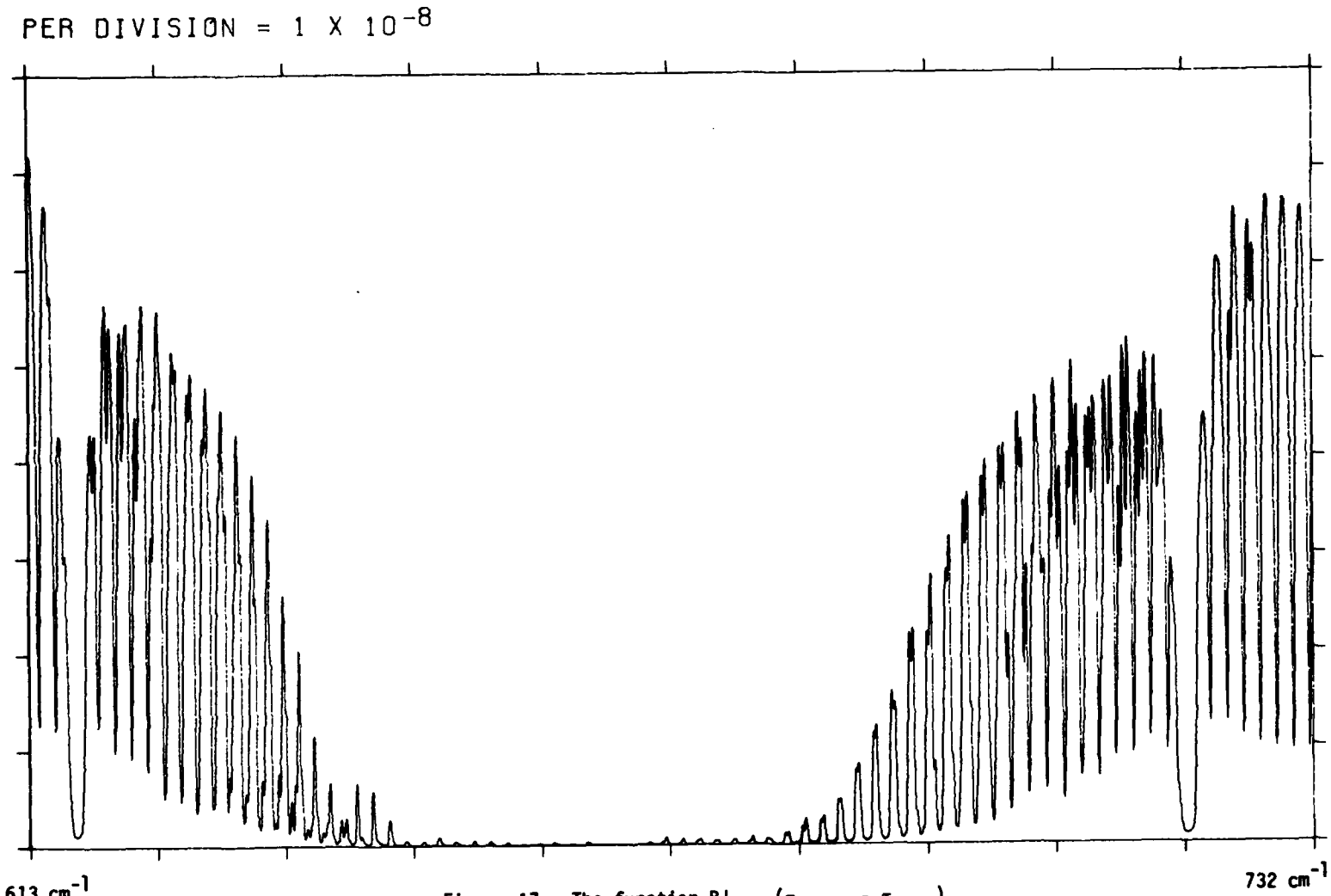

Figure 17. The function $B'_{242o}(\tau_{30\text{-}10} - \tau_{30\text{-}8})$.

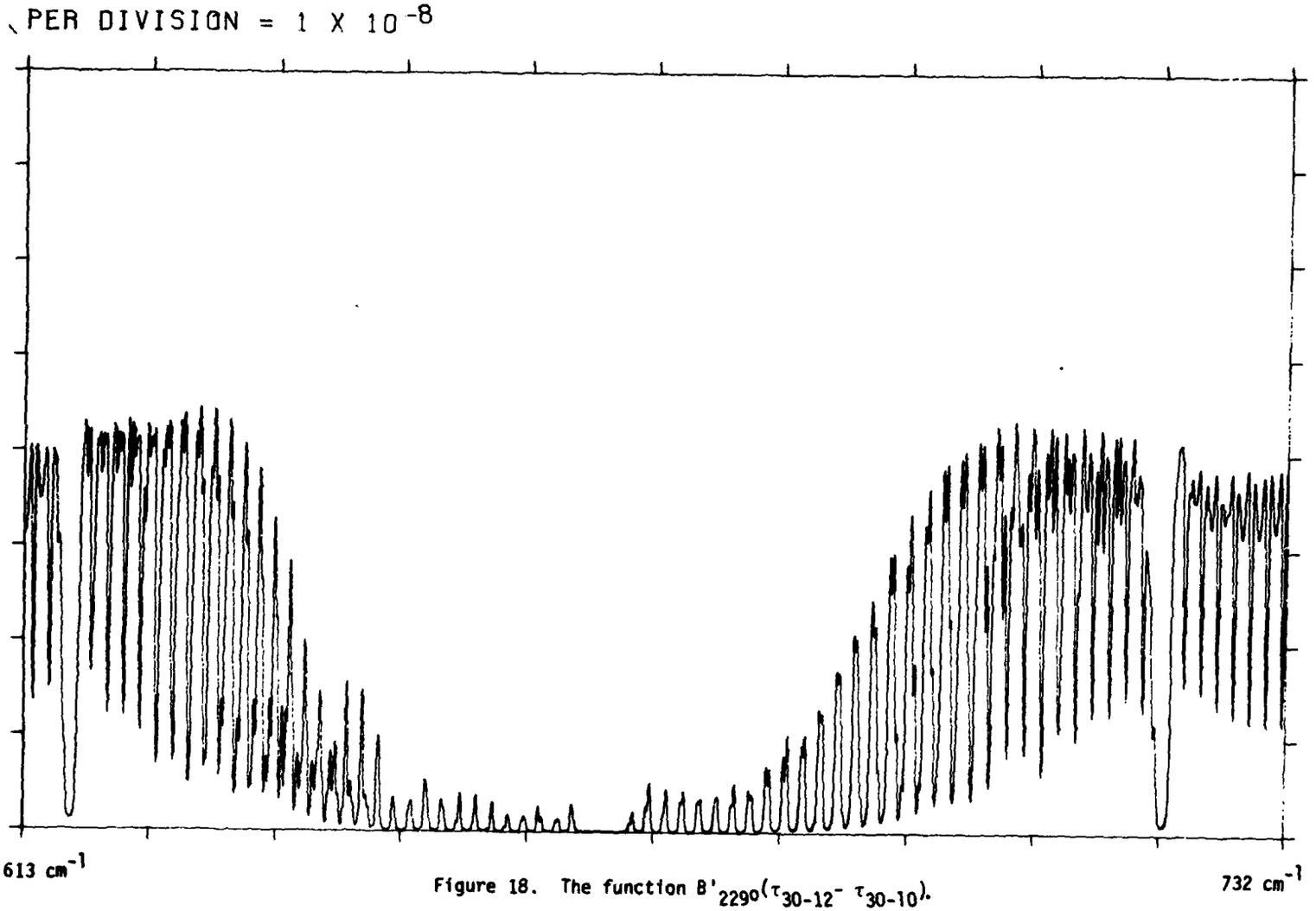

Figure 18. The function $B'_{2290}(\tau_{30-12} - \tau_{30-10})$.

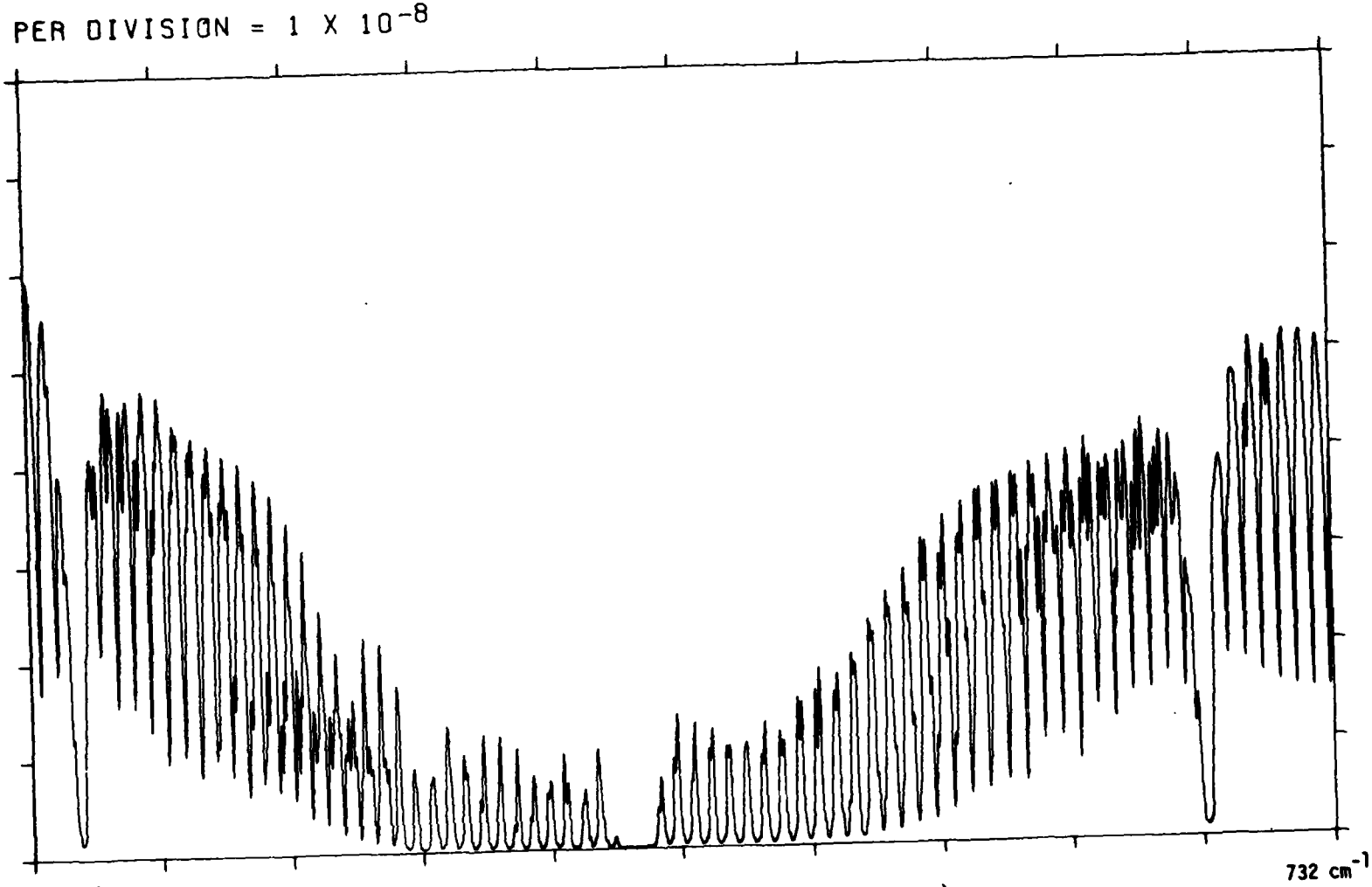

Figure 19. The function $B'_{216}o(\tau_{30-14} - \tau_{30-12})$.

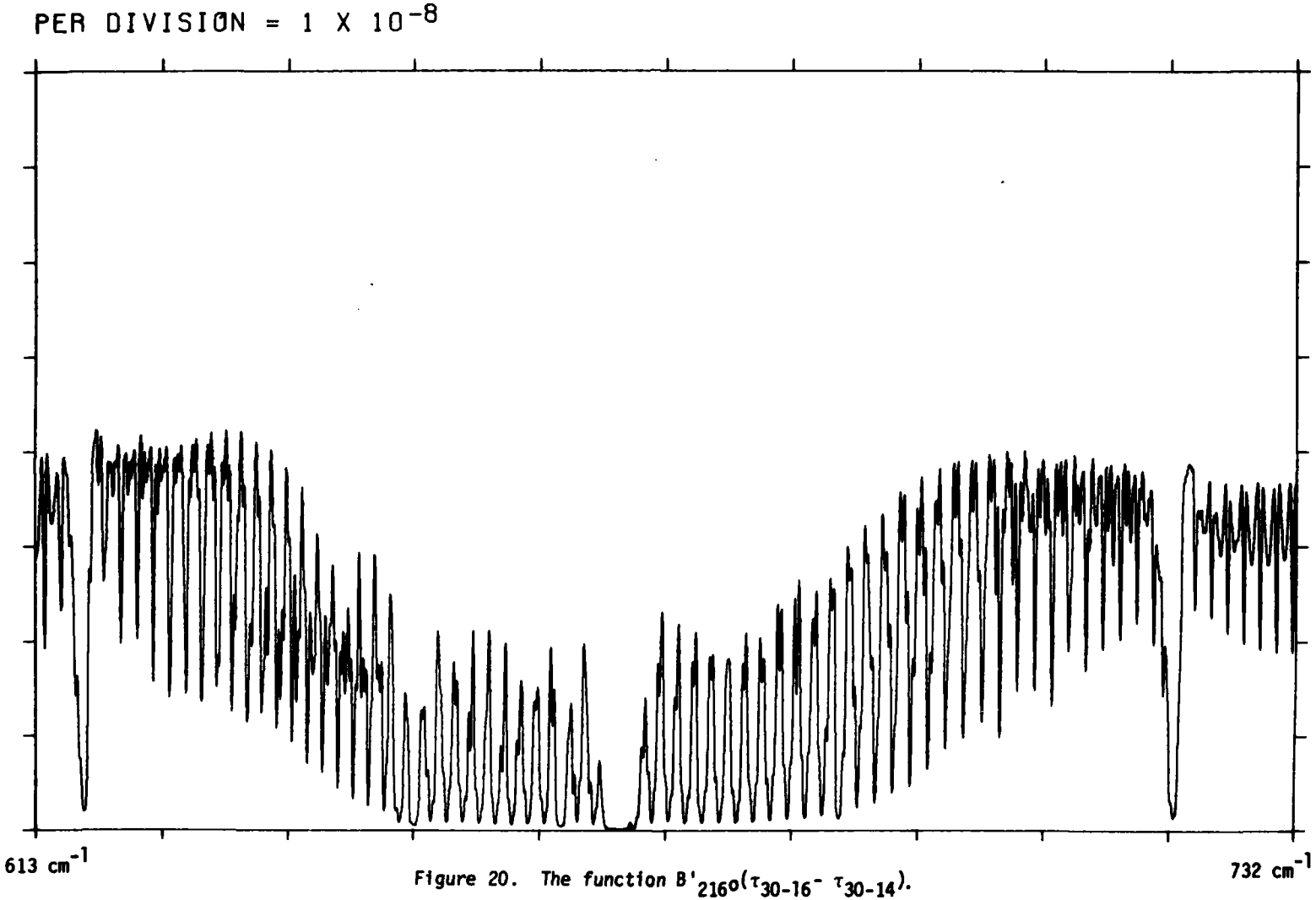

Figure 20. The function $B'_{216^0}(\tau_{30-16} - \tau_{30-14})$.

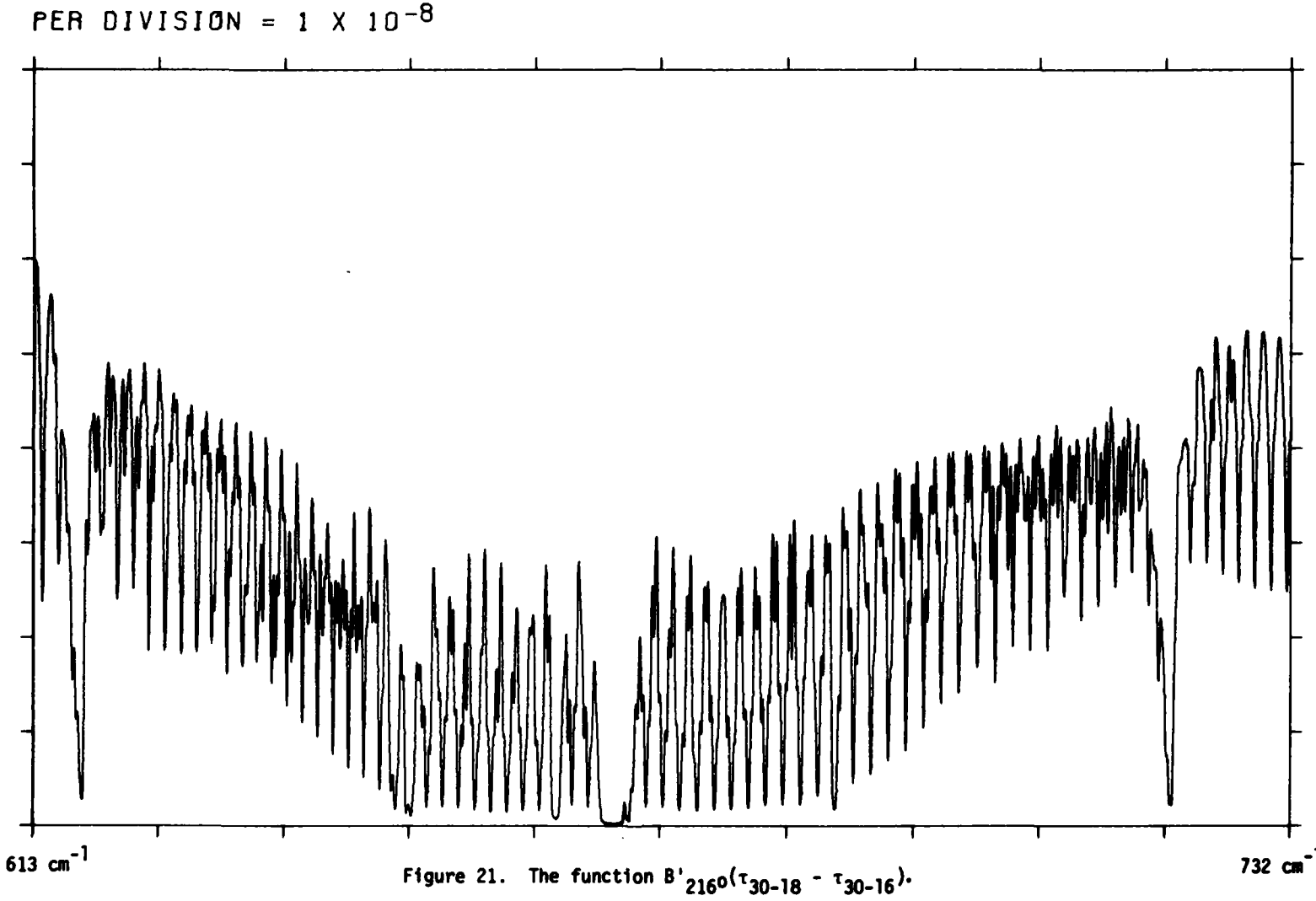

Figure 21. The function $B'_{216^0}(\tau_{30-18} - \tau_{30-16})$.

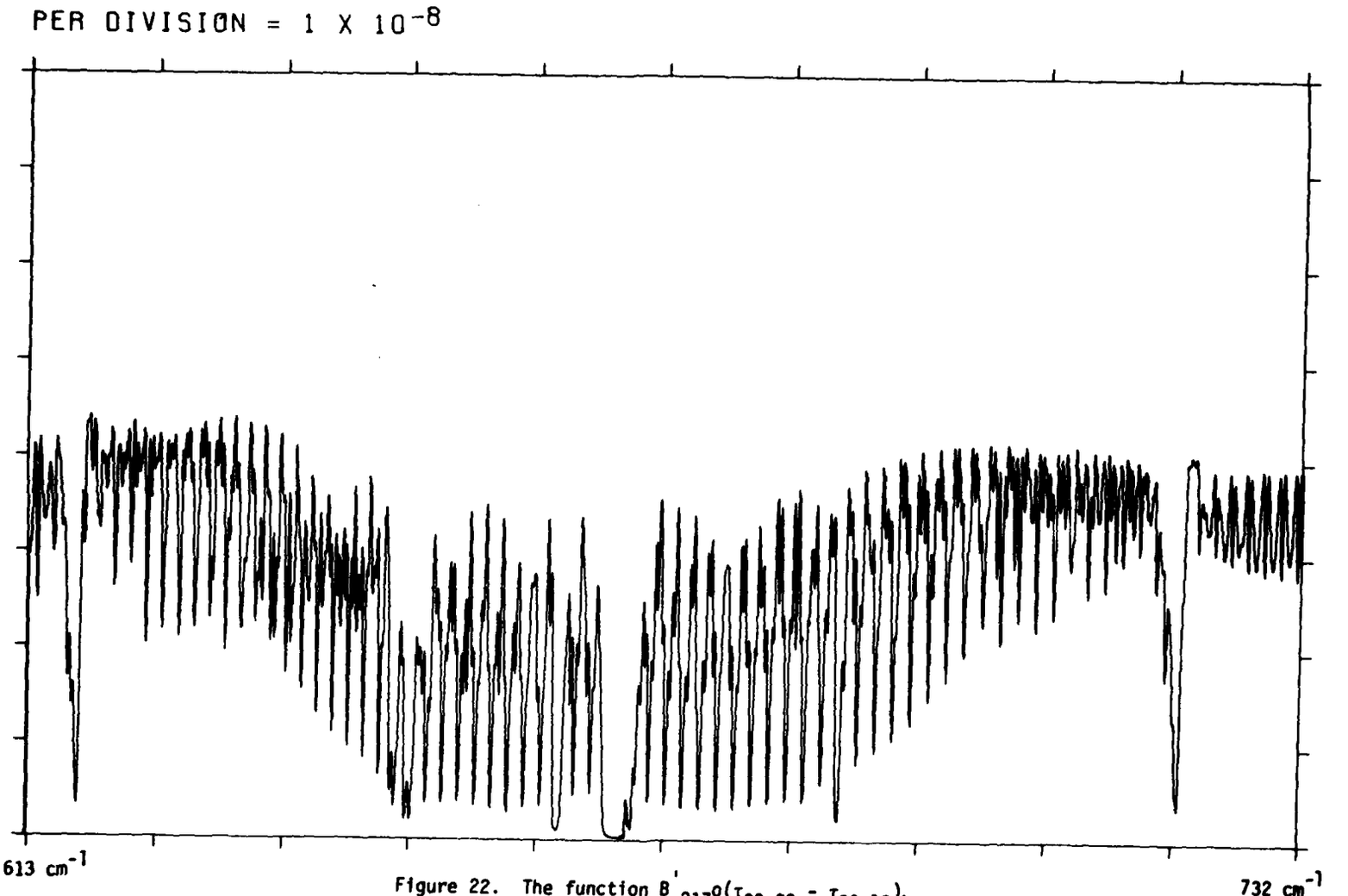

Figure 22. The function $B'_{217}{}^{o}(\tau_{30\text{-}20} - \tau_{30\text{-}18})$.

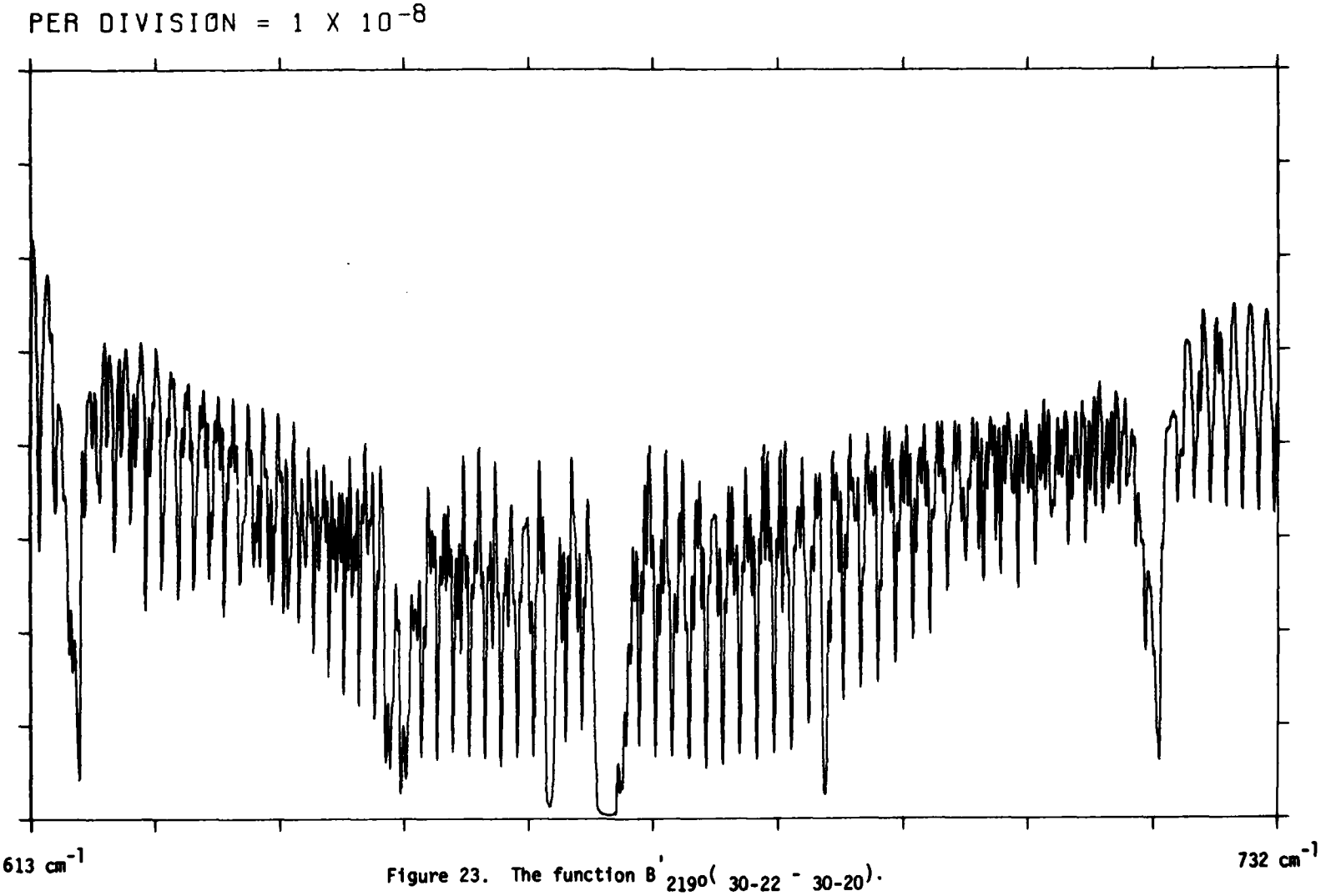

Figure 23. The function $B'_{219}{}^{o}(\ 30\text{-}22\ -\ 30\text{-}20)$.

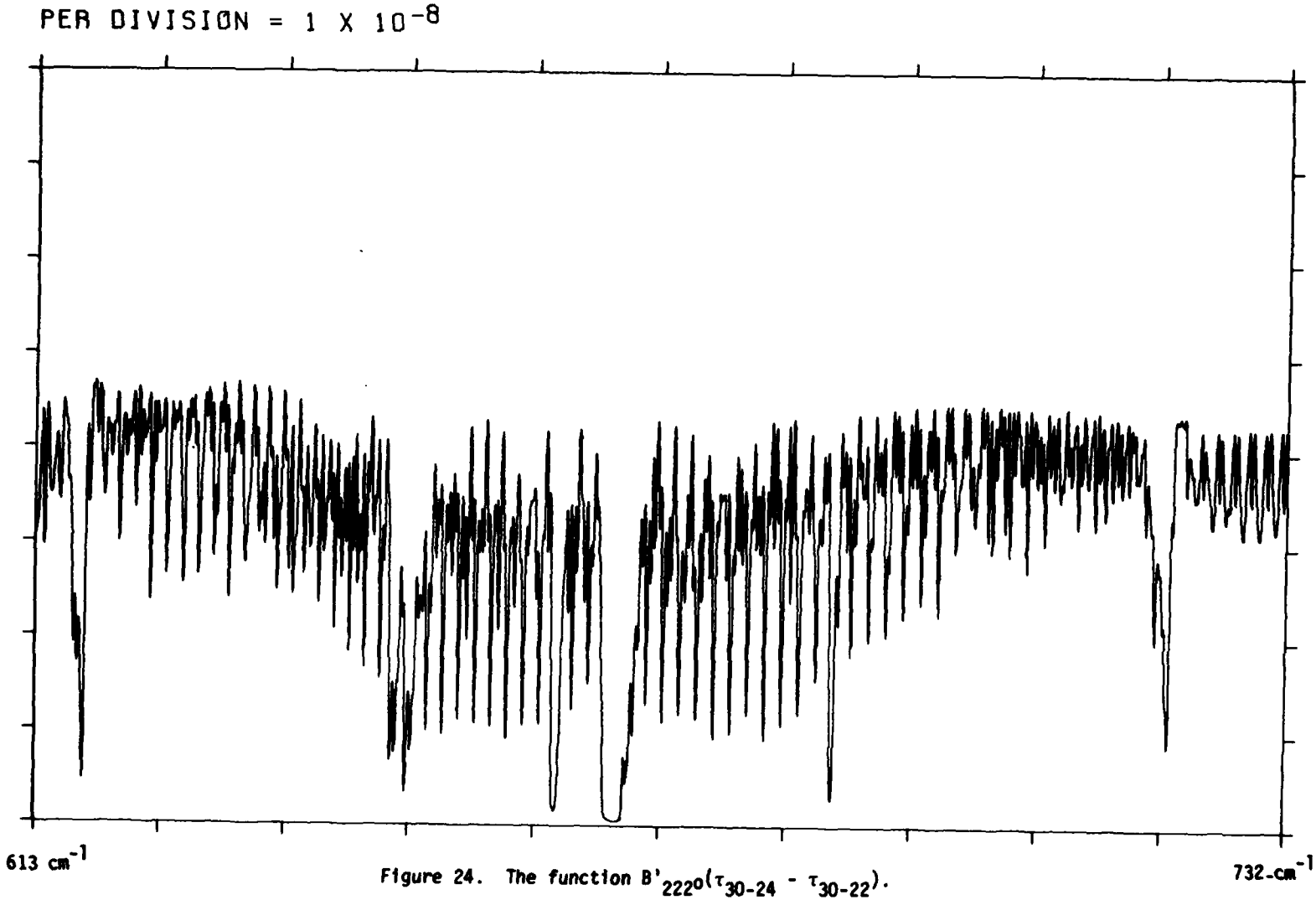

Figure 24. The function $B'_{222}{}^{o}(\tau_{30-24} - \tau_{30-22})$.

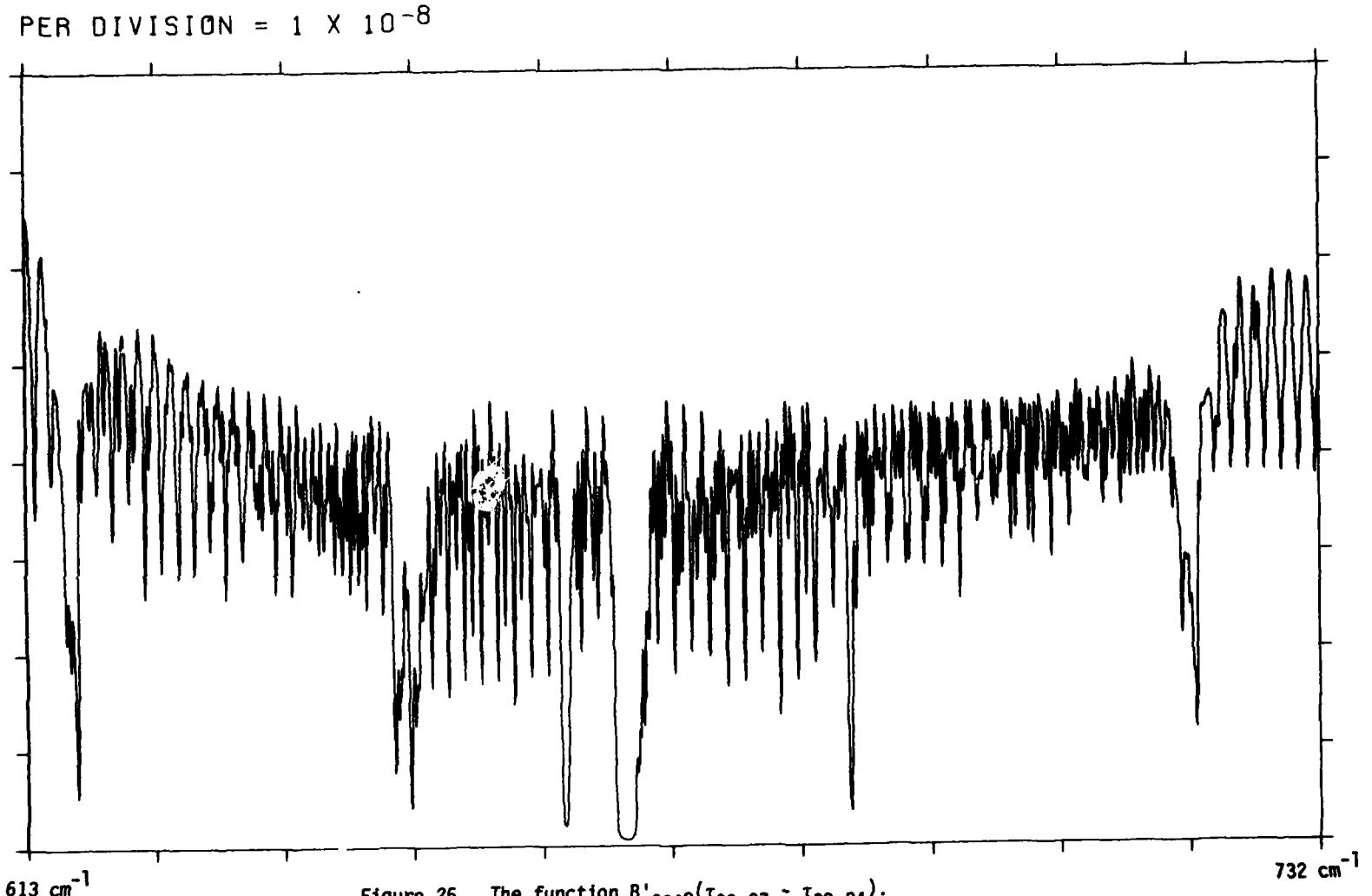

Figure 25. The function $B'_{2240}(\tau_{30-27} - \tau_{30-24})$.

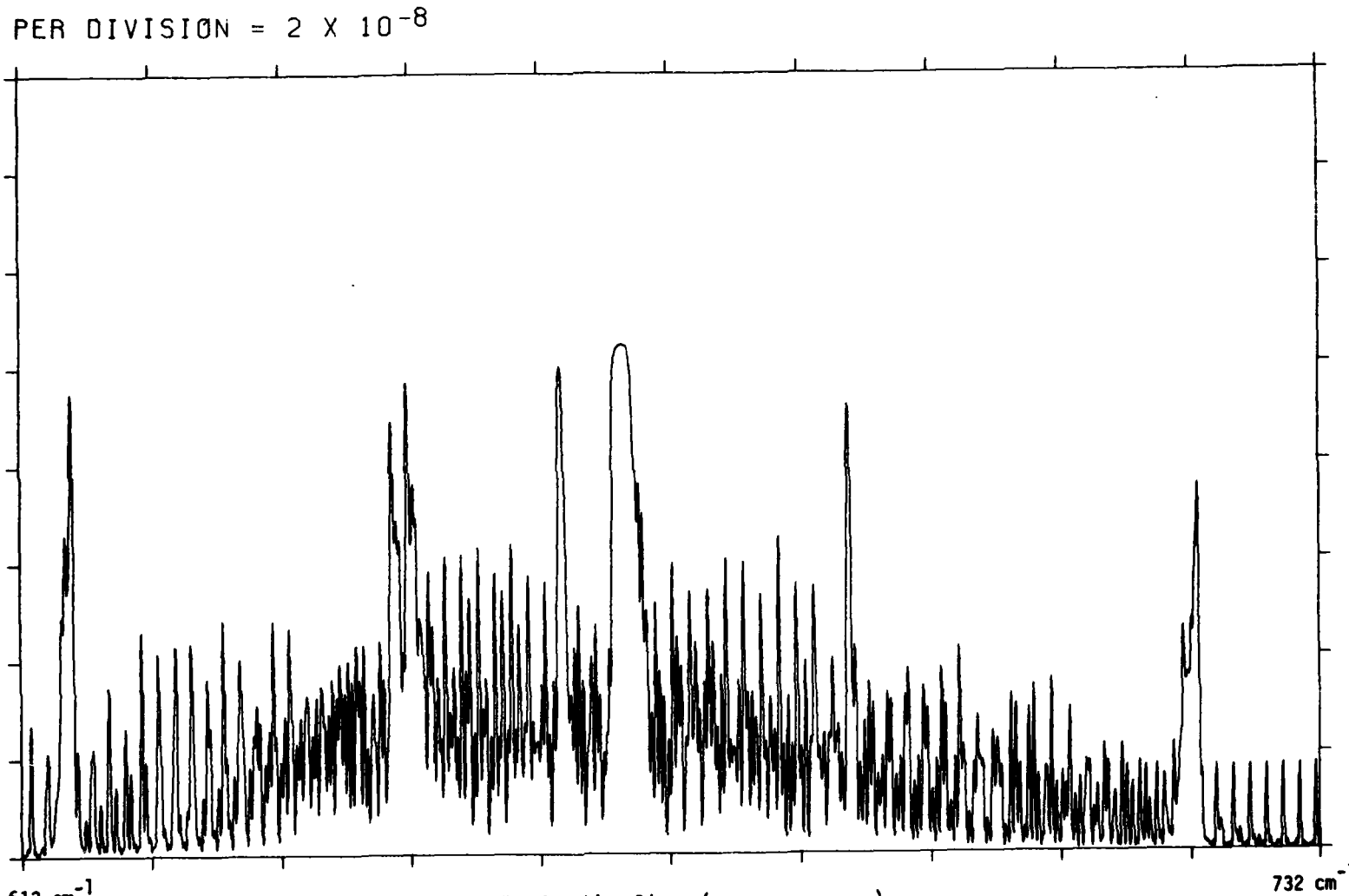

Figure 26. The function $B'_{2340}(\tau_{30-30} - \tau_{30-27})$.

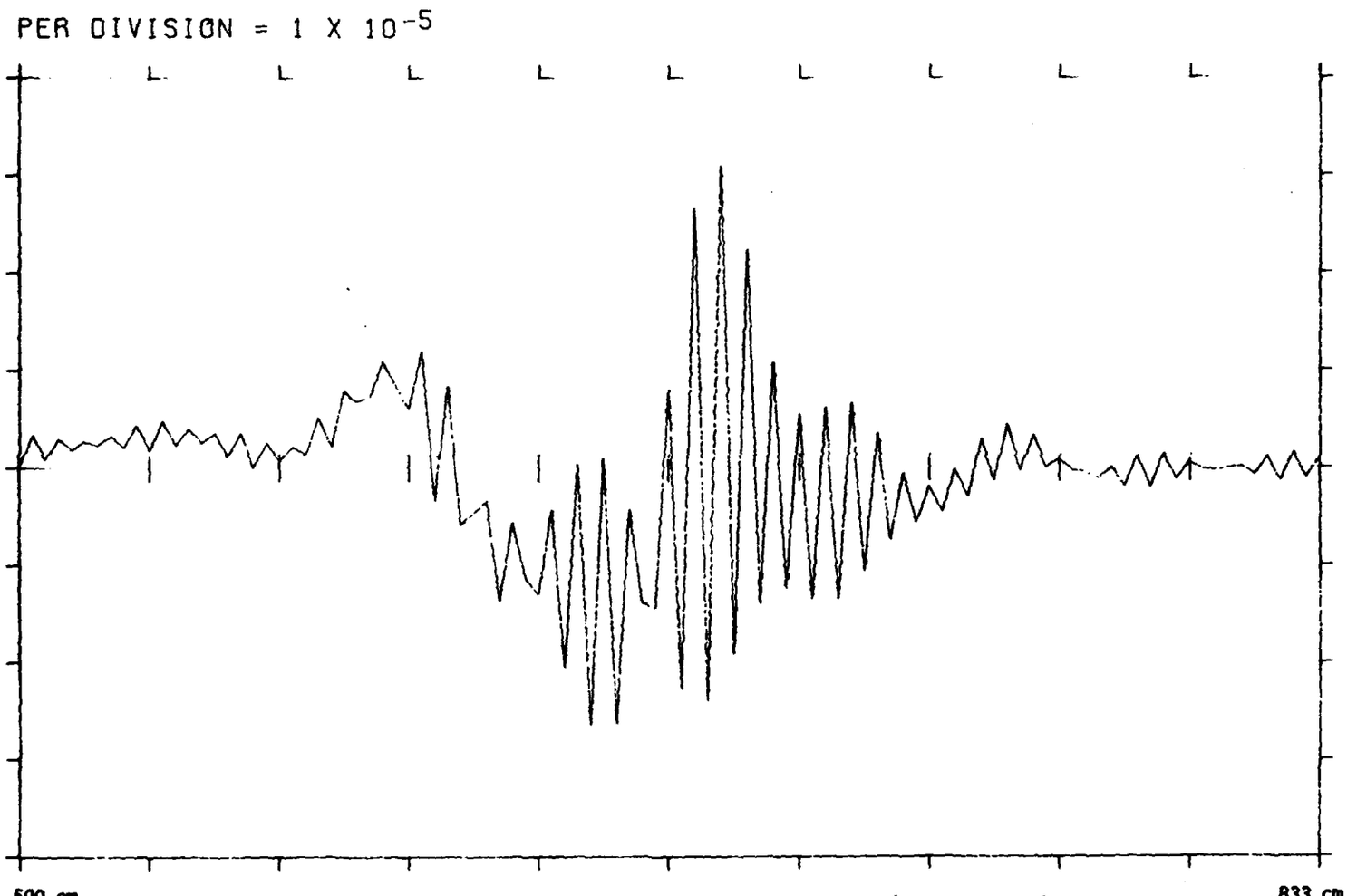

Figure 27. The Fourier transform of Figure 13, FT $B'_{290^0}(\tau_{30-2} - \tau_{30-0})$.

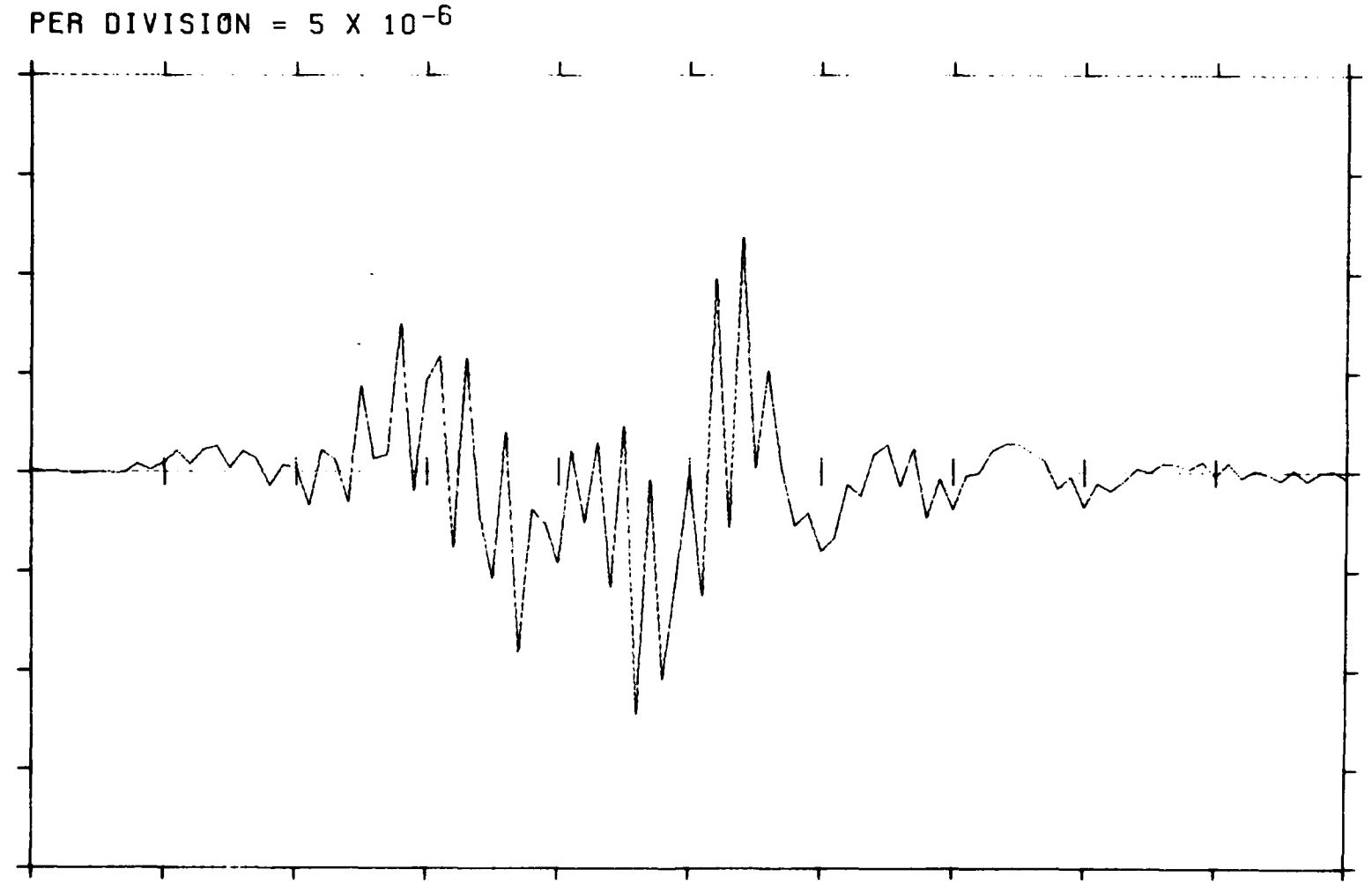

Figure 28. The Fourier transform of Figure 14, FT $B'_{279^o}(\tau_{30-4} - \tau_{30-2})$.

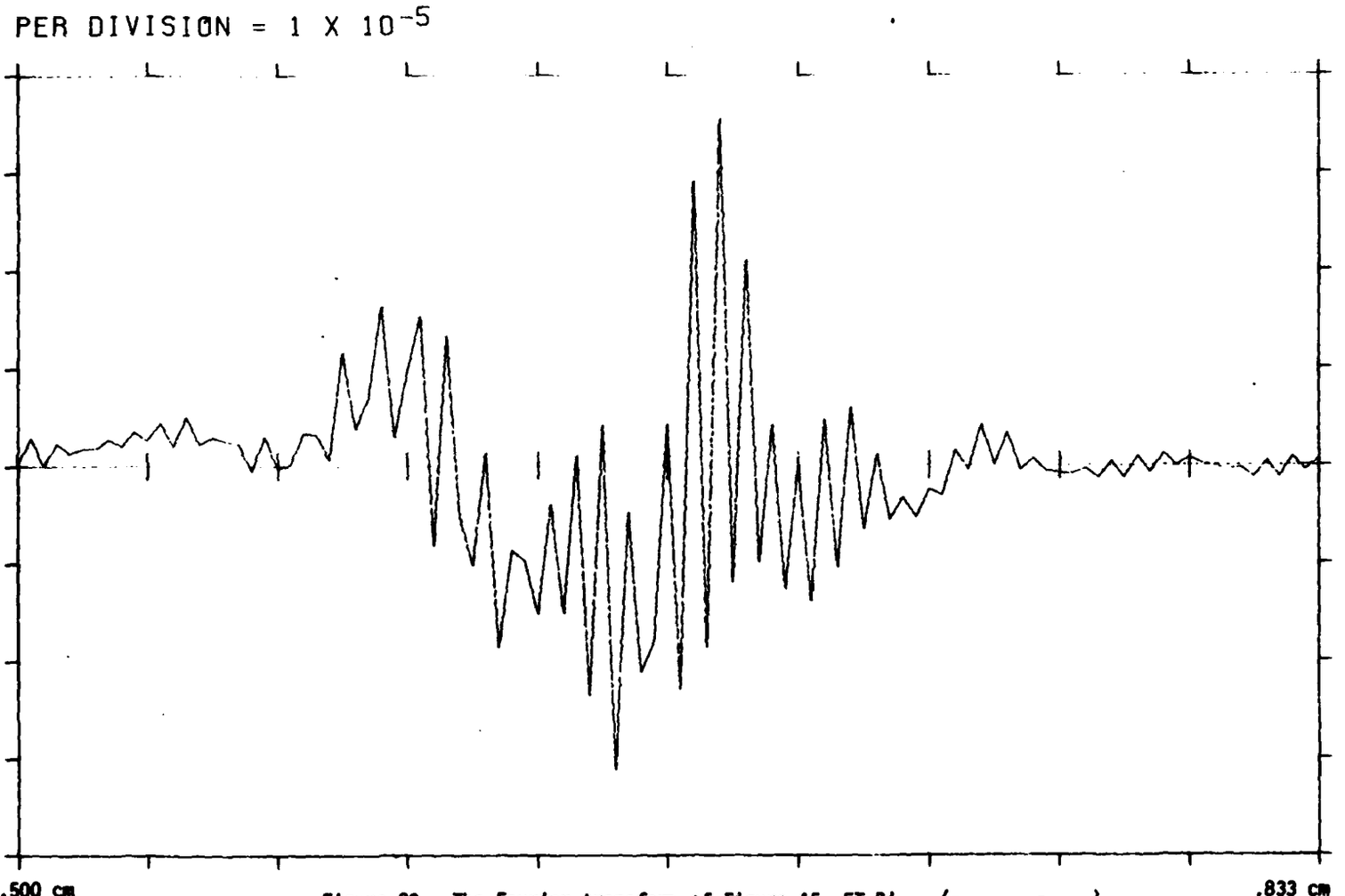

Figure 29. The Fourier transform of Figure 15, FT $B'_{267^0}(\tau_{30\text{-}6} - \tau_{30\text{-}4})$.

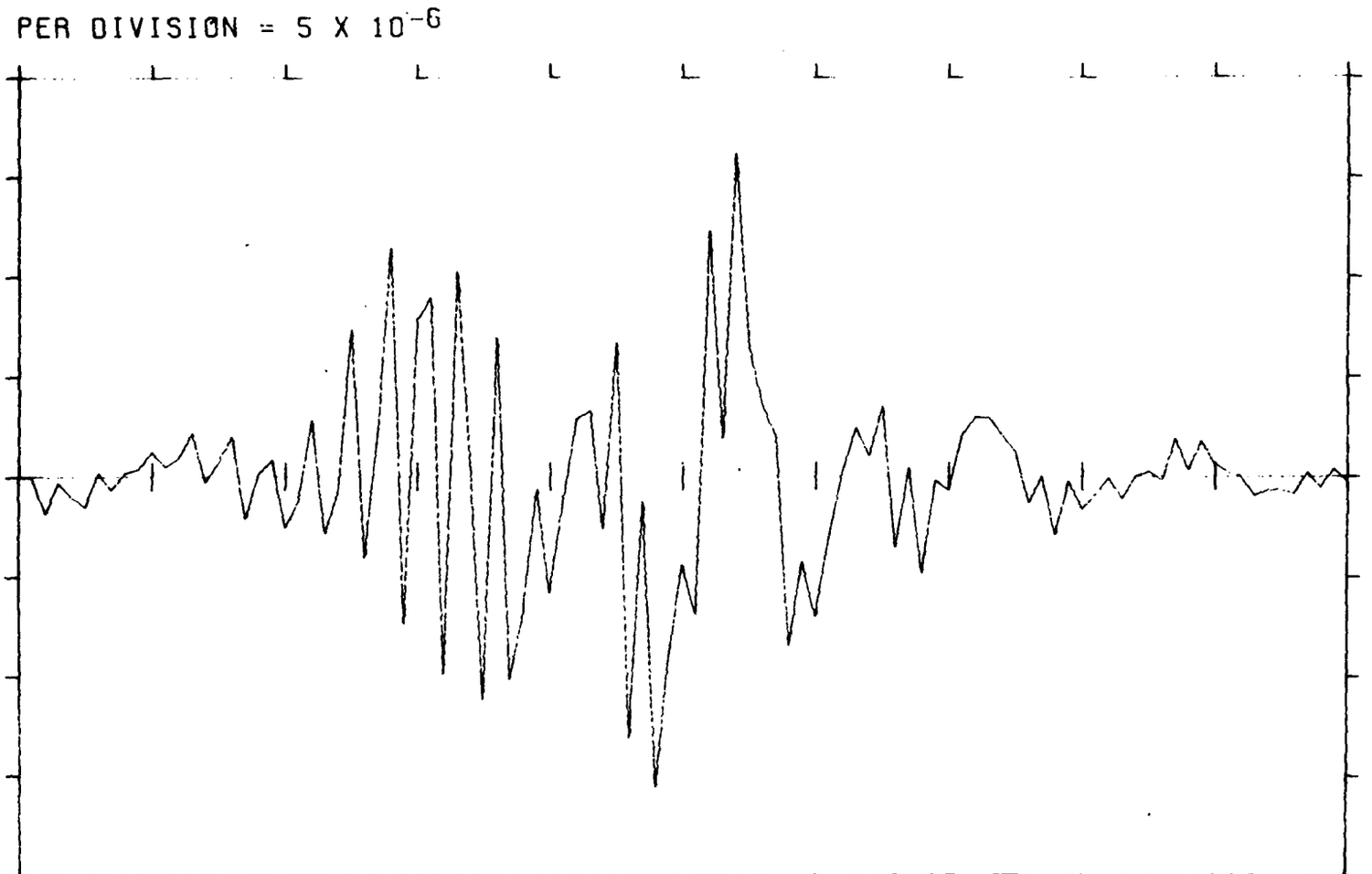

Figure 30. The Fourier transform of Figure 16, FT $B'_{2650}(\tau_{30-8} - \tau_{30-6})$.

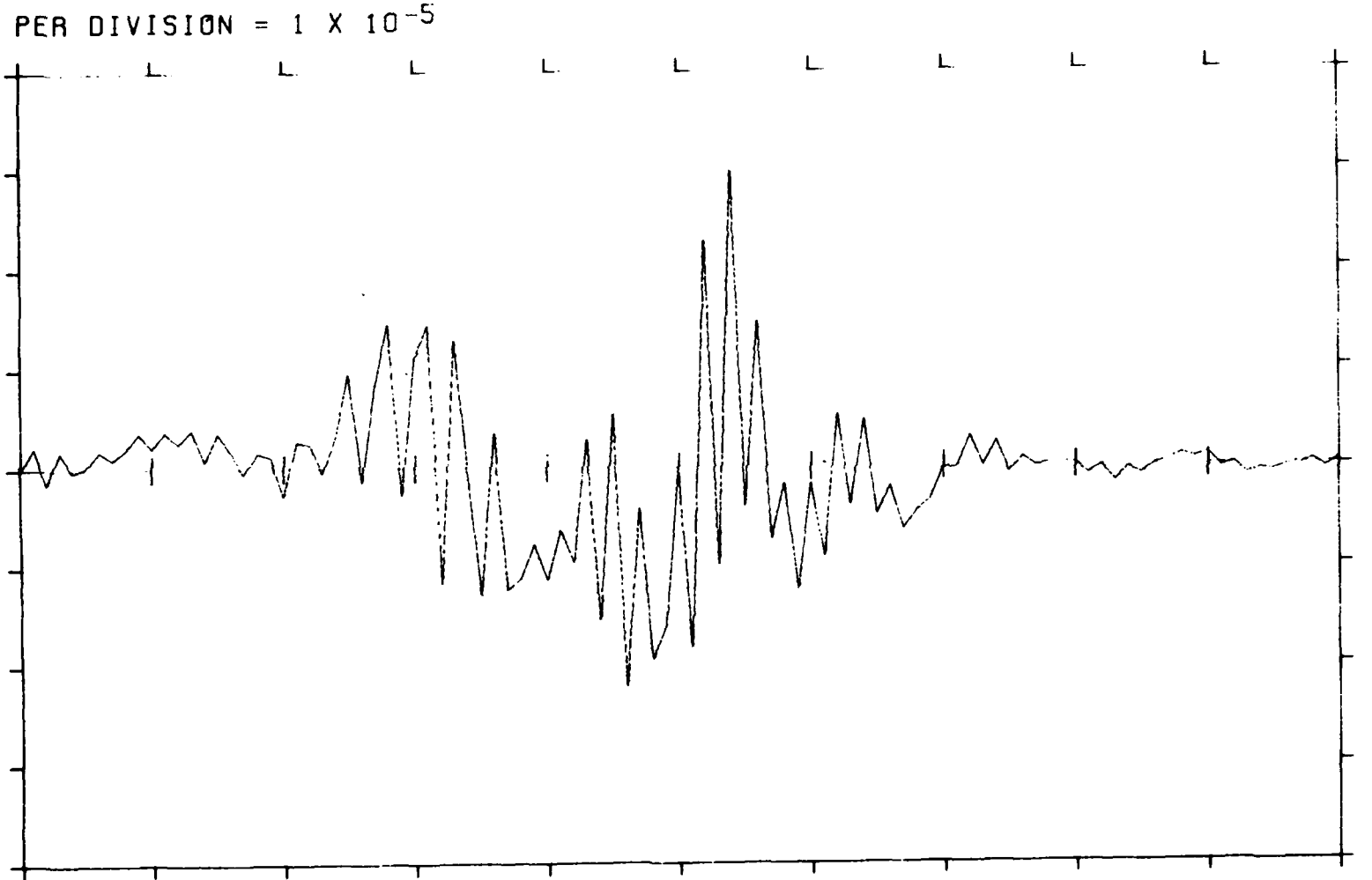

Figure 31. The Fourier transform of Figure 17, FT $B'_{2420}(\tau_{30-10} - \tau_{30-8})$.

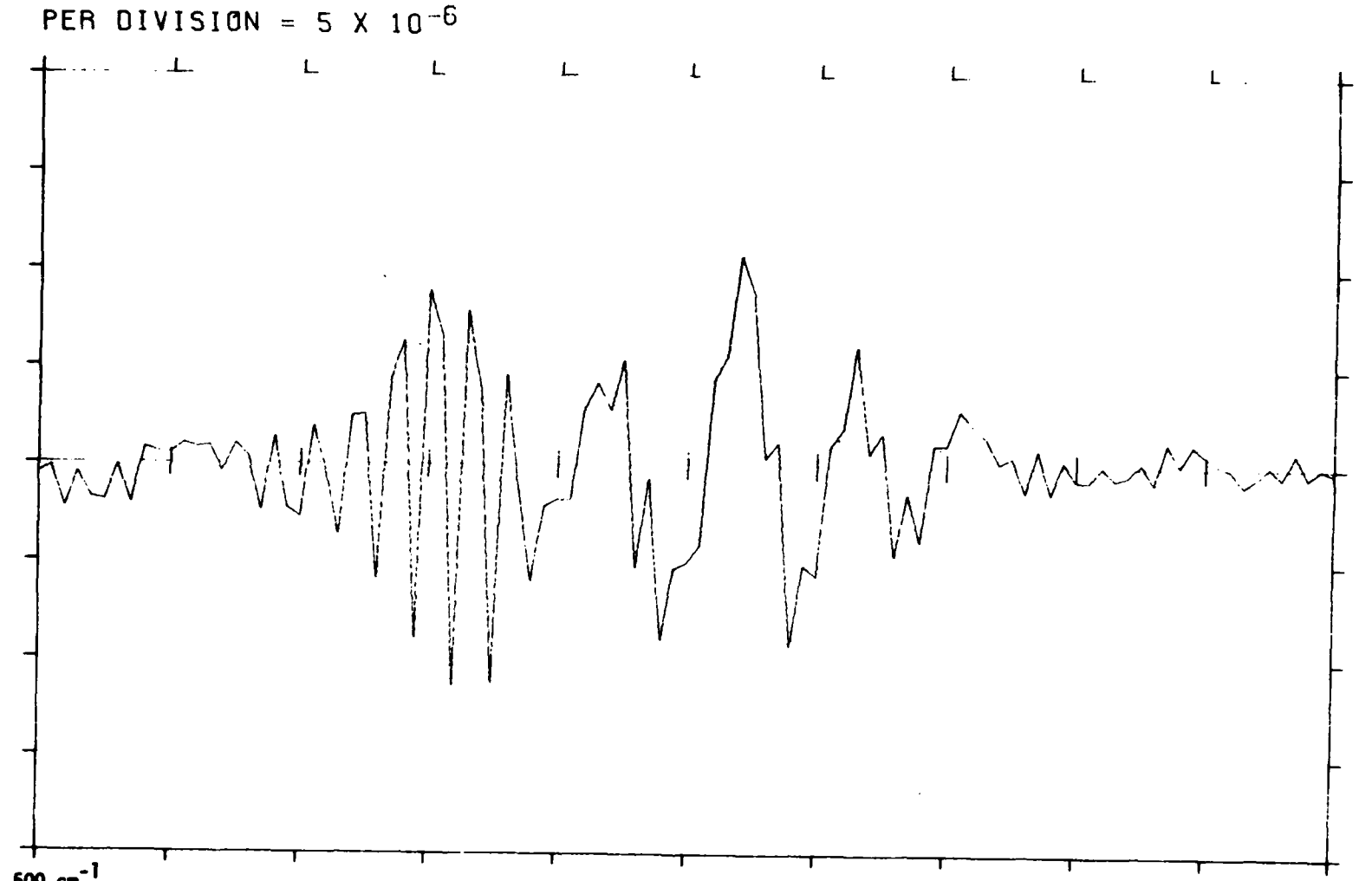

Figure 32. The Fourier transform of Figure 18, FT $B'_{2290}(\tau_{30\text{-}12} - \tau_{30\text{-}10})$.

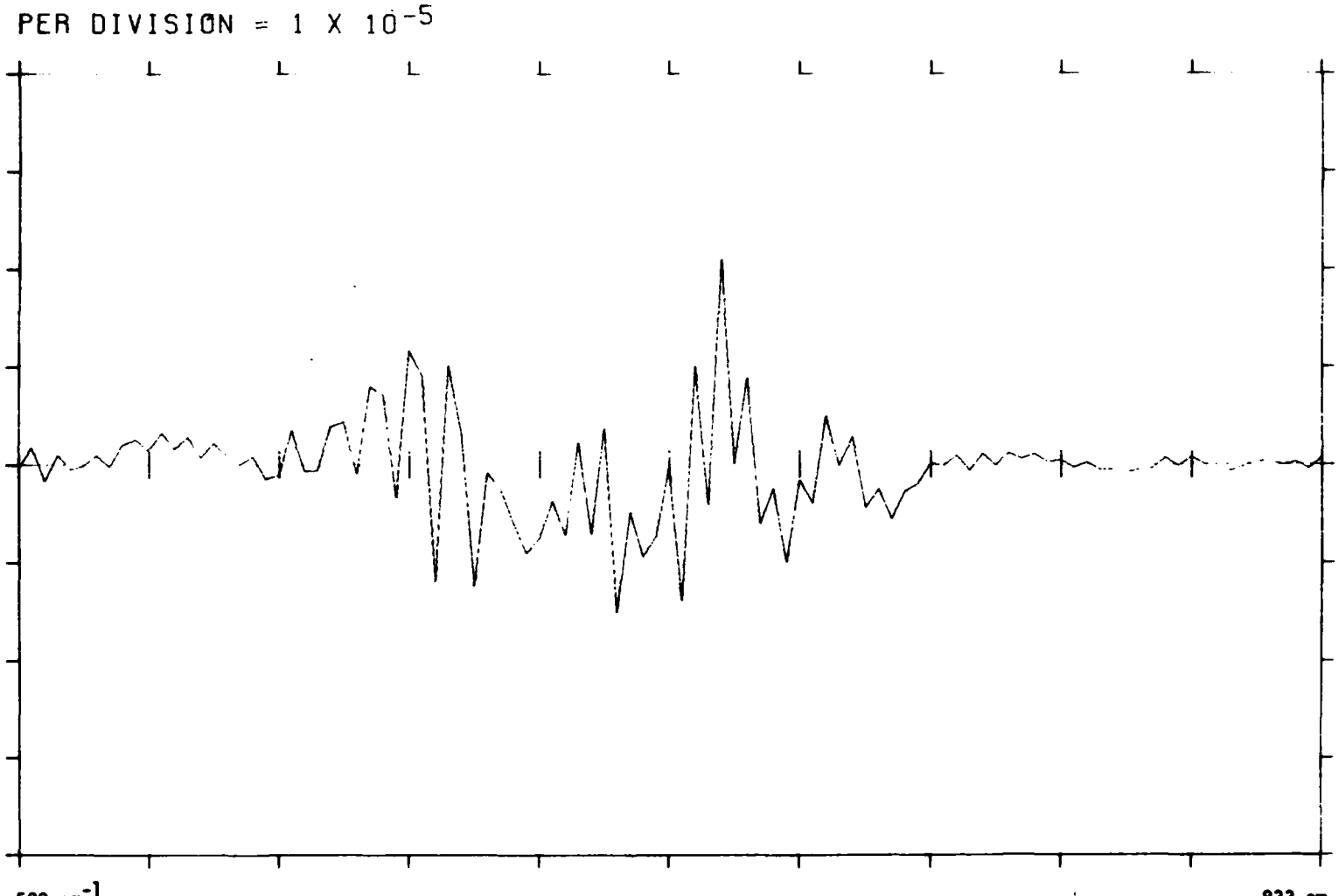

Figure 33. The Fourier transform of Figure 19, FT $B'_{2160}(\tau_{30-14} - \tau_{30-12})$.

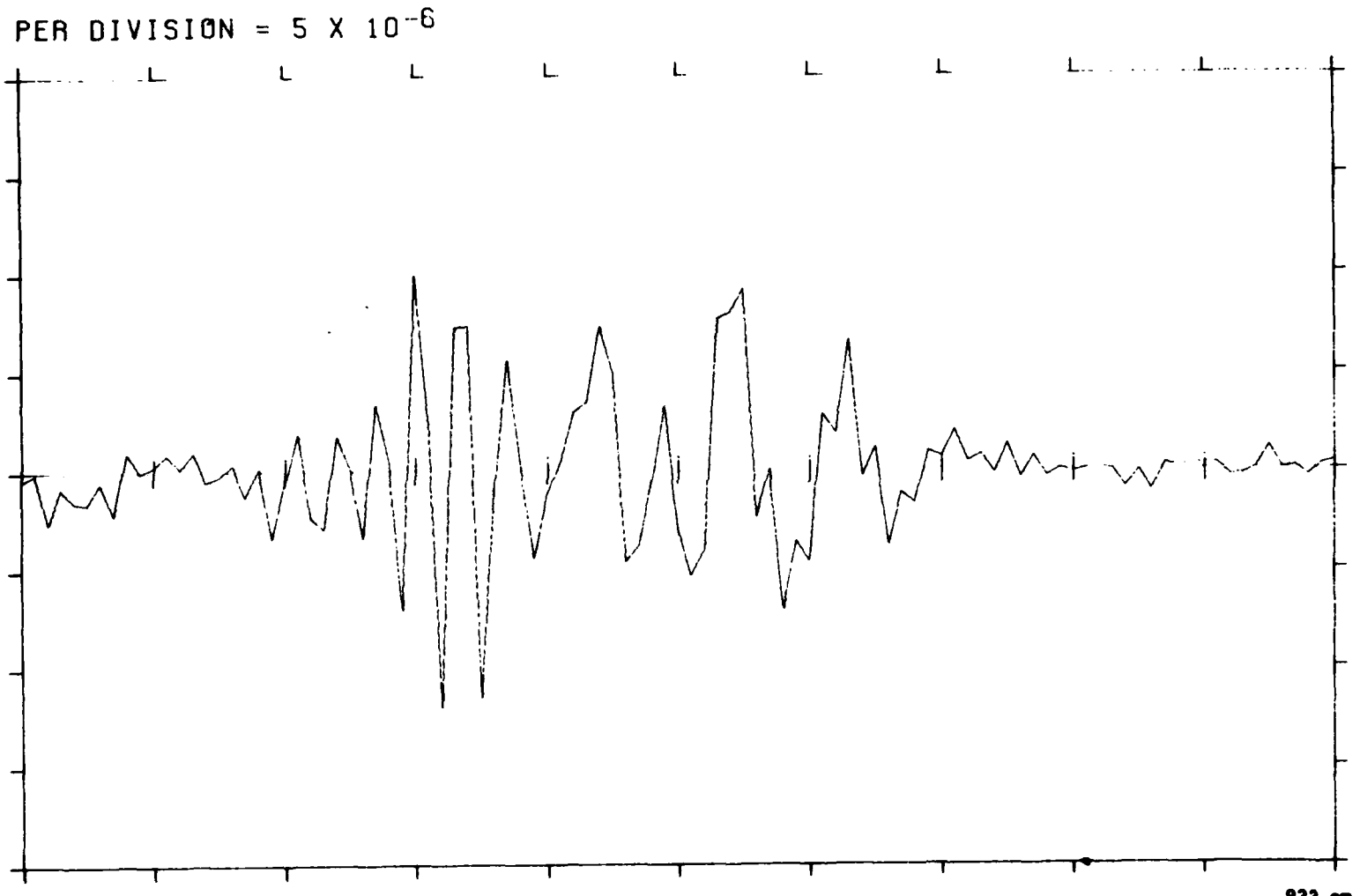

Figure 34. The Fourier transform of Figure 20, FT $B'_{216o}(\tau_{30\text{-}16} - \tau_{30\text{-}14})$.

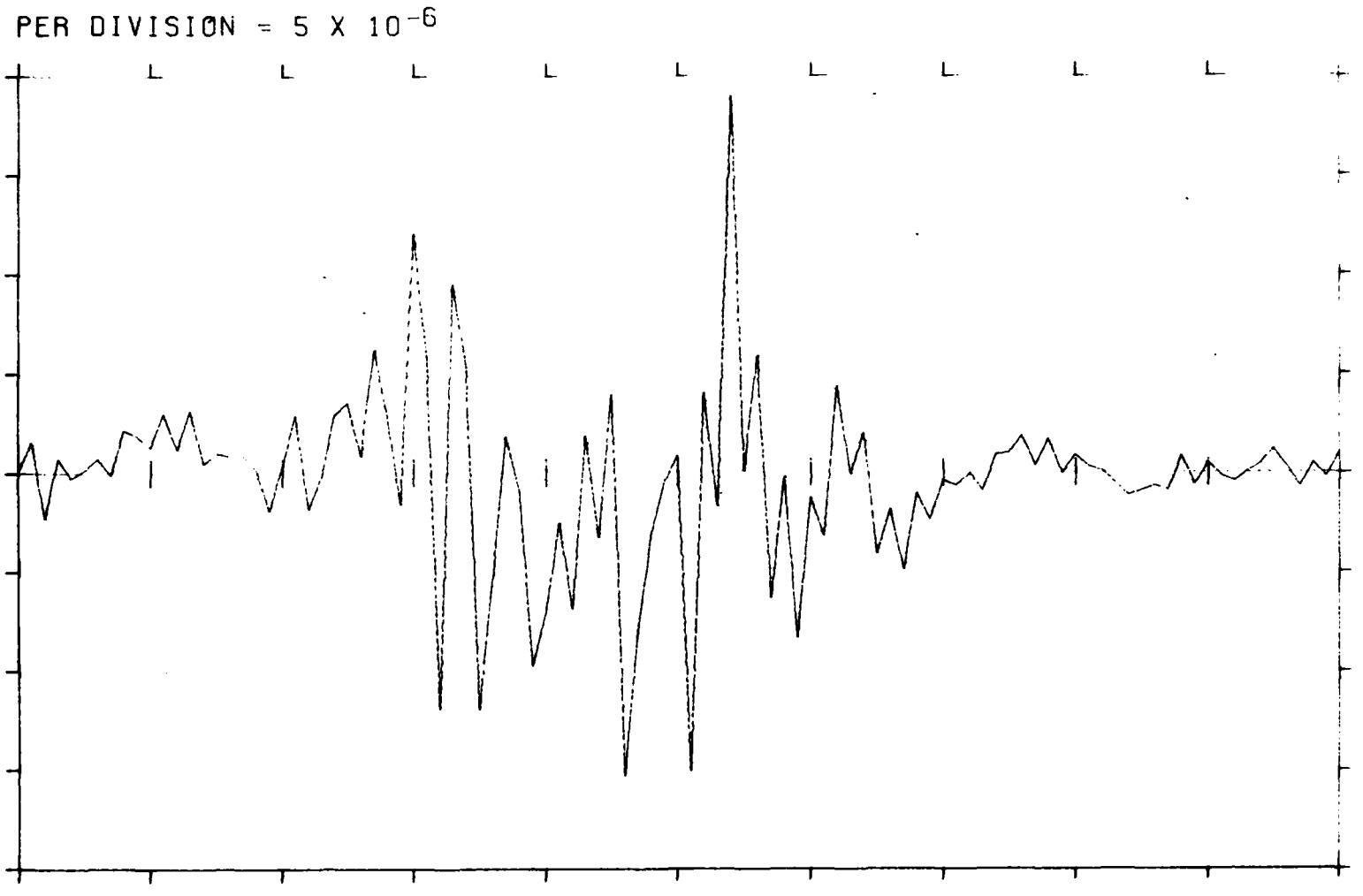

Figure 35. The Fourier transform of Figure 21, FT $B'_{216^o}(\tau_{30\text{-}18} - \tau_{30\text{-}16})$.

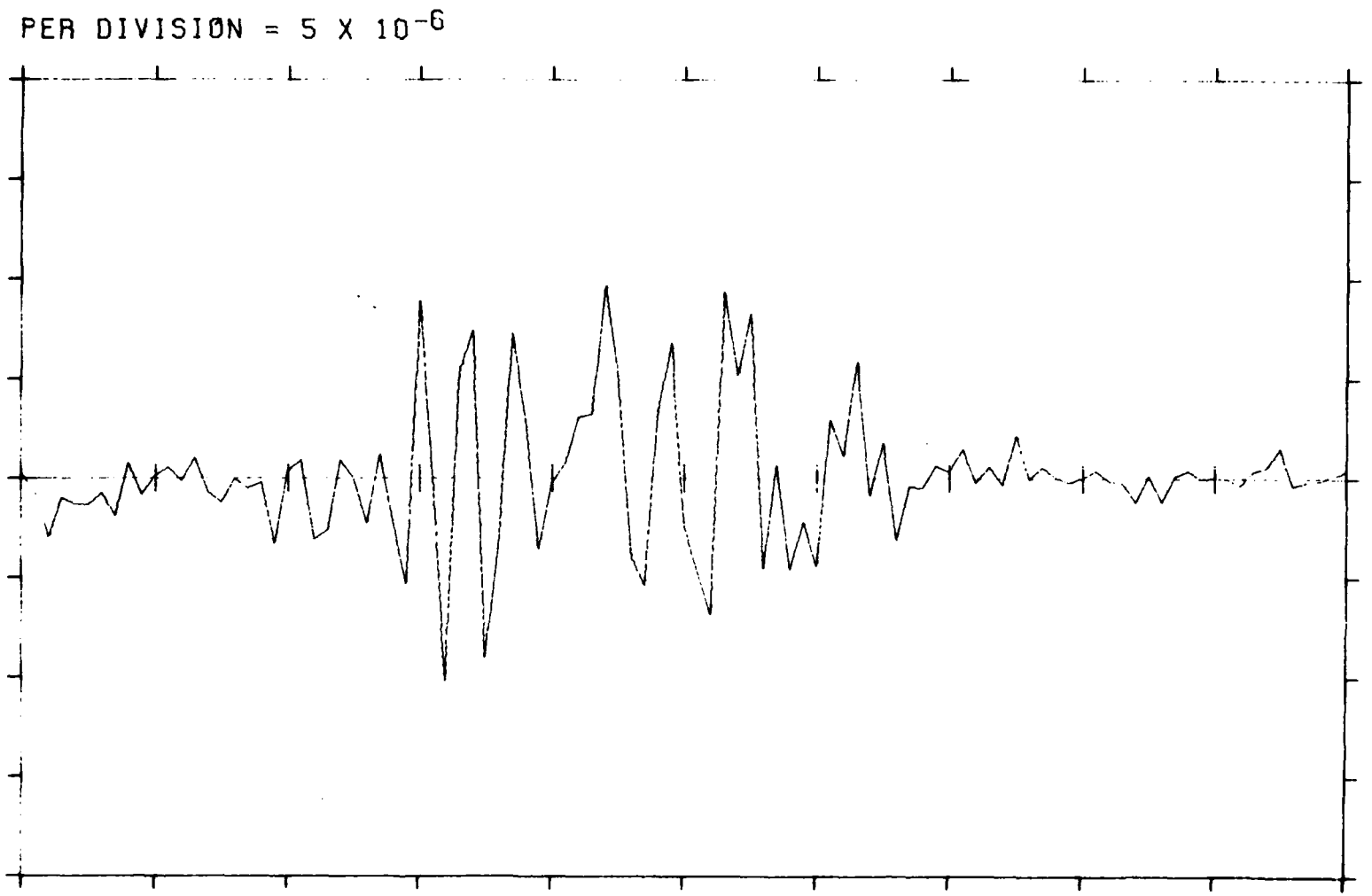

Figure 36. The Fourier transform of Figure 22, FT $B'_{2170}(\tau_{30-20} - \tau_{30-18})$.

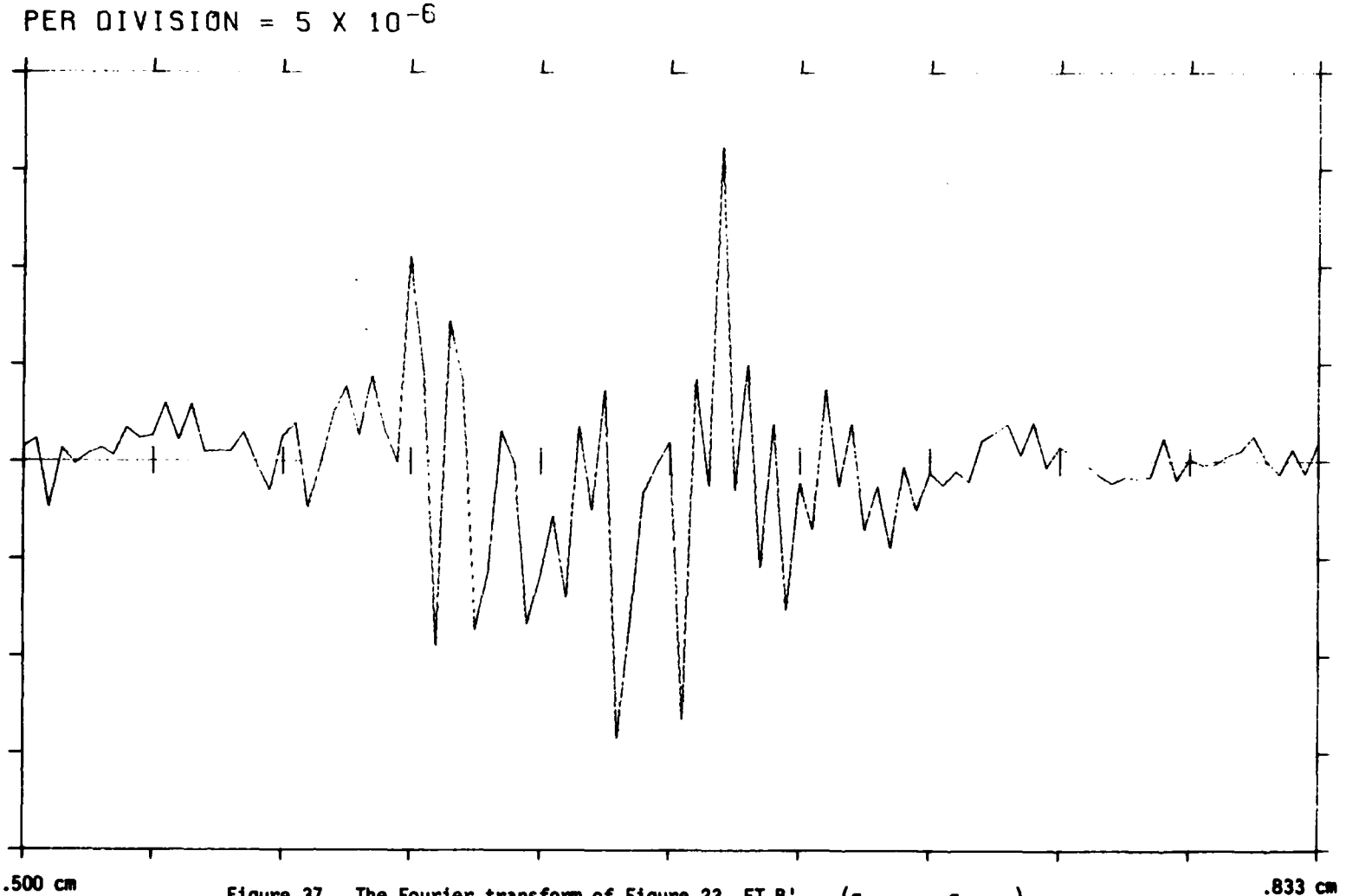

Figure 37. The Fourier transform of Figure 23, FT $B'_{219^o}(\tau_{30-22} - \tau_{30-20})$.

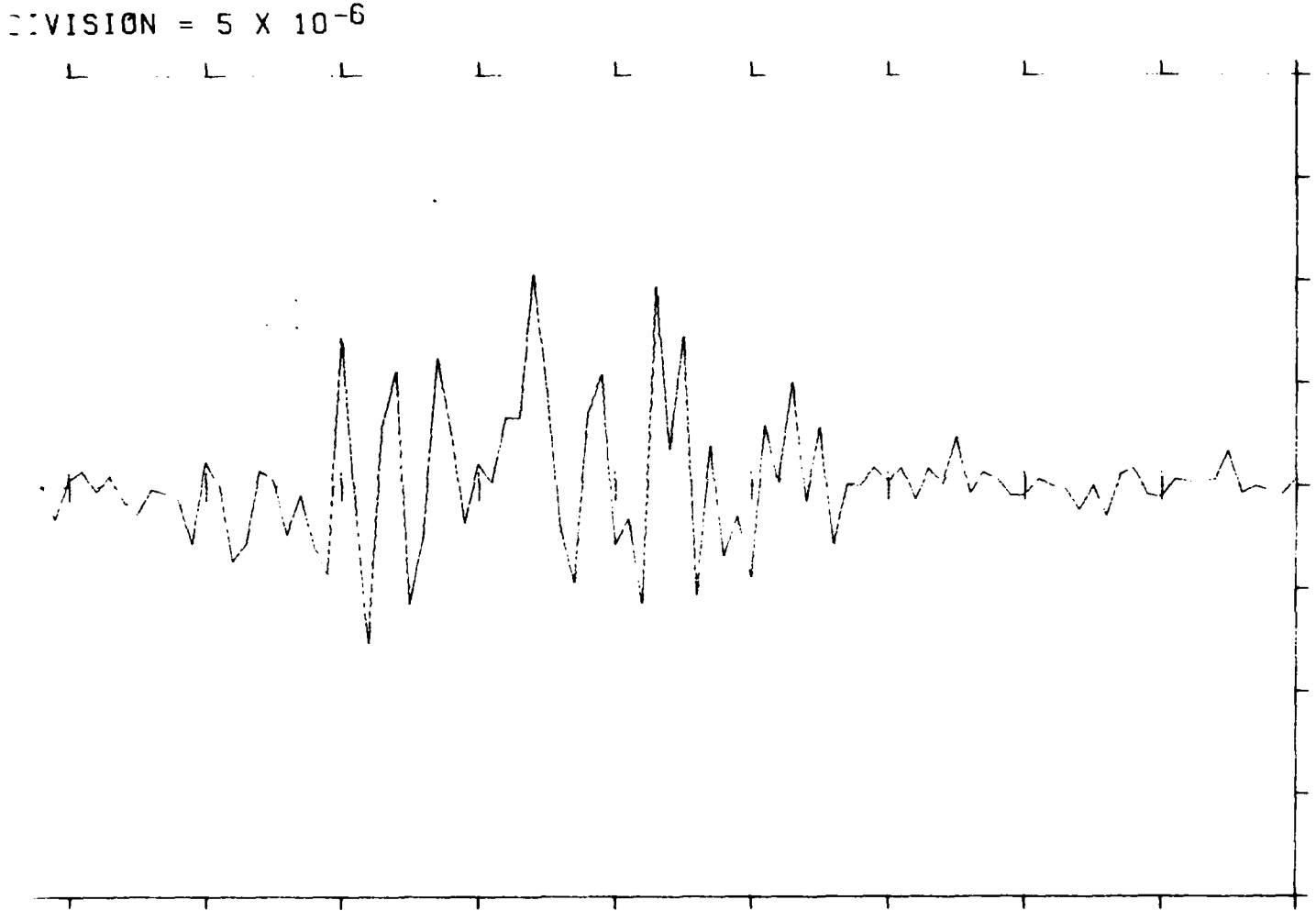

Figure 38. The Fourier transform of Figure 24, FT $B'_{222o}(\tau_{30-24} - \tau_{30-22})$.

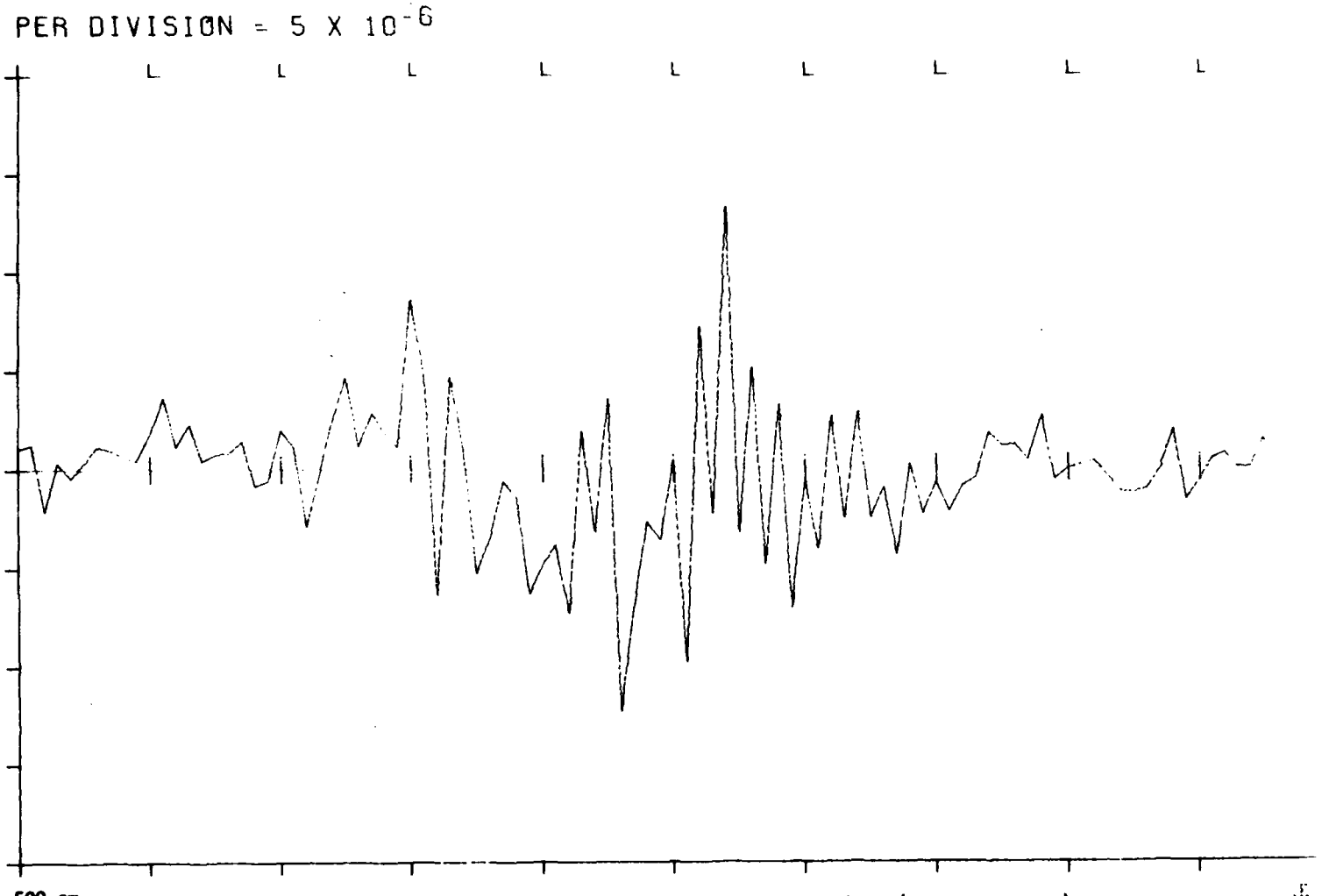

Figure 39. The Fourier transform of Figure 25, FT $B'_{2240}(\tau_{30-27} - \tau_{30-24})$.

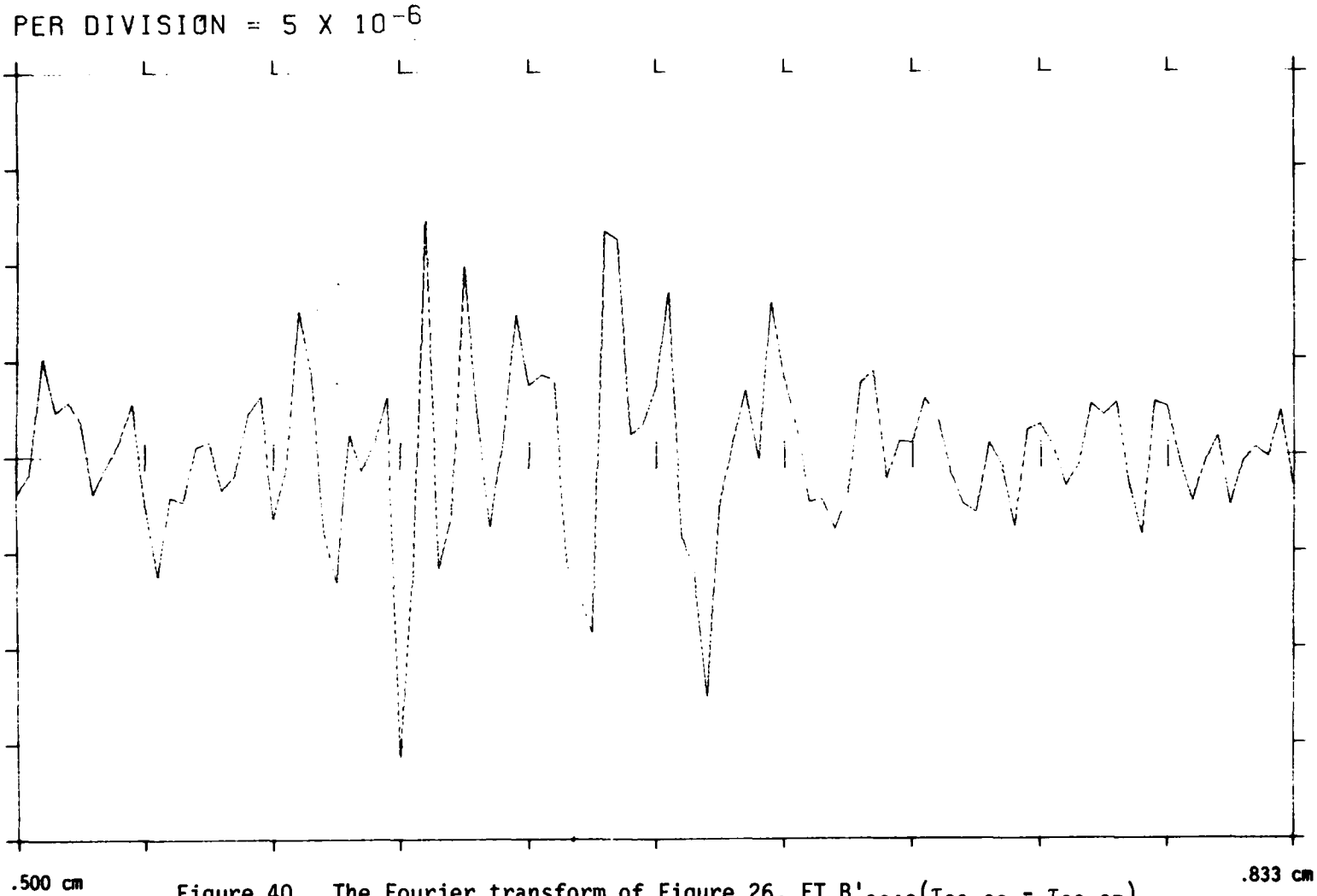

Figure 40. The Fourier transform of Figure 26, FT $B'_{2340}(\tau_{30-30} - \tau_{30-27})$.

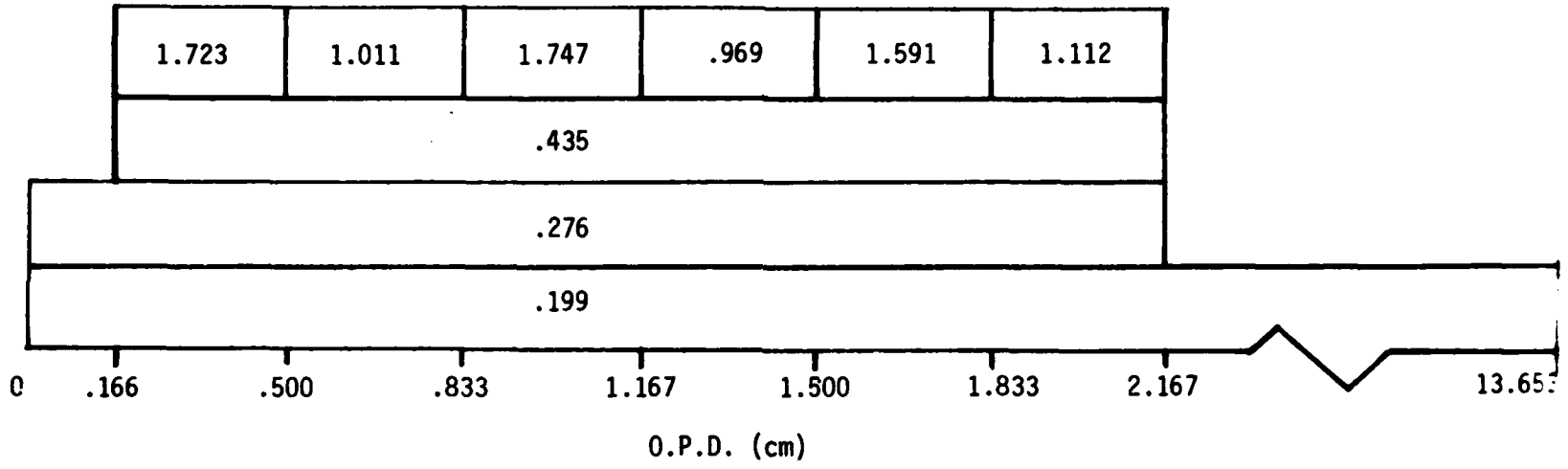

Figure 41. The r.m.s. noise temperature returned by various partial interferograms with 10^{-8} watts/cm^2-sr noise.

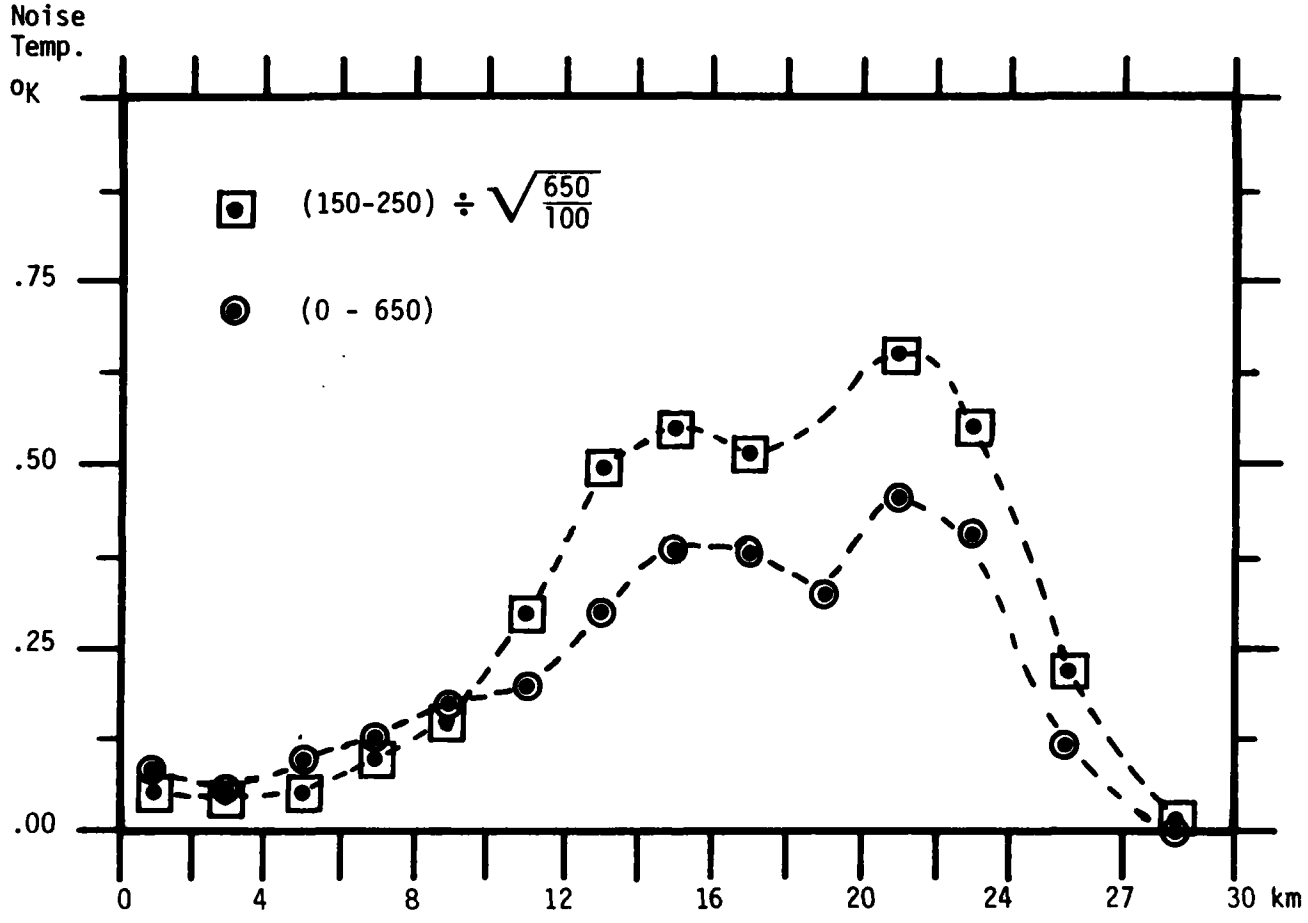

Figure 42. Noise temperatures from two partial interferograms.

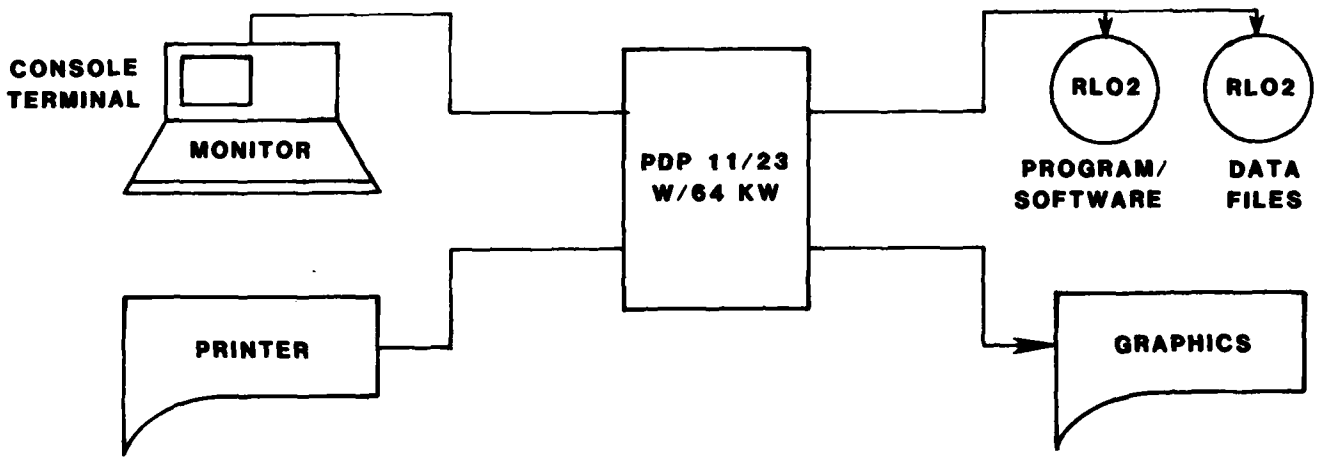

Figure 43. Diagram of PDP 11/23 Computer System Hardware.

The FAS program was designed to run on a PP PDP 11/23 computer with 32 KW of memory. Program and software are stored on one RLO2 disk and data files are stored on a separate RL102 disk using a random access file structure.

The FAS executive program allows the operator to interact with the data. From this program, the operator can issue separate commands with specified parameters to direct the flow of processing. Also, simple commands can be combined into more complex commands called "MACROS".

Using this structure, data can be generated and stored by the operator and complex computations can be defined by using a set of basic processing commands.

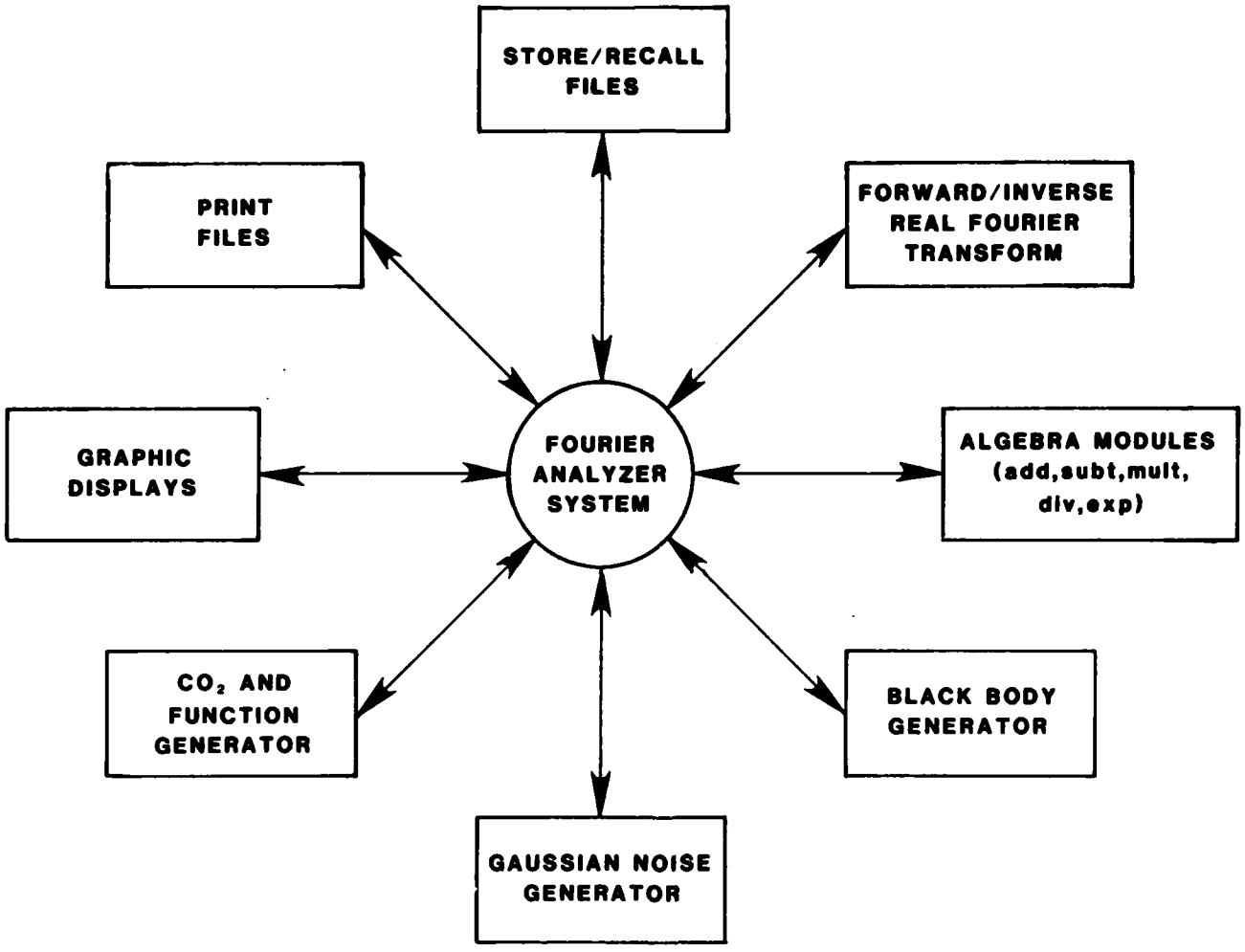

Figure 44. Block diagram of program used to generate and process CO_2 data files.

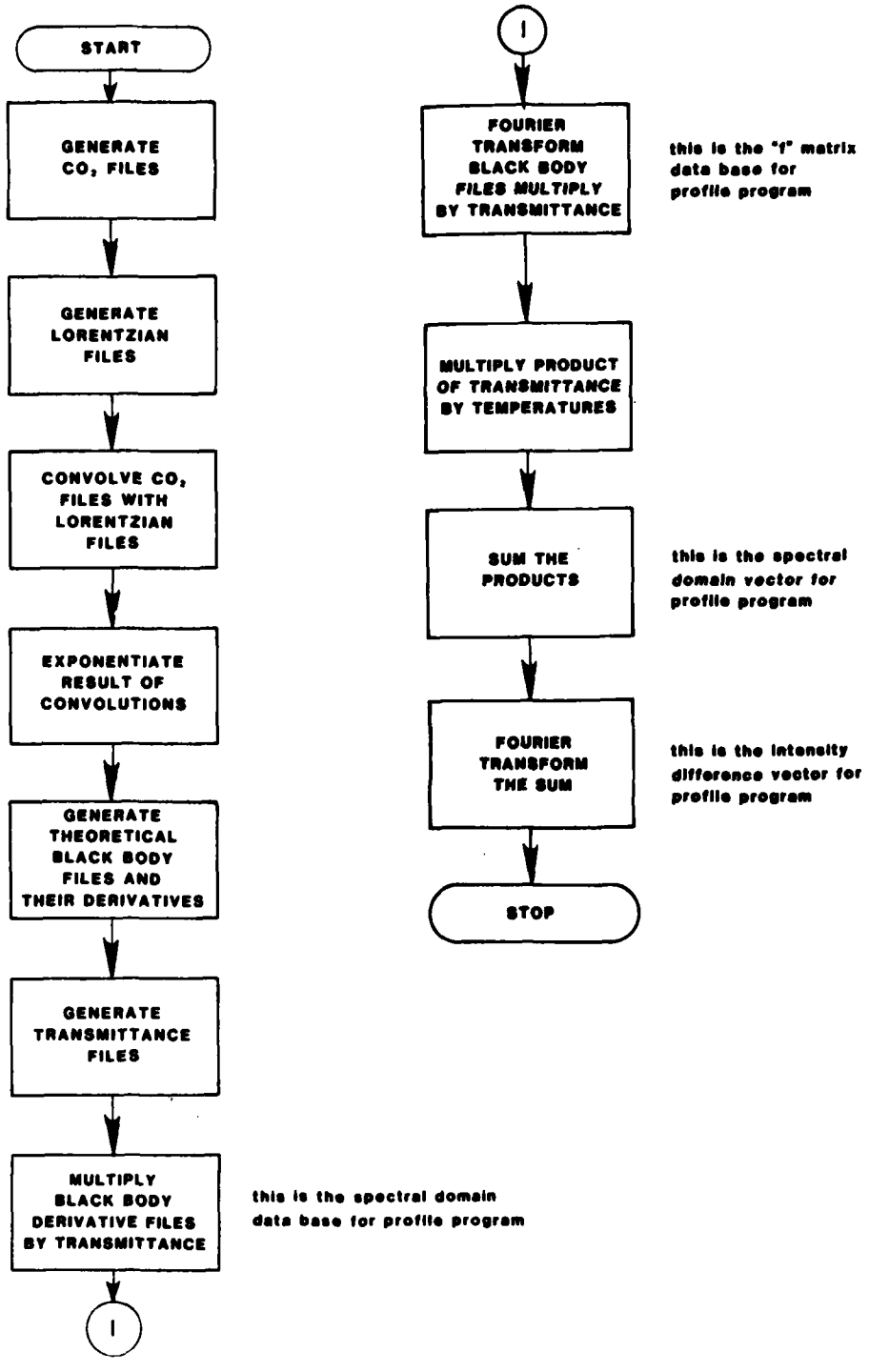

Figure 45. Computation procedure used to generate transmittance.

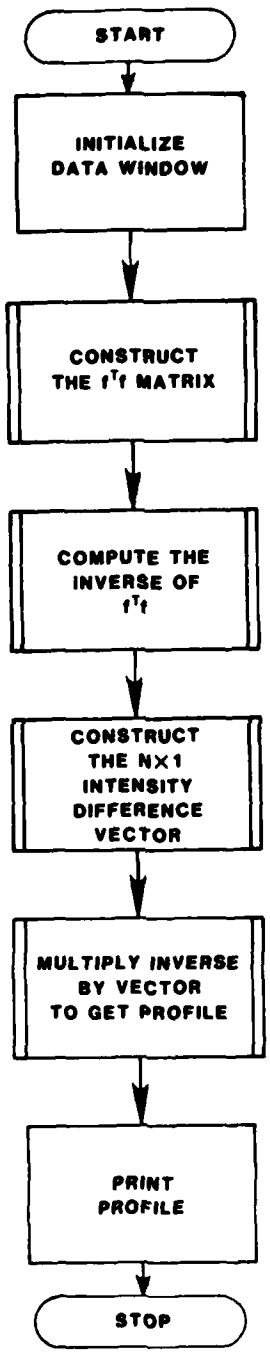

Figure 46. Program for Temperature Profile.

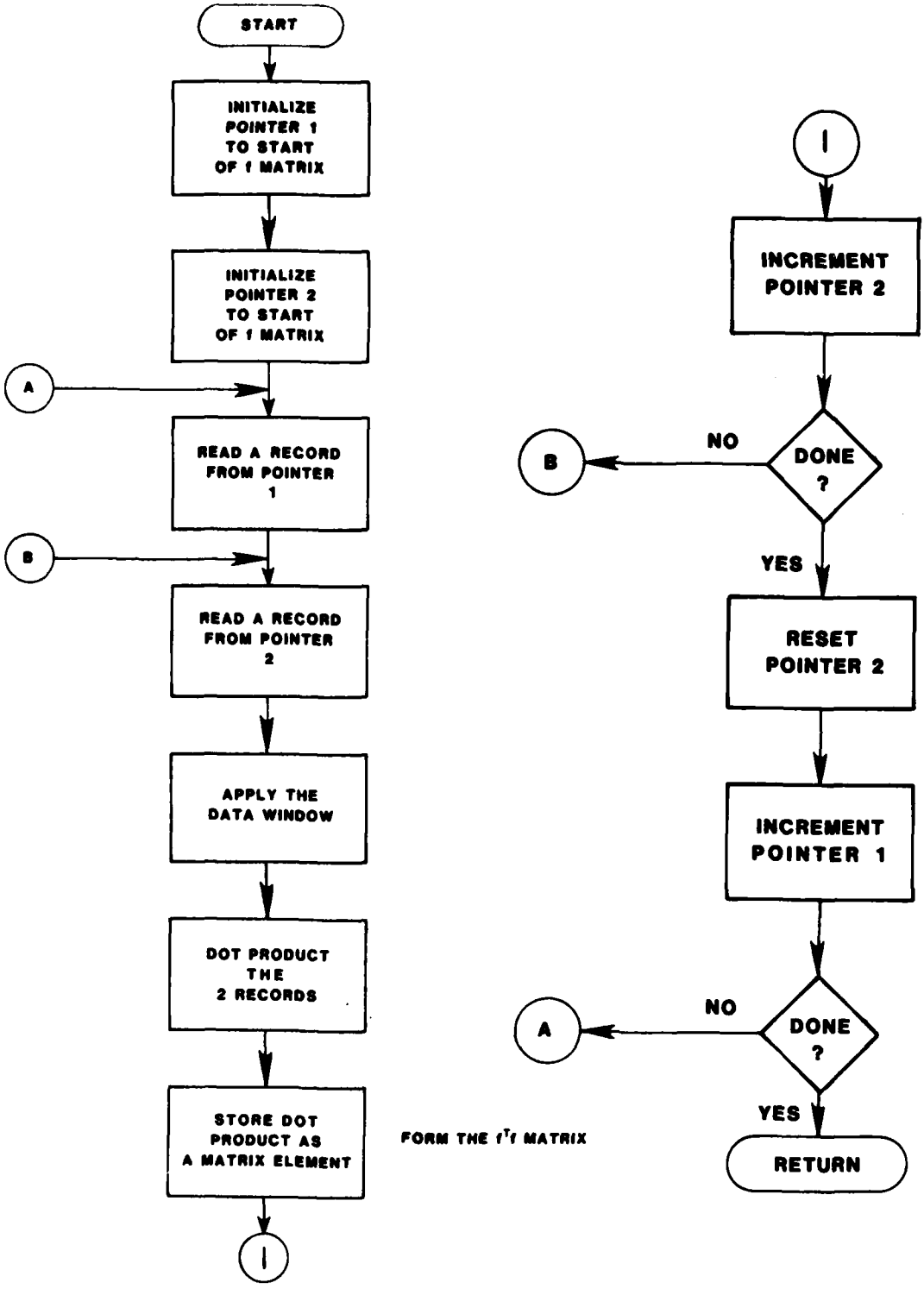

Figure 47. Construct the covariance matrix $f^T f$.

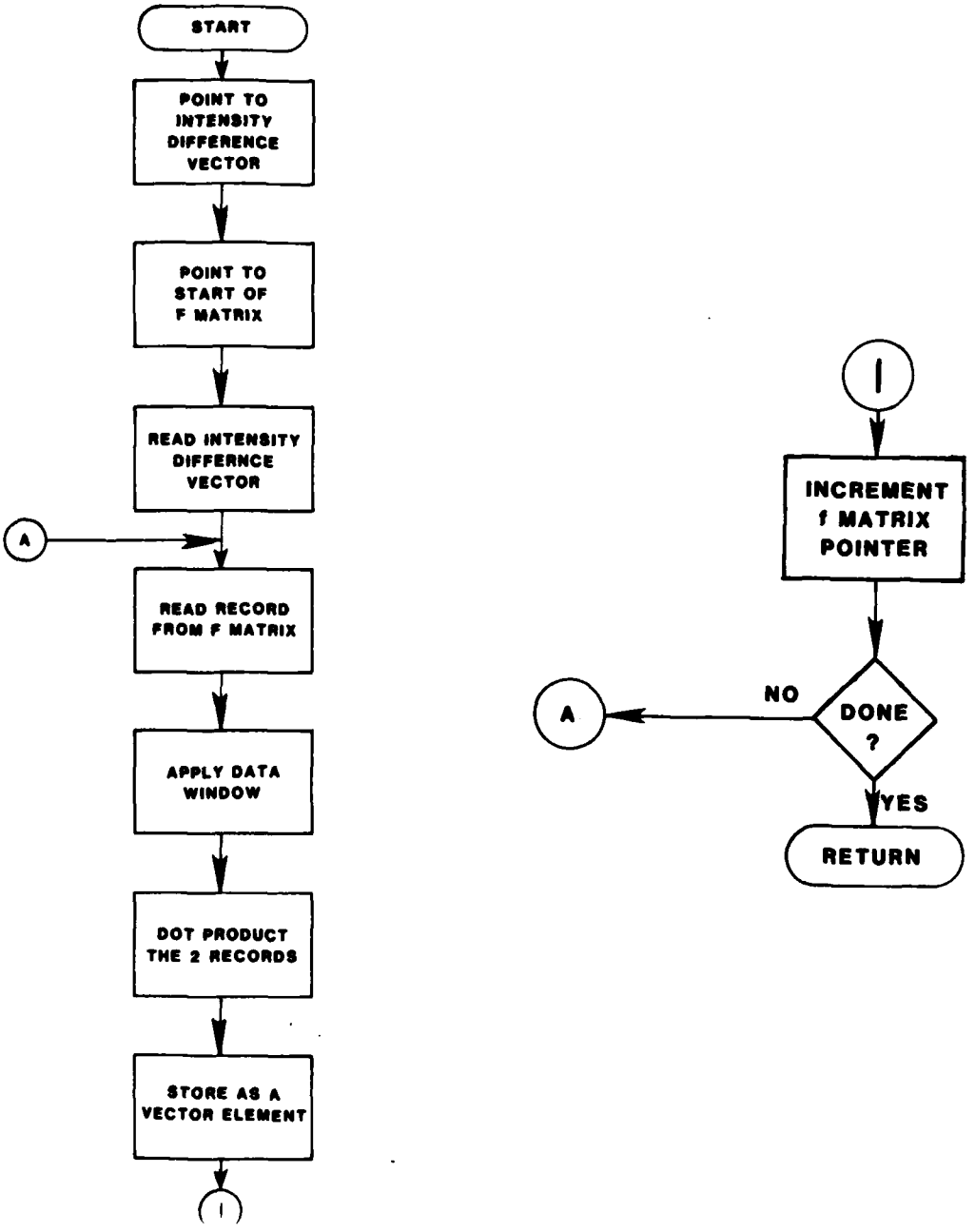
START
POINT TO INTENSITY DIFFERENCE VECTOR
POINT TO START OF F MATRIX
READ INTENSITY DIFFERNCE VECTOR
A
READ RECORD FROM F MATRIX
APPLY DATA WINDOW
DOT PRODUCT THE 2 RECORDS
STORE AS A VECTOR ELEMENT
I
I
INCREMENT f MATRIX POINTER
NO
A
DONE ?
YES
RETURN

TABLE 1. CO_2 BANDS

BAND CENTER	UPPER LEVEL	LOWER LEVEL	ISOTOPE	BAND STRENGTH (10^{22} mol^{-1}cm^{2}cm^{-1})
667.379	01101	00001	626	82580
647.058	11102	10002	626	222
648.484	01101	00001	636	860
688.678	11101	10001	626	148.8
622.368	01101	00001	628	330
668.109	03301	02201	626	382.4
667.750	02201	01101	626	6488
618.033	10002	01101	626	1436
720.808	10001	01101	626	1853

TABLE 2. STANDARD ATMOSPHERE -- MIDLATITUDE SUMMER

LAYER HEIGHT	TEMPERATURE	PRESSURE	ATM - CM
0	291	1.000	---
0-2	290	.792	58.9
2-4	279	.620	47.5
4-6	267	.481	37.6
6-8	255	.367	30.0
8-10	242	.277	23.1
10-12	229	.206	17.8
12-14	216	.151	13.4
14-16	216	.110	9.81
16-18	216	.0802	7.01
18-20	217	.0587	5.00
20-22	219	.0431	3.60
22-24	222	.0318	2.60
24-27	224	.0216	2.36
27-30	234	.0130	1.96
30-	243	.0130	----
		TOTAL	260.6 Atm. Cm.

TABLE 3. SPECTRAL CHANNELS FOR 15 μm CO_2^*

CHANNEL	CENTER FREQUENCY CM^{-1}	INTERGER POSITION
1	667.50	1844
2	668.70	1976
3	667.00	1829
4	666.00	1802
5	652.75	1440
6	646.65	1274
7	635.77	977
8	627.75	758
9	623.23	634
10	607.00	191

All channels have 0.5 cm^{-1} width.

* *Kaplan et al., see reference.*

TABLE 4. COVARIANCE ERROR MATRIX $(F^TF)^{-1}$

0.34394E+11	-0.10925E+11	-0.29315E+11	0.48036E+11	-0.50462E+11	0.27765E+11	0.79478E+10
-0.35115E+11	0.40790E+11	-0.23476E+11	0.32885E+09	0.67474E+10	-0.22449E+10	0.73254E+07
-0.10932E+11	0.20809E+11	-0.70297E+10	-0.20443E+11	0.39927E+11	-0.31423E+11	0.32049E+10
0.24099E+11	-0.32663E+11	0.18096E+11	0.40976E+10	-0.98049E+10	0.31227E+10	-0.76137E+07
-0.29291E+11	-0.70505E+10	0.47084E+11	-0.44173E+11	0.22829E+11	-0.25426E+10	-0.21236E+10
-0.23365E+10	-0.24748E+10	0.20665E+11	-0.35119E+11	0.25004E+11	-0.62059E+10	0.14373E+08
0.47978E+11	-0.20388E+11	-0.44192E+11	0.87408E+11	-0.10630E+12	0.82880E+11	-0.48303E+11
0.12078E+11	0.36592E+11	-0.91834E+11	0.11030E+12	-0.65948E+11	0.14533E+11	-0.43284E+08
-0.50290E+11	0.39780E+11	0.22834E+11	-0.10619E+12	0.20463E+12	-0.24291E+12	0.22663E+12
-0.13362E+12	-0.41918E+11	0.25298E+12	-0.33487E+12	0.20212E+12	-0.43677E+11	0.13929E+09
0.27389E+11	-0.31128E+11	-0.24644E+10	0.82422E+11	-0.24230E+12	0.40758E+12	-0.52435E+12
0.41827E+12	-0.41870E+11	-0.47239E+12	0.70727E+12	-0.43958E+12	0.95437E+11	-0.29291E+09
0.86117E+10	0.27077E+10	-0.23599E+10	-0.47244E+11	0.22483E+12	-0.52278E+12	0.87803E+12
-0.87105E+12	0.27256E+12	0.70464E+12	-0.12246E+13	0.79114E+12	-0.17434E+12	0.50421E+09
-0.35853E+11	0.24636E+11	-0.19971E+10	0.10692E+11	-0.13100E+12	0.41519E+12	-0.86873E+12
0.10433E+13	-0.51938E+12	-0.61235E+12	0.13507E+13	-0.93265E+12	0.21272E+12	-0.59523E+09
0.41122E+11	-0.32887E+11	-0.27073E+10	0.37430E+11	-0.43740E+11	-0.39105E+11	0.26909E+12
-0.51670E+12	0.48071E+12	0.35938E+11	-0.59725E+12	0.52184E+12	-0.13448E+12	0.39879E+09
-0.22980E+11	0.17708E+11	0.20548E+11	-0.91191E+11	0.25208E+12	-0.47219E+12	0.70636E+12
-0.61599E+12	0.39363E+11	0.71739E+12	-0.93542E+12	0.49826E+12	-0.89514E+11	0.18049E+09
-0.71174E+09	0.48727E+10	-0.34710E+11	0.10852E+12	-0.33168E+12	0.70403E+12	-0.12233E+13
0.13529E+13	-0.60201E+12	-0.93176E+12	0.19241E+13	-0.13156E+13	0.29739E+12	-0.81614E+09
0.74695E+10	-0.10335E+11	0.24689E+11	-0.64632E+11	0.19966E+12	-0.43680E+12	0.78927E+12
-0.93313E+12	0.52470E+12	0.49501E+12	-0.13141E+13	0.99508E+12	-0.24565E+12	0.78300E+09
-0.24118E+10	0.32439E+10	-0.61291E+10	0.14219E+11	-0.43080E+11	0.94728E+11	-0.17379E+12
0.21271E+12	-0.13509E+12	-0.88674E+11	0.29688E+12	-0.24553E+12	0.66074E+11	-0.25481E+09
0.78129E+07	-0.79647E+07	0.14149E+08	-0.42379E+08	0.13757E+09	-0.29087E+09	0.50266E+09
-0.59528E+09	0.40066E+09	0.17806E+09	-0.81478E+09	0.78276E+09	-0.25484E+09	0.18702E+08

RMS (DIAGONAL) = 0.702371E+06 Window 0.4096, (0-13.653 cm)

TABLE 5. COVARIANCE ERROR MATRIX $(F^TF)^{-1}$

0.37552E+13	-0.23835E+13	-0.23289E+13	0.55326E+13	-0.53924E+13	0.18859E+13	0.16364E+13
-0.34498E+13	0.37029E+13	-0.20542E+13	-0.75999E+12	0.16538E+13	-0.70694E+12	-0.57463E+11
-0.23837E+13	0.31958E+13	-0.66387E+12	-0.34424E+13	0.57194E+13	-0.41854E+13	0.19739E+13
0.15928E+12	-0.33442E+13	0.52179E+13	-0.20174E+13	-0.15078E+13	0.13061E+13	0.13748E+12
-0.23286E+13	-0.66425E+12	0.47041E+13	-0.41802E+13	0.49038E+11	0.41673E+13	-0.64408E+13
0.51467E+13	0.22734E+12	-0.55086E+13	0.40522E+13	0.23015E+12	-0.10656E+13	-0.12952E+12
0.55327E+13	-0.34420E+13	-0.41810E+13	0.96964E+13	-0.91292E+13	0.22481E+13	0.36346E+13
-0.49176E+13	0.36563E+13	-0.19270E+13	0.88250E+12	-0.42737E+12	0.25828E+11	-0.42732E+11
-0.53939E+13	0.57202E+13	0.50482E+11	-0.91318E+13	0.16841E+14	-0.15776E+14	0.10845E+14
-0.37093E+13	-0.76750E+13	0.17190E+14	-0.14521E+14	0.51599E+13	-0.16774E+12	0.11972E+12
0.18901E+13	-0.41889E+13	0.41661E+13	0.22547E+13	-0.15784E+14	0.28380E+14	-0.34503E+14
0.22806E+14	0.70036E+13	-0.35481E+14	0.34846E+14	-0.14452E+14	0.19049E+13	0.13644E+11
0.16289E+13	0.19802E+13	-0.64391E+13	0.36228E+13	0.10865E+14	-0.34518E+14	0.60236E+14
-0.57739E+14	0.87952E+13	0.57941E+14	-0.70658E+14	0.30551E+14	-0.25776E+13	0.22931E+12
-0.34421E+13	0.15400E+12	0.51434E+13	-0.49050E+13	-0.37311E+13	0.22830E+14	-0.57757E+14
0.79213E+14	-0.38323E+14	-0.54331E+14	0.91982E+14	-0.44664E+14	0.31683E+13	-0.64348E+12
0.37012E+13	-0.33448E+13	0.23023E+12	0.36529E+13	-0.76678E+13	0.69864E+13	0.88240E+13
-0.38348E+14	0.47369E+14	-0.72380E+13	-0.41924E+14	0.37754E+14	-0.93937E+13	-0.16023E+12
-0.20616E+13	0.52244E+13	-0.55070E+13	-0.19382E+13	0.17206E+14	-0.35485E+14	0.57922E+14
-0.54295E+14	-0.72679E+13	0.82921E+14	-0.69712E+14	0.65626E+13	0.12121E+14	0.16101E+13
-0.75027E+12	-0.20236E+13	0.40471E+13	0.89819E+12	-0.14545E+14	0.34867E+14	-0.70664E+14
0.91965E+14	-0.41889E+14	-0.69741E+14	0.11640E+15	-0.58063E+14	0.47775E+13	-0.82078E+12
0.16492E+13	-0.15056E+13	0.23348E+12	-0.43515E+12	0.51729E+13	-0.14469E+14	0.30567E+14
-0.44668E+14	0.37737E+14	0.65894E+13	-0.58078E+14	0.54178E+14	-0.17721E+14	-0.95433E+12
-0.70631E+12	0.13059E+13	-0.10661E+13	0.26949E+11	-0.17052E+12	0.19105E+13	-0.25854E+13
0.31732E+13	-0.93906E+13	0.12111E+14	0.47851E+13	-0.17723E+14	0.10320E+14	0.98835E+12
-0.57468E+11	0.13745E+12	-0.12947E+12	-0.42740E+11	0.11956E+12	0.14084E+11	0.22859E+12
-0.64291E+12	-0.16010E+12	0.16092E+13	-0.82007E+12	-0.95452E+12	0.98834E+12	0.13473E+12

RMS (DIAGONAL) = 0.607890E+07 Window 50-150, (.166-.500 cm)

TABLE 6. COVARIANCE ERROR MATRIX $(F^TF)^{-1}$

0.34490E+12	-0.18530E+12	-0.20138E+12	0.45889E+12	-0.54675E+12	0.32874E+12	0.23156E+12
-0.93009E+12	0.11693E+13	-0.46333E+12	-0.66163E+12	0.86321E+12	-0.32745E+12	-0.20120E+11
-0.18526E+12	0.22423E+12	-0.40684E+11	-0.24788E+12	0.50670E+12	-0.53153E+12	0.12435E+12
0.76436E+12	-0.13706E+13	0.77187E+12	0.58019E+12	-0.93717E+12	0.38621E+12	0.28122E+11
-0.20137E+12	-0.40700E+11	0.35532E+12	-0.34504E+12	0.51615E+11	0.39015E+12	-0.55000E+12
-0.38174E+11	0.76882E+12	-0.59629E+12	-0.24638E+12	0.48659E+12	-0.21617E+12	-0.23100E+11
0.45852E+12	-0.24756E+12	-0.34513E+12	0.78443E+12	-0.93314E+12	0.57608E+12	-0.19032E+11
-0.29471E+12	0.29883E+12	-0.37916E+12	0.52109E+12	-0.33292E+12	0.91864E+11	0.10549E+11
-0.54519E+12	0.50534E+12	0.51876E+11	-0.93266E+12	0.21846E+13	-0.32298E+13	0.34450E+13
-0.14339E+13	-0.17300E+13	0.37178E+13	-0.32522E+13	0.14473E+13	-0.26483E+12	-0.91691E+10
0.32487E+12	-0.52816E+12	0.38967E+12	0.57413E+12	-0.32269E+13	0.74670E+13	-0.11158E+14
0.75321E+13	0.26703E+13	-0.11127E+14	0.10403E+14	-0.43392E+13	0.72660E+12	0.36764E+11
0.23877E+12	0.11794E+12	-0.54923E+12	-0.13676E+11	0.34329E+13	-0.11142E+14	0.21075E+14
-0.19507E+14	0.16004E+13	0.19722E+14	-0.23509E+14	0.11482E+14	-0.24681E+13	-0.18778E+12
-0.93800E+12	0.77180E+12	-0.39109E+11	-0.30336E+12	-0.14089E+13	0.74861E+13	-0.19455E+14
0.26196E+14	-0.14336E+14	-0.13902E+14	0.30714E+14	-0.20407E+14	0.57151E+13	0.44020E+12
0.11725E+13	-0.13743E+13	0.76954E+12	0.30595E+12	-0.17563E+13	0.27281E+13	0.15080E+13
-0.14258E+14	0.23131E+14	-0.91573E+13	-0.17457E+14	0.20929E+14	-0.76136E+13	-0.53030E+12
-0.45773E+12	0.76741E+12	-0.59607E+12	-0.37720E+12	0.37188E+13	-0.11140E+14	0.19767E+14
-0.13990E+14	-0.90681E+13	0.27057E+14	-0.16338E+14	-0.11387E+13	0.30364E+13	0.20554E+12
-0.67192E+12	0.58989E+12	-0.24772E+12	0.51037E+12	-0.32216E+13	0.10347E+14	-0.23450E+14
0.30724E+14	-0.17563E+14	-0.16229E+14	0.38493E+14	-0.26196E+14	0.69837E+13	0.43542E+12
0.86981E+12	-0.94389E+12	0.48784E+12	-0.32404E+12	0.14181E+13	-0.42804E+13	0.11402E+14
-0.20370E+14	0.20982E+14	-0.12411E+13	-0.26138E+14	0.26617E+14	-0.95009E+13	-0.64915E+12
-0.32921E+12	0.38811E+12	-0.21660E+12	0.89062E+11	-0.25488E+12	0.70558E+12	-0.24372E+13
0.56951E+13	-0.76241E+13	0.30713E+13	0.69552E+13	-0.94926E+13	0.42279E+13	0.38953E+12
-0.20239E+11	0.28251E+11	-0.23128E+11	0.10351E+11	-0.84594E+10	0.35244E+11	-0.18550E+12
0.43864E+12	-0.53095E+12	0.20806E+12	0.43325E+12	-0.64844E+12	0.38949E+12	0.60773E+11

RMS (DIAGONAL) = 0.356789E+07 Window 150-250, (.500-.833 cm)

TABLE 7. COVARIANCE ERROR MATRIX $(F^TF)^{-1}$

0.41859E+13	-0.25692E+13	-0.66415E+12	0.32588E+13	-0.45219E+13	0.29423E+13	-0.21828E+12
-0.13853E+13	0.11427E+13	0.64290E+12	-0.20946E+13	0.13007E+13	-0.11004E+12	0.49843E+11
-0.25692E+13	0.27845E+13	-0.11184E+13	-0.13380E+13	0.30838E+13	-0.25678E+13	-0.51677E+11
0.20748E+13	-0.16396E+13	-0.12882E+13	0.37856E+13	-0.26408E+13	0.43752E+12	-0.46846E+11
-0.66412E+12	-0.11184E+13	0.26068E+13	-0.24980E+13	0.17478E+13	-0.13580E+12	-0.26963E+12
-0.50188E+12	0.35320E+12	0.15938E+13	-0.38888E+13	0.33263E+13	-0.10461E+13	-0.62187E+11
0.32587E+13	-0.13379E+13	-0.24981E+13	0.58039E+13	-0.80289E+13	0.52394E+13	-0.27304E+12
-0.25179E+13	0.38108E+13	-0.39922E+13	0.34331E+13	-0.24259E+13	0.10346E+13	0.14687E+12
-0.45218E+13	0.30838E+13	0.17478E+13	-0.80289E+13	0.15321E+14	-0.15559E+14	0.91504E+13
-0.64060E+12	-0.98874E+13	0.16644E+14	-0.12463E+14	0.42203E+13	-0.60091E+12	-0.12022E+12
0.29424E+13	-0.25679E+13	-0.13572E+12	0.52393E+13	-0.15558E+14	0.26612E+14	-0.32844E+14
0.23320E+14	0.64276E+13	-0.38028E+14	0.38739E+14	-0.15362E+14	0.15489E+13	0.84162E+11
-0.21864E+12	-0.51315E+11	-0.27001E+12	-0.27252E+12	0.91494E+13	-0.32843E+14	0.63762E+14
-0.63875E+14	0.13991E+14	0.57593E+14	-0.79917E+14	0.40160E+14	-0.63037E+13	-0.21254E+12
-0.13850E+13	0.20743E+13	-0.50130E+12	-0.25188E+13	-0.63881E+12	0.23318E+14	-0.63874E+14
0.80048E+14	-0.40151E+14	-0.43035E+14	0.92119E+14	-0.58485E+14	0.12777E+14	0.57764E+12
0.11426E+13	-0.16394E+13	0.35277E+12	0.38116E+13	-0.98891E+13	0.64300E+13	0.13988E+14
-0.40149E+14	0.51095E+14	-0.19060E+14	-0.37429E+14	0.44655E+14	-0.15842E+14	-0.11407E+13
0.64260E+12	-0.12879E+13	0.15936E+13	-0.39921E+13	0.16644E+14	-0.38028E+14	0.57595E+14
-0.43038E+14	-0.19057E+14	0.80852E+14	-0.67929E+14	0.14154E+14	0.61518E+13	0.10146E+13
-0.20943E+13	0.37852E+13	-0.38881E+13	0.34320E+13	-0.12461E+14	0.38737E+14	-0.79917E+14
0.92122E+14	-0.37433E+14	-0.67926E+14	0.12439E+15	-0.75143E+14	0.15129E+14	0.56542E+12
0.13006E+13	-0.26406E+13	0.33258E+13	-0.24249E+13	0.42182E+13	-0.15360E+14	0.40159E+14
-0.58487E+14	0.44658E+14	0.14151E+14	-0.75142E+14	0.64661E+14	-0.20652E+14	-0.15409E+13
-0.11006E+12	0.43751E+12	-0.10459E+13	0.10343E+13	-0.60027E+12	0.15484E+13	-0.63039E+13
0.12778E+14	-0.15843E+14	0.61523E+13	0.15129E+14	-0.20652E+14	0.96692E+13	0.10622E+13
0.49838E+11	-0.46842E+11	-0.62180E+11	0.14685E+12	-0.12018E+12	0.84152E+11	-0.21261E+12
0.57776E+12	-0.11408E+13	0.10146E+13	0.56551E+12	-0.15410E+13	0.10622E+13	0.17158E+12

RMS (DIAGONAL) = 0.616419E+07 Window 250-350, (.833-1.167 cm)

TABLE 8. COVARIANCE ERROR MATRIX $(F^TF)^{-1}$

0.82335E+12	-0.58044E+12	-0.18440E+12	0.87813E+12	-0.12816E+13	0.83255E+12	0.30022E+12
-0.12548E+13	0.12019E+13	-0.85256E+11	-0.98508E+12	0.79569E+12	-0.10054E+12	0.28736E+11
-0.58040E+12	0.84833E+12	-0.45968E+12	-0.45791E+12	0.12854E+13	-0.12019E+13	0.16941E+12
0.10808E+13	-0.14863E+13	0.47585E+12	0.11108E+13	-0.11886E+13	0.28678E+12	-0.92223E+10
-0.18439E+12	-0.45969E+12	0.99566E+12	-0.71629E+12	0.73105E+11	0.57954E+12	-0.83157E+12
0.31515E+12	0.52405E+12	-0.60230E+12	-0.55412E+12	0.99954E+12	-0.41710E+12	-0.38861E+11
0.87798E+12	-0.45781E+12	-0.71629E+12	0.16994E+13	-0.22077E+13	0.13069E+13	0.55172E+12
-0.17478E+13	0.14275E+13	-0.33655E+12	0.52566E+11	-0.32526E+12	0.36035E+12	0.83500E+11
-0.12812E+13	0.12851E+13	0.73045E+11	-0.22074E+13	0.44837E+13	-0.45933E+13	0.22111E+13
0.11664E+13	-0.33323E+13	0.32913E+13	-0.19189E+13	0.83947E+12	-0.54058E+12	-0.13639E+12
0.83173E+12	-0.12014E+13	0.57978E+12	0.13059E+13	-0.45920E+13	0.75923E+13	-0.86951E+13
0.51620E+13	0.16452E+13	-0.77281E+13	0.87826E+13	-0.49879E+13	0.15332E+13	0.17629E+12
0.30172E+12	0.16824E+12	-0.83207E+12	0.55423E+12	0.22068E+13	-0.86916E+13	0.17364E+14
-0.18131E+14	0.66872E+13	0.11555E+14	-0.21432E+14	0.14316E+14	-0.39059E+13	-0.24501E+12
-0.12567E+13	0.10825E+13	0.31569E+12	-0.17514E+13	0.11732E+13	0.51553E+13	-0.18128E+14
0.25883E+14	-0.17166E+14	-0.79238E+13	0.28134E+14	-0.21862E+14	0.62833E+13	0.35976E+12
0.12034E+13	-0.14878E+13	0.52383E+12	0.14303E+13	-0.33379E+13	0.16510E+13	0.66835E+13
-0.17164E+14	0.19760E+14	-0.52113E+13	-0.17451E+14	0.19632E+14	-0.69025E+13	-0.45942E+12
-0.84739E+11	0.47563E+12	-0.60263E+12	-0.33587E+12	0.32904E+13	-0.77278E+13	0.11556E+14
-0.79262E+13	-0.52090E+13	0.16979E+14	-0.11329E+14	-0.19559E+12	0.21691E+13	0.23918E+12
-0.98770E+12	0.11131E+13	-0.55346E+12	0.48097E+11	-0.19109E+13	0.87758E+13	-0.21431E+14
0.28140E+14	-0.17457E+14	-0.11326E+14	0.34994E+14	-0.27045E+14	0.77319E+13	0.45389E+12
0.79802E+12	-0.11907E+13	0.99908E+12	-0.32126E+12	0.83223E+12	-0.49819E+13	0.14316E+14
-0.21868E+14	0.19638E+14	-0.19743E+12	-0.27045E+14	0.27920E+14	-0.10025E+14	-0.74646E+12
-0.10132E+12	0.28749E+12	-0.41697E+12	0.35906E+12	-0.53826E+12	0.15315E+13	-0.39064E+13
0.62859E+13	-0.69051E+13	0.21695E+13	0.77331E+13	-0.10026E+14	0.44316E+13	0.45421E+12
0.28676E+11	-0.91694E+10	-0.38852E+11	0.83412E+11	-0.13624E+12	0.17622E+12	-0.24517E+12
0.36012E+12	-0.45973E+12	0.23918E+12	0.45419E+12	-0.74671E+12	0.45427E+12	0.73600E+11

RMS (DIAGONAL) = 0.342102E+07 Window 350-450, (1.167-1.500 cm)

TABLE 9. COVARIANCE ERROR MATRIX $(F^TF)^{-1}$

0.36135E+13	-0.19747E+13	-0.64447E+12	0.23547E+13	-0.32982E+13	0.23500E+13	-0.20735E+12
-0.18324E+13	0.21626E+13	-0.48337E+12	-0.23013E+13	0.29766E+13	-0.17449E+13	-0.28178E+12
-0.19746E+13	0.19977E+13	-0.76613E+12	-0.83188E+12	0.19699E+13	-0.20495E+13	0.15236E+13
-0.48668E+12	-0.25744E+12	0.17828E+12	0.69714E+12	-0.10053E+13	0.66276E+12	0.12776E+12
-0.64454E+12	-0.76609E+12	0.21006E+13	-0.21341E+13	0.19603E+13	-0.95837E+12	-0.64838E+12
0.21285E+13	-0.26667E+13	0.21355E+13	-0.13660E+13	0.46175E+12	0.16289E+12	0.49367E+11
0.23549E+13	-0.83195E+12	-0.21341E+13	0.43328E+13	-0.61728E+13	0.53377E+13	-0.25073E+13
-0.16277E+13	0.47055E+13	-0.54542E+13	0.45000E+13	-0.20029E+13	-0.15778E+12	-0.13655E+12
-0.32984E+13	0.19700E+13	0.19603E+13	-0.61729E+13	0.11546E+14	-0.13569E+14	0.11510E+14
-0.37031E+13	-0.54078E+13	0.12467E+14	-0.15266E+14	0.95350E+13	-0.18803E+13	0.42528E+11
0.23502E+13	-0.20496E+13	-0.95852E+12	0.53381E+13	-0.13570E+14	0.22672E+14	-0.28933E+14
0.21109E+14	-0.30686E+13	-0.19226E+14	0.36226E+14	-0.28251E+14	0.90649E+13	0.63119E+12
-0.20745E+12	0.15236E+13	-0.64797E+12	-0.25081E+13	0.11511E+14	-0.28934E+14	0.50862E+14
-0.50372E+14	0.23692E+14	0.22141E+14	-0.64438E+14	0.56771E+14	-0.21469E+14	-0.19817E+13
-0.18325E+13	-0.48643E+12	0.21280E+13	-0.16268E+13	-0.37048E+13	0.21111E+14	-0.50373E+14
0.62311E+14	-0.42187E+14	-0.11247E+14	0.68297E+14	-0.65921E+14	0.26940E+14	0.27830E+13
0.21630E+13	-0.25779E+12	-0.26663E+13	0.47048E+13	-0.54064E+13	-0.30707E+13	0.23694E+14
-0.42189E+14	0.44113E+14	-0.13626E+14	-0.37053E+14	0.47650E+14	-0.22296E+14	-0.25451E+13
-0.48378E+12	0.17850E+12	0.21355E+13	-0.54542E+13	0.12467E+14	-0.19225E+14	0.22137E+14
-0.11242E+14	-0.13629E+14	0.35445E+14	-0.29252E+14	0.70755E+13	0.29348E+13	0.77764E+12
-0.23011E+13	0.69723E+12	-0.13666E+13	0.45011E+13	-0.15268E+14	0.36227E+14	-0.64437E+14
0.68294E+14	-0.37048E+14	-0.29257E+14	0.94722E+14	-0.83218E+14	0.30283E+14	0.27112E+13
0.29766E+13	-0.10056E+13	0.46251E+12	-0.20043E+13	0.95375E+13	-0.28254E+14	0.56772E+14
-0.65921E+14	0.47647E+14	0.70815E+13	-0.83222E+14	0.88907E+14	-0.37694E+14	-0.38773E+13
-0.17450E+13	0.66289E+12	0.16254E+12	-0.15711E+12	-0.18816E+13	0.90667E+13	-0.21471E+14
0.26942E+14	-0.22296E+14	0.29319E+13	0.30287E+14	-0.37696E+14	0.18498E+14	0.22587E+13
-0.28180E+12	0.12778E+12	0.49325E+11	-0.13647E+12	0.42355E+11	0.63145E+12	-0.19820E+13
0.27832E+13	-0.25451E+13	0.77728E+12	0.27117E+13	-0.38776E+13	0.22588E+13	0.34930E+12

RMS (DIAGONAL) = 0.561547E+07 Window 450-550 (1.500-1.833 cm)

TABLE 10. COVARIANCE ERROR MATRIX $(F^TF)^{-1}$

0.17680E+13	-0.12120E+13	-0.32557E+12	0.16166E+13	-0.24807E+13	0.24341E+13	-0.17636E+13
0.10381E+12	0.18338E+13	-0.21689E+13	0.44431E+12	0.63308E+12	-0.24549E+12	0.30678E+11
-0.12119E+13	0.14940E+13	-0.61713E+12	-0.82923E+12	0.19771E+13	-0.23515E+13	0.21299E+13
-0.64982E+12	-0.14521E+13	0.21627E+13	-0.47125E+12	-0.79193E+12	0.39053E+12	-0.62948E+10
-0.32568E+12	-0.61704E+12	0.14070E+13	-0.11124E+13	0.42851E+12	0.50356E+12	-0.13561E+13
0.14000E+13	-0.47500E+12	-0.64543E+12	0.28733E+12	0.55507E+12	-0.44038E+12	-0.47291E+11
0.16166E+13	-0.82940E+12	-0.11123E+13	0.25599E+13	-0.32853E+13	0.25594E+13	-0.10347E+13
-0.10872E+13	0.28345E+13	-0.24817E+13	0.84366E+12	-0.13804E+12	0.22068E+12	0.82002E+11
-0.24811E+13	0.19777E+13	0.42810E+12	-0.32856E+13	0.63952E+13	-0.78202E+13	0.73351E+13
-0.28127E+13	-0.44267E+13	0.86463E+13	-0.63539E+13	0.21618E+13	-0.59086E+12	-0.17155E+12
0.24357E+13	-0.23534E+13	0.50429E+12	0.25608E+13	-0.78228E+13	0.13434E+14	-0.17242E+14
0.11997E+14	0.21209E+13	-0.15727E+14	0.17005E+14	-0.83855E+13	0.22411E+13	0.31635E+12
-0.17673E+13	0.21337E+13	-0.13572E+13	-0.10382E+13	0.73432E+13	-0.17250E+14	0.27963E+14
-0.25647E+14	0.52312E+13	0.22223E+14	-0.31257E+14	0.17631E+14	-0.47727E+13	-0.46687E+12
0.10861E+12	-0.65448E+12	0.14009E+13	-0.10821E+13	-0.28253E+13	0.12014E+14	-0.25662E+14
0.30661E+14	-0.15573E+14	-0.16298E+14	0.34488E+14	-0.22742E+14	0.66383E+13	0.57120E+12
0.18305E+13	-0.14493E+13	-0.47503E+12	0.28306E+13	-0.44160E+13	0.21024E+13	0.52564E+13
-0.15593E+14	0.21012E+14	-0.81015E+13	-0.15328E+14	0.18835E+14	-0.73834E+13	-0.66373E+12
-0.21704E+13	0.21646E+13	-0.64641E+12	-0.24827E+13	0.86480E+13	-0.15725E+14	0.22210E+14
-0.16275E+14	-0.81241E+13	0.30727E+14	-0.21777E+14	0.18103E+13	0.25850E+13	0.32714E+12
0.45016E+12	-0.47702E+12	0.28852E+12	0.84974E+12	-0.63689E+13	0.17024E+14	-0.31272E+14
0.34483E+14	-0.15301E+14	-0.21805E+14	0.43404E+14	-0.29090E+14	0.84005E+13	0.68097E+12
0.62823E+12	-0.78739E+12	0.55446E+12	-0.14333E+12	0.21753E+13	-0.84051E+13	0.17652E+14
-0.22750E+14	0.18821E+14	0.18364E+13	-0.29104E+14	0.29135E+14	-0.11240E+14	-0.10682E+13
-0.24381E+12	0.38901E+12	-0.44023E+12	0.22254E+12	-0.59558E+12	0.22481E+13	-0.47805E+13
0.66420E+13	-0.73791E+13	0.25757E+13	0.84066E+13	-0.11241E+14	0.55672E+13	0.73256E+12
0.30827E+11	-0.64319E+10	-0.47277E+11	0.82165E+11	-0.17194E+12	0.31687E+12	-0.46736E+12
0.57127E+12	-0.66318E+12	0.32642E+12	0.68118E+12	-0.10680E+13	0.73247E+12	0.15409E+12

RMS (DIAGONAL) = 0.392502E+07 Window 550-650, (1.833-2.167 cm)

TABLE 11. COVARIANCE ERROR MATRIX $(F^TF)^{-1}$

0.79824E+11	-0.35849E+11	-0.62792E+11	0.12054E+12	-0.12405E+12	0.34178E+11	0.10778E+12
-0.18232E+12	0.12553E+12	0.22054E+11	-0.10632E+12	0.65735E+11	-0.11477E+11	0.15594E+09
-0.35828E+11	0.52932E+11	-0.95017E+10	-0.65823E+11	0.11429E+12	-0.67293E+11	-0.56094E+11
0.16070E+12	-0.15262E+12	0.15273E+11	0.11137E+12	-0.93112E+11	0.21850E+11	-0.15088E+09
-0.62807E+11	-0.94877E+10	0.99738E+11	-0.95472E+11	0.32412E+11	0.43869E+11	-0.75242E+11
0.21647E+11	0.54546E+11	-0.52942E+11	-0.34105E+11	0.65001E+11	-0.21890E+11	-0.29755E+07
0.12047E+12	-0.65784E+11	-0.95444E+11	0.21089E+12	-0.23043E+12	0.84214E+11	0.12619E+12
-0.21355E+12	0.12844E+12	0.16520E+11	-0.40289E+11	-0.10292E+11	0.12289E+11	0.21541E+09
-0.12369E+12	0.11402E+12	0.32315E+11	-0.23008E+12	0.40089E+12	-0.33768E+12	0.59229E+11
0.23237E+12	-0.30920E+12	0.16907E+12	-0.67407E+11	0.56822E+11	-0.23153E+11	-0.30976E+09
0.33340E+11	-0.66600E+11	0.44065E+11	0.83145E+11	-0.33639E+12	0.56179E+12	-0.57884E+12
0.20762E+12	0.26473E+12	-0.52660E+12	0.52614E+12	-0.30905E+12	0.72289E+11	0.34354E+08
0.10911E+12	-0.57274E+11	-0.75487E+11	0.12812E+12	0.55975E+11	-0.57603E+12	0.12200E+13
-0.12031E+13	0.32263E+12	0.91675E+12	-0.14538E+13	0.87924E+12	-0.18017E+12	0.72567E+09
-0.18334E+12	0.16174E+12	0.21727E+11	-0.21536E+12	0.23649E+12	0.20177E+12	-0.11972E+13
0.19756E+13	-0.14308E+13	-0.62302E+12	0.21824E+13	-0.15533E+13	0.33613E+12	-0.10725E+10
0.12527E+12	-0.15261E+12	0.54751E+11	0.12874E+12	-0.31180E+12	0.27162E+12	0.31045E+12
-0.14196E+13	0.19544E+13	-0.57582E+12	-0.16146E+13	0.17077E+13	-0.46034E+12	0.62777E+09
0.23644E+11	0.13977E+11	-0.53262E+11	0.18282E+11	0.16750E+12	-0.52858E+12	0.92573E+12
-0.63805E+12	-0.56176E+12	0.14772E+13	-0.73567E+12	-0.24457E+12	0.19703E+12	0.19360E+08
-0.10779E+12	0.11282E+12	-0.33951E+11	-0.42736E+11	-0.62271E+11	0.51955E+12	-0.14482E+13
0.21844E+13	-0.16297E+13	-0.71786E+12	0.27875E+13	-0.21172E+13	0.48349E+12	-0.59672E+09
0.66181E+11	-0.93694E+11	0.65010E+11	-0.89814E+10	0.52845E+11	-0.30154E+12	0.86827E+12
-0.15458E+13	0.17131E+13	-0.26147E+12	-0.21060E+13	0.22171E+13	-0.63576E+12	0.99132E+09
-0.11467E+11	0.21896E+11	-0.21907E+11	0.12068E+11	-0.22191E+11	0.70062E+11	-0.17638E+12
0.33269E+12	-0.46049E+12	0.20161E+12	0.47876E+12	-0.63417E+12	0.20642E+12	-0.56729E+09
0.15582E+09	-0.15085E+09	-0.30144E+07	0.21589E+09	-0.31193E+09	0.39679E+08	0.71606E+09
-0.10628E+10	0.62609E+09	0.92224E+07	-0.58354E+09	0.98521E+09	-0.56657E+09	0.72072E+08

RMS (DIAGONAL) = 0.972643E+06 Window 0-650, (0-2.167 cm)

TABLE 12. COVARIANCE ERROR MATRIX $(F^TF)^{-1}$

0.11219E+12	-0.57394E+11	-0.69712E+11	0.15602E+12	-0.19200E+12	0.12639E+12	0.18278E+11
-0.17362E+12	0.23567E+12	-0.12049E+12	-0.66614E+11	0.10389E+12	-0.33889E+11	-0.94003E+09
-0.57383E+11	0.75987E+11	-0.16254E+11	-0.85470E+11	0.16913E+12	-0.15632E+12	0.42816E+11
0.13453E+12	-0.24817E+12	0.15654E+12	0.63773E+11	-0.12760E+12	0.46514E+11	0.16179E+10
-0.69731E+11	-0.16235E+11	0.11905E+12	-0.11375E+12	0.39679E+11	0.55081E+11	-0.96346E+11
0.26502E+11	0.82405E+11	-0.87750E+11	-0.42393E+11	0.10295E+12	-0.48481E+11	-0.41070E+10
0.15602E+12	-0.85486E+11	-0.11371E+12	0.26773E+12	-0.33312E+12	0.22706E+12	-0.43266E+11
-0.10856E+12	0.17278E+12	-0.16018E+12	0.14377E+12	-0.10656E+12	0.46732E+11	0.63243E+10
-0.19190E+12	0.16908E+12	0.39591E+11	-0.33296E+12	0.67000E+12	-0.81081E+12	0.70169E+12
-0.22888E+12	-0.40143E+12	0.80830E+12	-0.75537E+12	0.38672E+12	-0.10235E+12	-0.10630E+11
0.12612E+12	-0.15613E+12	0.55230E+11	0.22658E+12	-0.81026E+12	0.15195E+13	-0.20175E+13
0.13877E+13	0.25834E+12	-0.18732E+13	0.21595E+13	-0.11449E+13	0.26166E+12	0.18442E+11
0.18747E+11	0.42450E+11	-0.96544E+11	-0.42424E+11	0.70038E+12	-0.20165E+13	0.36101E+13
-0.34516E+13	0.77731E+12	0.29724E+13	-0.44223E+13	0.25755E+13	-0.59972E+12	-0.35210E+11
-0.17402E+12	0.13486E+12	0.26647E+11	-0.10931E+12	-0.22755E+12	0.13863E+13	-0.34507E+13
0.45027E+13	-0.25590E+13	-0.21939E+13	0.53848E+13	-0.37537E+13	0.99670E+12	0.59223E+11
0.23567E+12	-0.24819E+12	0.82433E+11	0.17280E+12	-0.40159E+12	0.25875E+12	0.77669E+12
-0.25585E+13	0.33616E+13	-0.10189E+13	-0.28926E+13	0.32953E+13	-0.11719E+13	-0.80240E+11
-0.12002E+12	0.15618E+12	-0.87962E+11	-0.15933E+12	0.80696E+12	-0.18722E+13	0.29723E+13
-0.21945E+13	-0.10184E+13	0.39825E+13	-0.29402E+13	0.26651E+12	0.41109E+12	0.49578E+11
-0.67135E+11	0.64179E+11	-0.42164E+11	0.14282E+12	-0.75390E+12	0.21584E+13	-0.44223E+13
0.53858E+13	-0.28932E+13	-0.29405E+13	0.69508E+13	-0.48672E+13	0.12623E+13	0.65949E+11
0.10410E+12	-0.12776E+12	0.10284E+12	-0.10617E+12	0.38621E+12	-0.11447E+13	0.25761E+13
-0.37548E+13	0.32957E+13	0.26734E+12	-0.48681E+13	0.47835E+13	-0.16817E+13	-0.12128E+12
-0.33908E+11	0.46529E+11	-0.48468E+11	0.46700E+11	-0.10237E+12	0.26186E+12	-0.60019E+12
0.99723E+12	-0.11721E+13	0.41061E+12	0.12629E+13	-0.16819E+13	0.75900E+12	0.76772E+11
-0.93922E+09	0.16173E+10	-0.41070E+10	0.63267E+10	-0.10643E+11	0.18475E+11	-0.35271E+11
0.59286E+11	-0.80256E+11	0.49522E+11	0.66030E+11	-0.12132E+12	0.76779E+11	0.12370E+11

RMS (DIAGONAL) = 0.148149E+07 Window 25-650, (.083-2.167 cm)

TABLE 13. COVARIANCE ERROR MATRIX $(F^TF)^{-1}$

0.11941E+12	-0.61186E+11	-0.73862E+11	0.16545E+12	-0.20180E+12	0.12890E+12	0.27963E+11
-0.19195E+12	0.25101E+12	-0.11947E+12	-0.82113E+11	0.11650E+12	-0.37111E+11	-0.91435E+09
-0.61187E+11	0.80285E+11	-0.16475E+11	-0.91055E+11	0.17815E+12	-0.16249E+12	0.41714E+11
0.14307E+12	-0.25952E+12	0.16195E+12	0.68877E+11	-0.13507E+12	0.49253E+11	0.15956E+10
-0.73864E+11	-0.16473E+11	0.12477E+12	-0.11952E+12	0.41332E+11	0.60605E+11	-0.10991E+12
0.41801E+11	0.75776E+11	-0.96410E+11	-0.27084E+11	0.94777E+11	-0.47722E+11	-0.42294E+10
0.16546E+12	-0.91070E+11	-0.11952E+12	0.28269E+12	-0.35215E+12	0.24000E+12	-0.42910E+11
-0.12267E+12	0.19218E+12	-0.17023E+12	0.14072E+12	-0.10195E+12	0.47149E+11	0.69690E+10
-0.20188E+12	0.17821E+12	0.41331E+11	-0.35220E+12	0.71396E+12	-0.87589E+12	0.77817E+12
-0.28054E+12	-0.40909E+12	0.87764E+12	-0.84463E+12	0.44273E+12	-0.12186E+12	-0.13101E+11
0.12909E+12	-0.16265E+12	0.60598E+11	0.24019E+12	-0.87616E+12	0.16617E+13	-0.22345E+13
0.15785E+13	0.21797E+12	-0.20360E+13	0.24237E+13	-0.13239E+13	0.32012E+12	0.23778E+11
0.27609E+11	0.42027E+11	-0.10989E+12	-0.43350E+11	0.77903E+12	-0.22354E+13	0.39884E+13
-0.38184E+13	0.89385E+12	0.32369E+13	-0.48970E+13	0.29037E+13	-0.70436E+12	-0.43473E+11
-0.19154E+12	0.14269E+12	0.41777E+11	-0.12207E+12	-0.28191E+12	0.15803E+13	-0.38201E+13
0.48932E+13	-0.27179E+13	-0.24375E+13	0.58699E+13	-0.40953E+13	0.11055E+13	0.67832E+11
0.25080E+12	-0.25933E+12	0.75797E+11	0.19177E+12	-0.40800E+12	0.21606E+12	0.89656E+12
-0.27201E+13	0.34692E+13	-0.96871E+12	-0.30728E+13	0.34409E+13	-0.12237E+13	-0.85079E+11
-0.11972E+12	0.16216E+12	-0.96411E+11	-0.17045E+12	0.87798E+12	-0.20360E+13	0.32358E+13
-0.24349E+13	-0.97135E+12	0.42013E+13	-0.32676E+13	0.46561E+12	0.35852E+12	0.46482E+11
-0.81573E+11	0.68389E+11	-0.27115E+11	0.14148E+12	-0.84628E+12	0.24258E+13	-0.48986E+13
0.58691E+13	-0.30695E+13	-0.32706E+13	0.75733E+13	-0.52994E+13	0.13983E+13	0.76821E+11
0.11613E+12	-0.13473E+12	0.94808E+11	-0.10253E+12	0.44406E+12	-0.13258E+13	0.29056E+13
-0.40957E+13	0.34392E+13	0.46822E+12	-0.53007E+13	0.51097E+13	-0.17967E+13	-0.13188E+12
-0.37013E+11	0.49162E+11	-0.47731E+11	0.47310E+11	-0.12223E+12	0.32066E+12	-0.70493E+12
0.11057E+13	-0.12233E+13	0.35776E+12	0.13988E+13	-0.17968E+13	0.80834E+12	0.82729E+11
-0.90887E+09	0.15902E+10	-0.42294E+10	0.69773E+10	-0.13119E+11	0.23801E+11	-0.43492E+11
0.67828E+11	-0.85046E+11	0.46447E+11	0.76827E+11	-0.13187E+12	0.82724E+11	0.13430E+11

RMS (DIAGONAL) = 0.153622E+07 Window 50-650, (.167-2.167 cm)

TABLE 14. COVARIANCE ERROR MATRIX $(F^TF)^{-1}$

```
      E-04 -0.11587E-03 -0.79155E-04 -0.61512E-04 -0.84400E-04 -0.15163E-03  0.99996E+00

 0.12495E+12 -0.63333E+11 -0.76232E+11  0.17027E+12 -0.20691E+12  0.12956E+12  0.36107E+11
-0.20625E+12  0.26082E+12 -0.11486E+12 -0.96687E+11  0.12733E+12 -0.40739E+11 -0.11727E+10

-0.63339E+11  0.82504E+11 -0.16716E+11 -0.93815E+11  0.18404E+12 -0.16915E+12  0.44246E+11
 0.14925E+12 -0.27071E+12  0.16767E+12  0.71978E+11 -0.13986E+12  0.51593E+11  0.18804E+10

-0.76222E+11 -0.16724E+11  0.12763E+12 -0.12242E+12  0.42084E+11  0.64130E+11 -0.11566E+12
 0.41811E+11  0.85150E+11 -0.10678E+12 -0.27383E+11  0.10135E+12 -0.52250E+11 -0.50964E+10

 0.17028E+12 -0.93818E+11 -0.12243E+12  0.29089E+12 -0.36466E+12  0.25214E+12 -0.51361E+11
-0.11785E+12  0.18797E+12 -0.17022E+12  0.15560E+12 -0.12102E+12  0.56956E+11  0.85522E+10

-0.20701E+12  0.18411E+12  0.42128E+11 -0.36478E+12  0.74439E+12 -0.92417E+12  0.83709E+12
-0.32129E+12 -0.40724E+12  0.91662E+12 -0.91281E+12  0.49884E+12 -0.14505E+12 -0.15821E+11

 0.12984E+12 -0.16937E+12  0.64040E+11  0.25252E+12 -0.92460E+12  0.17659E+13 -0.23942E+13
 0.17096E+13  0.20251E+12 -0.21528E+13  0.26036E+13 -0.14529E+13  0.36886E+12  0.28383E+11

 0.35595E+11  0.44667E+11 -0.11554E+12 -0.52077E+11  0.83815E+12 -0.23950E+13  0.42761E+13
-0.40971E+13  0.97351E+12  0.34368E+13 -0.52452E+13  0.31561E+13 -0.80161E+12 -0.53131E+11

-0.20575E+12  0.14881E+12  0.41740E+11 -0.11715E+12 -0.32253E+12  0.17109E+13 -0.40981E+13
 0.52272E+13 -0.29032E+13 -0.25779E+13  0.62696E+13 -0.44294E+13  0.12452E+13  0.84205E+11

 0.26072E+12 -0.27056E+12  0.85082E+11  0.18779E+12 -0.40659E+12  0.20118E+12  0.97571E+12
-0.29053E+13  0.36972E+13 -0.10380E+13 -0.32891E+13  0.37084E+13 -0.13506E+13 -0.10237E+12

-0.11533E+12  0.16801E+12 -0.10661E+12 -0.17081E+12  0.91715E+12 -0.21523E+13  0.34346E+13
-0.25747E+13 -0.10407E+13  0.44392E+13 -0.34417E+13  0.49964E+12  0.36504E+12  0.50144E+11

-0.96046E+11  0.71416E+11 -0.27491E+11  0.15649E+12 -0.91422E+12  0.26048E+13 -0.52457E+13
 0.62688E+13 -0.32863E+13 -0.34451E+13  0.80746E+13 -0.57242E+13  0.15720E+13  0.96413E+11

 0.12700E+12 -0.13953E+12  0.10135E+12 -0.12154E+12  0.49996E+12 -0.14545E+13  0.31581E+13
-0.44310E+13  0.37076E+13  0.50309E+12 -0.57268E+13  0.55508E+13 -0.19935E+13 -0.15614E+12

-0.40679E+11  0.51516E+11 -0.52237E+11  0.57083E+11 -0.14542E+12  0.36956E+12 -0.80276E+12
 0.12464E+13 -0.13508E+13  0.36372E+12  0.15736E+13 -0.19941E+13  0.90492E+12  0.96381E+11

-0.11707E+10  0.18762E+10 -0.50947E+10  0.85605E+10 -0.15852E+11  0.28450E+11 -0.53252E+11
 0.84337E+11 -0.10241E+12  0.50030E+11  0.96588E+11 -0.15623E+12  0.96396E+11  0.15852E+11
```

RMS (DIAGONAL) = 0.158840E+07 Window 100-650, (.333-2.167 cm)

TABLE 15. THE SPECTRAL SPACE COVARIANCE MATRIX $(f^T f)^{-1}$ USING THE FILTERS OF KAPLAN et al., (1977).

0.16677E+15	-0.10257E+08	-0.97713E+07	0.33984E+08	-0.13865E+10	0.91388E+09	0.85895E+08	0.96980E+06	0.38896E+08	0.73400E+04
-0.10257E+08	0.35642E+15	-0.85356E+09	-0.51483E+08	-0.51850E+11	0.27506E+09	0.18793E+10	-0.70241E+07	0.16821E+09	0.75677E+05
-0.97713E+07	-0.85356E+09	0.25590E+15	0.48204E+07	-0.29359E+12	-0.86051E+08	0.31989E+10	0.70929E+07	0.19663E+09	-0.18816E+06
0.33984E+08	-0.51483E+08	0.48204E+07	0.28837E+16	0.47166E+10	-0.60239E+10	0.80211E+10	-0.49287E+07	0.44511E+10	-0.61350E+06
-0.13865E+10	-0.51850E+11	-0.29359E+12	0.47166E+10	0.15587E+18	-0.82092E+11	0.48596E+11	0.15992E+09	-0.10498E+11	-0.16909E+08
0.91388E+09	0.27506E+09	-0.86051E+08	-0.60239E+10	-0.82092E+11	0.78012E+17	0.45139E+11	-0.85774E+10	-0.32397E+10	0.28609E+07
0.85895E+08	0.18793E+10	0.31989E+10	0.80211E+10	0.48596E+11	0.45139E+11	0.11528E+18	-0.24438E+11	-0.71043E+12	-0.66807E+09
0.96980E+06	-0.70241E+07	0.70929E+07	-0.49287E+07	0.15992E+09	-0.85774E+10	-0.24438E+11	0.67363E+15	-0.30694E+11	-0.14425E+09
0.38896E+08	0.16821E+09	0.19663E+09	0.44511E+10	-0.10498E+11	-0.32397E+10	-0.71043E+12	-0.30694E+11	0.25662E+17	-0.29868E+10
0.73400E+04	0.75677E+05	-0.18816E+06	-0.61350E+06	-0.16909E+08	0.28609E+07	-0.66807E+09	-0.14425E+09	-0.29868E+10	0.11640E+14

RMS (Diagonal) = 1.9472×10^8.

TABLE 16. COVARIANCE ERROR MATRIX $(f^T f)^{-1}$

0.26613E+15	-0.78826E+14	-0.23298E+15	0.36623E+15	-0.36386E+15	0.17347E+15	0.97543E+14
-0.27235E+15	0.27651E+15	-0.13492E+15	-0.19221E+14	0.55035E+14	-0.17292E+14	0.88715E+11
-0.78851E+14	0.16267E+15	-0.62022E+14	-0.14946E+15	0.29722E+15	-0.23172E+15	0.25020E+14
0.16300E+15	-0.21516E+15	0.12133E+15	0.16441E+14	-0.55940E+14	0.18764E+14	-0.89912E+11
-0.23294E+15	-0.62060E+14	0.37981E+15	-0.34082E+15	0.13529E+15	0.67885E+14	-0.14264E+15
0.93637E+14	-0.46016E+14	0.60517E+14	-0.10798E+15	0.88108E+14	-0.24397E+14	0.84880E+11
0.36620E+15	-0.14940E+15	-0.34086E+15	0.64107E+15	-0.70203E+15	0.41202E+15	-0.42673E+14
-0.19645E+15	0.33285E+15	-0.41692E+15	0.40362E+15	-0.23176E+15	0.52295E+14	-0.14756E+12
-0.36382E+15	0.29713E+15	0.13536E+15	-0.70204E+15	0.12829E+16	-0.13217E+16	0.88994E+15
-0.19573E+15	-0.55562E+15	0.11975E+16	-0.13194E+16	0.75650E+15	-0.16353E+15	0.48058E+12
0.17334E+15	-0.23159E+15	0.67847E+14	0.41191E+15	-0.13215E+16	0.21056E+16	-0.23513E+16
0.14638E+16	0.30212E+15	-0.22055E+16	0.28477E+16	-0.16947E+16	0.36676E+15	-0.11161E+13
0.97856E+14	0.24819E+14	-0.14277E+15	-0.42250E+14	0.88927E+15	-0.23508E+16	0.39328E+16
-0.36498E+16	0.86595E+15	0.31172E+16	-0.49884E+16	0.31496E+16	-0.69562E+15	0.21659E+13
-0.27278E+15	0.16318E+15	0.93967E+14	-0.19710E+15	-0.19481E+15	0.14629E+16	-0.36492E+16
0.46574E+16	-0.25231E+16	-0.23300E+16	0.55894E+16	-0.39463E+16	0.92027E+15	-0.29749E+13
0.27678E+15	-0.21518E+15	-0.46360E+14	0.33331E+15	-0.55610E+15	0.30262E+15	0.86529E+15
-0.25224E+16	0.29443E+16	-0.58396E+15	-0.26346E+16	0.26577E+16	-0.72938E+15	0.26449E+13
-0.13473E+15	0.12114E+15	0.60551E+14	-0.41671E+15	0.11970E+16	-0.22050E+16	0.31174E+16
-0.23309E+16	-0.58308E+15	0.36057E+16	-0.36373E+16	0.14824E+16	-0.16863E+15	-0.77994E+11
-0.19786E+14	0.16725E+14	-0.10764E+15	0.40284E+15	-0.13183E+16	0.28468E+16	-0.49882E+16
0.55902E+16	-0.26358E+16	-0.36365E+16	0.78961E+16	-0.55146E+16	0.12679E+16	-0.38303E+13
0.55476E+14	-0.56127E+14	0.87783E+14	-0.23112E+15	0.75570E+15	-0.16941E+16	0.31494E+16
-0.39466E+16	0.26583E+16	0.14819E+16	-0.55143E+16	0.45978E+16	-0.12181E+16	0.44920E+13
-0.17406E+14	0.18811E+14	-0.24308E+14	0.52124E+14	-0.16332E+15	0.36661E+15	-0.69558E+15
0.92033E+15	-0.72951E+15	-0.16848E+15	0.12678E+16	-0.12180E+16	0.36340E+15	-0.16226E+13
0.89148E+11	-0.90106E+11	0.84546E+11	-0.14687E+12	0.47971E+12	-0.11155E+13	0.21657E+13
-0.29750E+13	0.26453E+13	-0.78596E+11	-0.38296E+13	0.44917E+13	-0.16226E+13	0.16311E+12

RMS (DIAGONAL) = 0.502[illegible]7E+08 WINDOW 0-4096 (600-750 cm^{-1})

END

FILMED

DTIC